Rheological properties of aqueous nanometric alumina suspensions

by

Chuanping Li

A dissertation submitted to the graduate faculty

in partial fulfillment of the requirements for the degree of

DOCTOR OF PHILOSOPHY

Major: Materials Science and Engineering

Program of Study Committee:
Mufit Akinc, Major Professor
David Cann
Vladimir Tsukruk
Klaus Schmidt-Rohr
Kristen Constant

Iowa State University

Ames, Iowa

2004

Graduate College
Iowa State University

This is to certify that the doctoral dissertation of

Chuanping Li

has met the dissertation requirements of Iowa State University

Signature was redacted for privacy.

Major Professor

Signature was redacted for privacy.

For the Major Program

Table of Contents

Acknowledgments

Sincere gratitude is expressed to my major professor, Dr. Mufit Akinc, for his assistance in the preparation of this manuscript and many helpful guidance and discussions. I would like to thank the member of my supervisory committee Dr. Vladimir Tsukruk, Dr. David Cann, Dr. Kristen Constant, in MSE, Dr. Klaus Schmidt-Rohr in Chemistry, and Dr. Surya K. Mallapragada in Chemical Engineering at Iowa State University for their guidance and time. Sincere gratitude is also expressed to Dr. C. Schilling for his encouragement and helpful discussions. Thanks to Drs. P. Tomasik, M. Sikora, J. Wiench, P. Marek, J. Anderegg, Mr. S. Hennady, Drs. G. Tuttle, T. Oja, B. Mavis, Andrew Thom, M. Kramer, and our research group members for their support on experiments and discussions. Thanks also to the staffs and some of the faculty and graduate students in MSE department at ISU for their helps. Deepest thanks go to my wife, Weihua Du and my daughter, Xueqian, for their encouragement and patient devotion.

Finally, I would like to thank the Office of Basic Energy Sciences at the U. S. Department of Energy, for funding this research. This work was performed at Ames Laboratory under Contract No. W-7405-Eng-82 with the U.S. Department of Energy. The United States government has assigned the DOE Report number IS-T 2097 to this thesis.

Abstract

Colloidal processing is an effective and reliable approach in the fabrication of the advanced ceramic products. Successful colloidal processing of fine ceramic powders requires accurate control of the rheological properties. The accurate control relies on the understanding the influences of various colloidal parameters on the rheological properties.

Almost all research done on the rheology paid less attention to the interactions of particle and solvent. However, the interactions of the particles are usually built up through the media in which the particles are suspended. Therefore, interactions of the particle with the media, the adsorbed layers on the particle surface, and chemical and physical properties of media themselves must influence the rheology of the suspension, especially for the dense suspensions containing nanosized particles. Relatively little research work has been reported in this area.

This thesis addresses the rheological properties of nanometric alumina aqueous suspensions, and paying more attention to the interactions between particle and solvent, which in turn influence the particle-particle interactions. Dense nanometric alumina aqueous suspensions with low viscosity were achieved by environmentally-benign fructose additives.

The rheology of nanometric alumina aqueous suspensions and its variation with the particle volume fraction and concentration of fructose were explored by rheometry. The adsorptions of solute (fructose) and solvent (water) on the nanometric alumina particle surfaces were measured and analyzed by TG/DSC, TOC, and NMR techniques. The mobility of water molecules in the suspensions and its variation with particle volume fractions and fructose additive were determined by the ^{17}O NMR relaxation method. The interactions between the nanometric alumina particles in water and fructose solutions were investigated by AFM.

The results indicated that a large number of water layers were physically bound on the particles' surfaces in the aqueous suspension. The viscosity of the suspension increases dramatically when the solid volume fraction exceeds 30 vol.%. The overlap of physically adsorbed water layers at this level causes the sharp increase in viscosity. Fructose molecules can weaken the interactions between the particle surfaces and water molecules, as a consequence, they release some bound water layers from the surfaces to the bulk medium. It

is believed that fraction of the water that is bound by the solid surface is reduced hence becoming available for flow. The oxygen-17 relaxation time decreased with the increase of particle volume fractions in the suspension. Fructose addition increased the overall water mobility in the suspension. Only part of the alumina particle surfaces was covered with fructose molecules. This adsorption of fructose molecules on the particle surfaces increased the pH of the suspension with a concomitant decrease in ζ-potential of the alumina nanoparticles. The interactions between the nanometric alumina particles in water to a large extent can be explained by the DLVO theory. However, the interactions between particles in fructose solutions cannot be well described by the DLVO theory. The interaction forces (magnitude and range) as well as adhesive force and surface tension between nanometric alumina particles were decreased with the fructose concentration.

Chapter 1: Introduction

Thesis Organization

This thesis adopts a journal paper format described in the Graduate College Thesis Manual, such that each paper or manuscript will appear as a separate chapter. In addition, a general introduction is given in this, the first chapter, and an overall conclusion is included as the last chapter of the thesis. The First paper, Chapter 2, which has been submitted to the *Journal of the American Ceramic Society*, is in the review process (Manuscript Number: JACS-10513) and titled "Role of Bound water on the Viscosity of Nanometric Alumina Suspension". The viscosity of aqueous nanometric alumina suspensions with various solid volume fraction and fructose concentrations was examined in this paper. The adsorbed water layer on the particle surfaces with and without fructose was measured through the freezing behavior of water in the suspensions, and the effect of this layer on the rheology was discussed in this paper. Chapter 3, "Relationship between Water Mobility and Rheological Behavior of Nanometric Alumina Aqueous Suspension", will be submitted to *Journal of the American Ceramic Society*. This paper studied the changes in mobility of water molecules in the suspensions with and without fructose and how the mobility related with the viscosity. Chapter 4, "Interactions between Nanometric Alumina Particles in Fructose Solutions," discusses the interparticle forces between nanoparticles in water and fructose solution using colloidal probe atomic force microscopy and relates the experimental findings to the well-known DLVO theory.

Note that although all three manuscripts are largely the work of this author, Dr. Mufit Akinc (major professor) has made significant contributions throughout the study and appears as co-author on these papers. Drs. C. Schilling, J. Wiench, M. Pruski, and J. Anderegg have made contributions to some parts of these papers and appear as co-authors on one of these papers.

1.1 Background

1.1.1 The Reliability of Ceramics and Colloidal Route

Among the various powder-processing techniques, colloidal processing has been well-recognized as one of the common approaches in the fabrication of advanced ceramics primarily because it offers such advantages as low cost and more reliable properties in the resulting ceramic products [1,2], which are difficult to achieve through the use of other alternatives, e.g., dry-pressing. In colloidal processing, a number of liquids were used as carrier media, and among them, water has always been preferred simply because environmental concerns have become an increasingly important issue. In powder processing via colloidal processing, a stable suspension with high solids content and with appropriate rheological properties is needed. Moreover, it may be of interest to further realize the rheological properties of highly concentrated aqueous suspensions with nano-size powders, since many applications need the components forming from nanoparticles. In general, an increase in solids content and a decrease in particle size result in increase in the suspension viscosity and give rise to a high yield value [3-5]. This would make green shape processing, such as slip or tape casting, more difficult.

Experience indicates that the higher the green density, the less the shrinkage during drying, debinding and sintering, and in consequence, the easier it is to sinter reliable, crack-free parts. Unfortunately, the green density is often limited by the low concentrations of solid needed to maintain acceptable flow properties during shape forming. For example, suspensions that are used for extrusion, injection molding, or ram pressing, must contain large concentrations (up to 60 to 70 vol.%) of carrier liquids in order to maintain acceptable flow characteristics [6,7]. Costly trial-and-error methods are typically used to find the right suspension composition that will maintain fluidity/plasticity while keeping the solids concentration as high as possible. A schematic picture (Figure 1) shows the objective of these efforts.

Successful colloidal processing of fine ceramic powders requires on accurate control of the rheological behavior of the suspension. The accurate control in turn, relies on the

understanding of the influences of various colloidal interactions on the rheological properties. A better science base is needed to elucidate how the chemistry and physics of the solid-liquid interface controls interparticle interaction, agglomeration, and the rheology of ceramic particle suspensions.

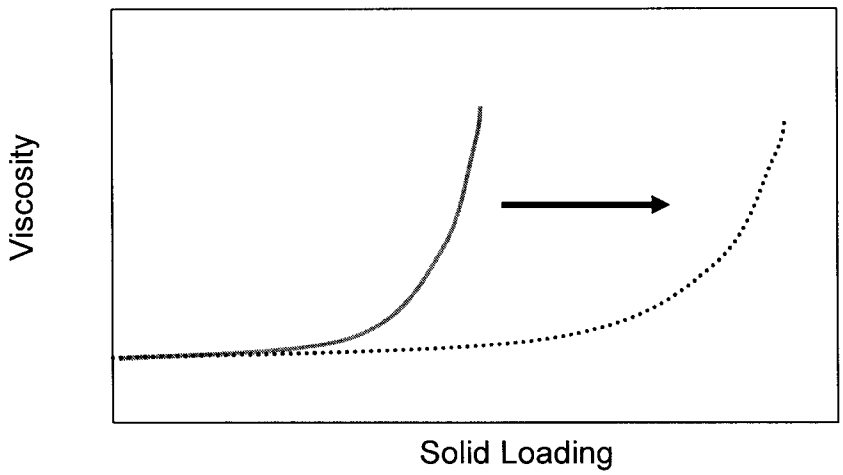

Fig. 1 Increasing solid loading in suspension but keeping the viscosity at a low level.

1.1.2 Previous work

Schilling and co-workers [8-10] in Ames Lab developed an environmentally- benign gelcasting method to form ceramics by using polysaccharides. It shows that polysaccharides can be added to reduce viscosity and in turn provide highly dense suspensions of micron-sized oxide particles. They performed rheological measurements to show that a range of dextrin and maltodextrin molecular-weights produce a similar, dramatic reduction in viscosity of aqueous systems of alumina (as shown in Fig. 2). The authors performed electrokinetic and sorption-isotherm experiments to demonstrate that short-range, steric repulsion forces are responsible for significant reductions in the viscosity of aqueous suspensions of micron-sized, α-Al_2O_3 powder upon the addition of maltodextrin. They subsequently evaluated whether the same approach can be used to form highly dense, low-viscosity, aqueous suspensions of aluminum oxide nanoparticles [11, 12]. A key result of these experiments is that the polysaccharide molecular weight must be below a certain limit

in order to produce a reduction in viscosity. For example, Figure 3 illustrates that sugar alcohols, pentoses, and some hexoses are effective in reducing the suspension viscosity. Although different molecules have varying degree of influence on the rheology in the suspensions, in general, they reduce the viscosity of the suspension, especially mono-saccharides like fructose. Therefore, it seems possible to achieve high solids loadings for nanometric particle slurries by adding mono- or di- saccharides. On the contrary, excessively high viscosities were obtained after adding longer polysaccharide molecules to aqueous suspensions of nanometric alumina.

The mechanism of saccharide addition on rheology of suspensions is unknown. Mono- and di-saccharides are neither electrolytes nor polymers. Therefore, not much electrostatic forces and steric repulsion forces can be induced by adding them in the suspensions. The question is how do they reduce the viscosity of the suspension so dramatically? This research was set up in order to answer this question.

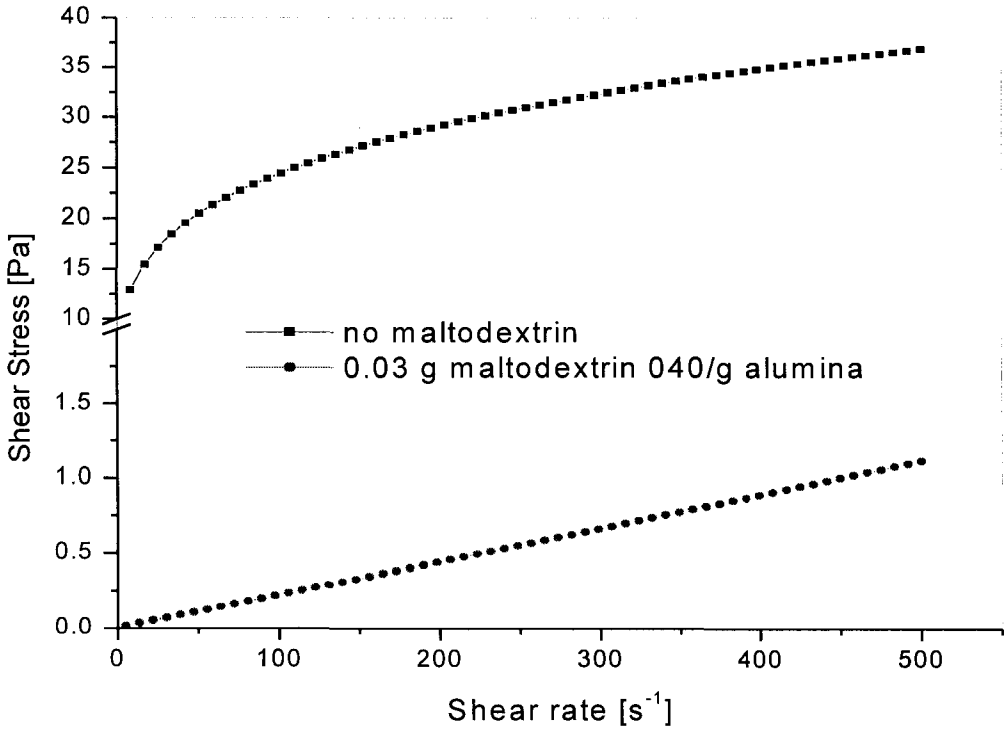

Fig. 2 Effect of Maltodextrin M040 (AMW: 3,600 Dalton) on rheology of the 30 vol.% suspension of microsized alumina particles

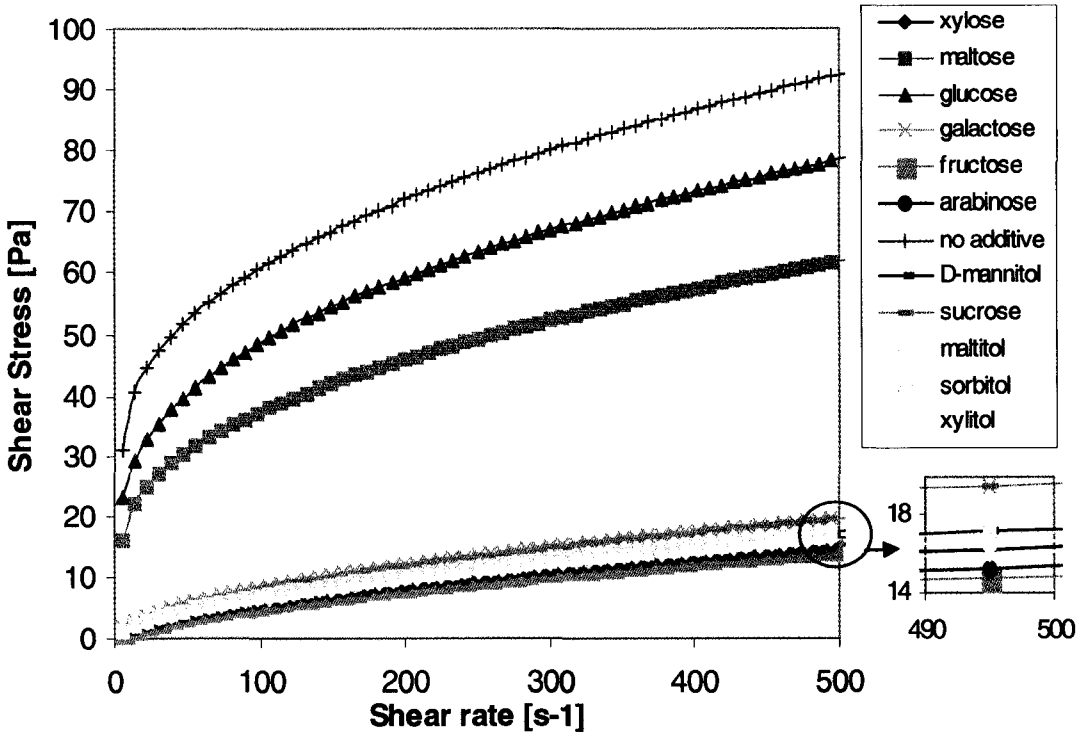

Fig. 3 Effect of 5 wt.% different saccharides on the rheology of 30 vol.% suspensions of nanometric alumina particles.

1.1.3 Application of the dense nanometric particle aqueous suspensions with low viscosity

Ability to increase the solid fraction of the suspension while maintaining flowability provides numerous advantages in colloidal processing of ceramics. These dense suspensions under appropriate processing conditions lead to reliable, defect-free components.

Figure 4 shows two different yttria-stabilized zirconia (YSZ) films that were fabricated by spray-coating an aqueous suspension of nanometric powder onto a porous substrate of (La, Sr)MnO_3. Both films were sintered to 1000 °C in air. Notice the extensive cracking in the sample at the right. This cracked coating was spray-coated using an aqueous suspension of YSZ (18 vol.%) without any additives. Denser suspensions were tried to form the thin film by spray-coating. However, the viscosity of the suspension was too high when the solid volume fraction reaches 25 vol.%. The crack-free coating for the sample shown on the left

was spray-coated using a suspension (25 vol.%) containing 5 wt.% saccharide additives (based on the solids). Chemical vapor deposition has traditionally been used to produce prototype zirconia electrolytes for solid-oxide fuel cells. Because this process is difficult to scale up [13], alternative methods involving spray deposition of zirconia nanoparticles are being explored.

Figure 5 shows another example of the possible route for producing a photonic band gap component employing 28 vol.% nanometric alumina suspension with 8 wt.% fructose (based on the solids) and calcined at 600 °C. Low shrinkage, crack-free components with smooth surface were obtained. Sol-gel methods had been used to form the components, but resulted in large shrinkage and a rough surface, making the precise feature size control of the components nearly impossible.

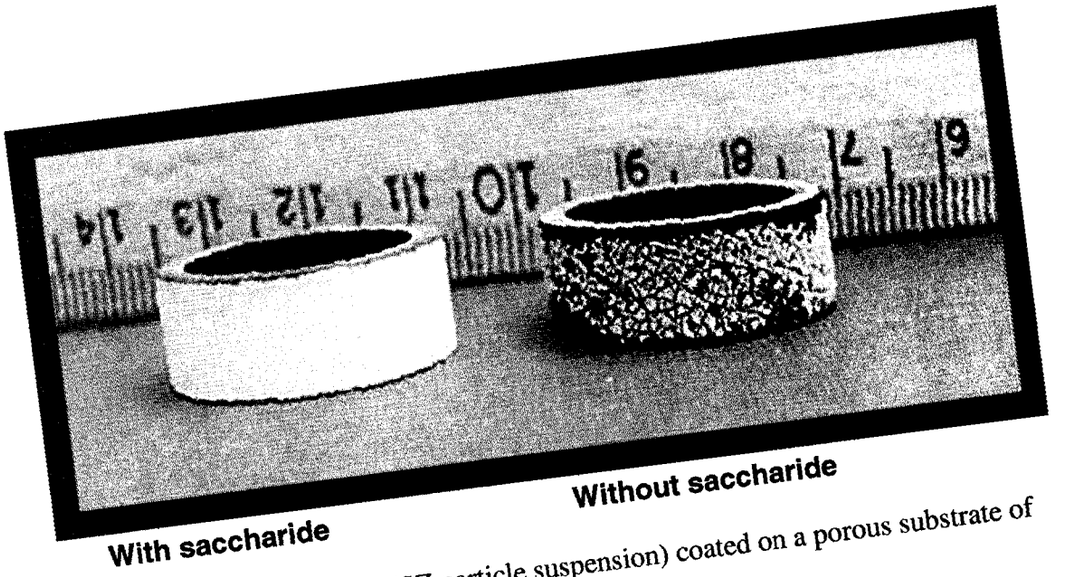

Fig. 4 YSZ films (nano-YSZ particle suspension) coated on a porous substrate of (La, Sr)MnO_3 and calcined at 1000 °C

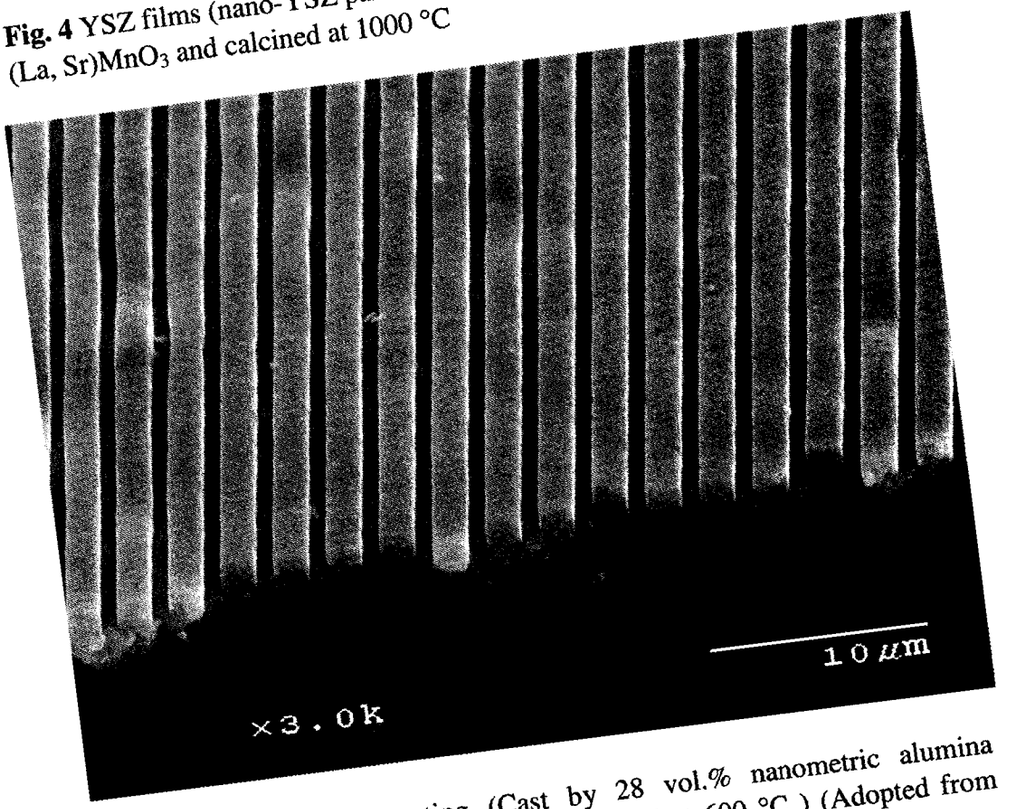

Fig. 5 Ceramic line grating (Cast by 28 vol.% nanometric alumina suspension with 8 wt.% fructose and calcined at 600 °C) (Adopted from Henry Kang's work, unpublished.)

1.2 Viscosity of a Colloidal Suspension

Conventionally, as is well known, the rheological properties (e.g., flow properties) of liquids such as water or oils are characterized by their viscosity, η, which can be thought of as the resistance of a liquid to flow or internal friction. Suppose that a liquid is confined between two plates, one fixed and the other moveable, of area A and separated by a distance x. A constant force $\boldsymbol{F}$ is then applied to the moveable plane and after acceleration it assumes a constant velocity v. The liquid between the planes is sheared and a velocity gradient is set up, intermediate layers moving with intermediate velocities. The force $\boldsymbol{F}$ between two adjacent layers of liquid is given by

$$F = \eta A \frac{dv}{dx} \qquad (1\text{-}1)$$

($F = \eta A\dot{\gamma}$ or $\tau = \eta\dot{\gamma}$, $\dot{\gamma}$--shear rate, τ--shear stress)

where dv/dx is the velocity gradient.

As the shearing force or stress is increased so the rate of flow and for liquid media a plot of shearing stress against rate of shear yields a straight line passing through the origin (Fig. 6b), the slope of the line being the viscosity, η. The rheological behaviour of such systems is described as *Newtonian.* However, for many suspensions there is no such linear relation between the rate of shear and the shearing stress, and the rheological behaviour is said to be non-Newtonian. Fig. 6 shows the different types of basic flow behavior that can occur.

Materials exhibiting *plastic flow* (Fig. 6d) require a certain minimum shear stress before flow commences; this minimum stress is designated the *yield value, f.* This type of flow, which is called Bingham flow, is shown by some dispersions of finely divided solids in liquids such as paints, printing inks, clay pastes and particle slurries used in ceramics, etc.

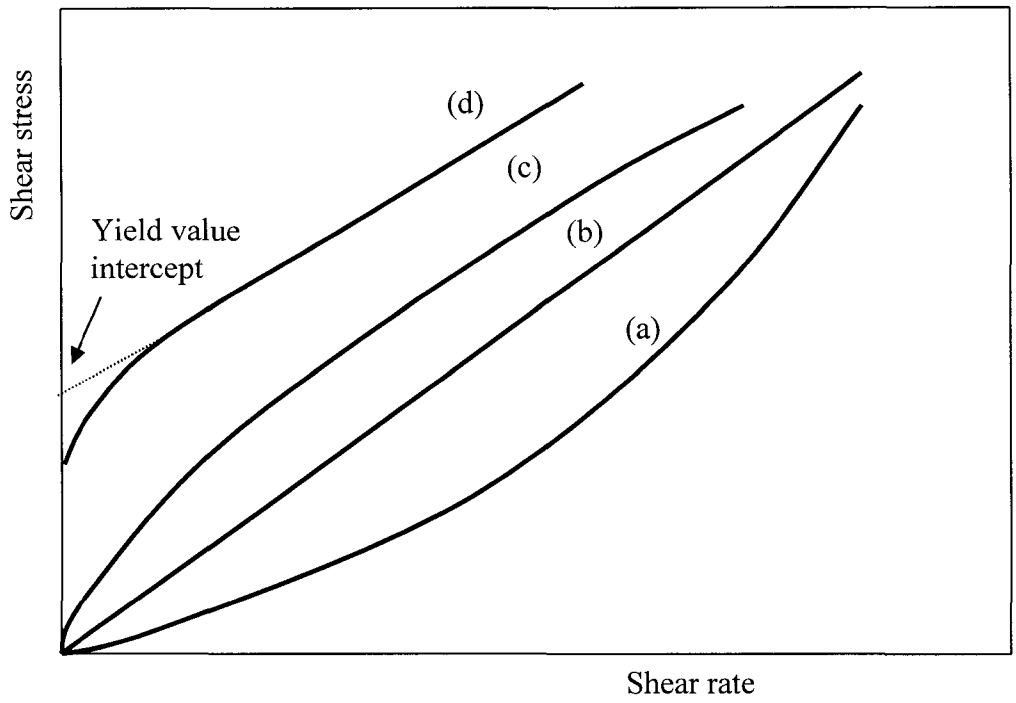

Fig. 6 Basic type of rheological behaviour of dispersions: (a) dilatant; (b) Newtonian; (c) pseudeoplastic; (d) plastic. [14]

Bingham [15] suggested that in a suspension showing plastic flow the individual particles touch each other in a flocculated array and that in order for flow to commence it is necessary to apply sufficient stress to break some of these interparticle bonds. During shear an equilibrium is set up between the breaking and reforming of these bonds, so that at a constant rate of shear an equilibrium value for the shear stress is attained, and increasing the rate of shear produces a different equilibrium.

Other dispersions exhibit *pseudoplastic flow* (Fig. 6c) in which there is no initial yield value and with increasing rate of shear an apparent decrease in viscosity occurs, the shear stress against rate of shear curve being convex to the shear stress axis. The fourth type of behaviour shown in Fig. 6a is *dilatant flow*; the apparent viscosity increases with increasing shear rate, the shear stress/shear rate curve being concave to the shear stress axis. This behaviour is shown by deflocculated dispersions of pigments and other powders at high volume concentrations. At these high concentrations of the solid phase, the particles are

closely packed and disturbance by shear introduces irregularities into the packing, with bridging effects occurring between the particles. Since the packing becomes looser, the total volume of interparticle space becomes greater and the liquid present is no longer sufficient to fill the space between the particles: consequently, the lubricating effect of the liquid, which enables the particles to slide over one another, is lost.

A further type of rheological behaviour exhibited by certain systems is *thixotropic flow*, which is a time-dependent phenomenon. In this case, the existing structure of the system, for example a flocculated network of particles, is broken down on stirring but does not re-form immediately the stirring action is ceased. The time taken for the structure to re-assemble itself may range from seconds to hours. Fig. 7 illustrates the type of flow curves which may be obtained using a rotational viscometer with such systems.

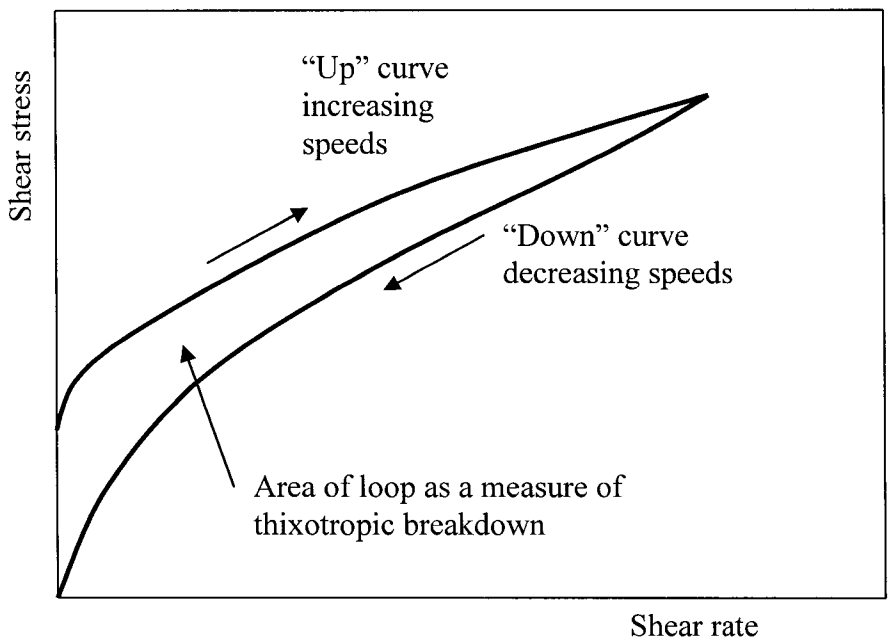

Fig. 7 Rheological behaviour of a thixotropic system as measured with a rotational viscometer. [14]

Thus, the flow properties of dispersions is rather complex and at the present, no universal theory exists for the interpretation of flow behaviors and their relationship to parameters (e.g., particle size, volume fraction, and interparticle interaction) of the media and suspended phase.

Generally, the viscosity of colloidal suspensions is affected by the following factors [16]: (i) medium of the suspension; (ii) shape, density, size and size distribution of the particles; (iii) volume actually occupied by the particles in suspension; (v) thermodynamic conditions of the system (T, P); (vi) presence and concentration of electric charges in the system; (vii) shear rate.

The equation of state for the viscosity of a colloidal suspension of hard spheres can be written [17]

$$\eta = f\left(\dot{\gamma}, t, \eta_0, \rho_0, R, n, \rho_p, kT\right) \qquad (1\text{-}2)$$

where, $\dot{\gamma}$ (or, alternatively, the shear stress τ)--shear rate, t--the time. Since the particles are much larger than the molecules of the medium, only continuum properties of the medium are of interest: its viscosity η_0 and its density ρ_0. The radius, R, of the particles, their concentration (number density) n, and their density ρ_p are relevant, and, whenever Brownian movement is significant, a thermal energy variable kT is include, where k is Boltzmann's constant and T the temperature.

For a system of charged particles, additional structural variables must be present in the equation of state. These include the particle charge q, the ionic strength, *I*, and the dielectric constant, ε, of the medium.

For a given colloid system (e.g., particles, medium, temperature, pressure and shear rate are fixed), the viscosity can be expressed as

$$\eta = f(\phi, \psi) \qquad (1\text{-}3)$$

ϕ--volume fraction of suspended particles; ψ--the term of interactions between particles and particle with medium.

1.3 Particle-particle Interaction and DLVO Theory

A well-established theory for the study of interparticle interaction in colloidal suspension is the DLVO theory. The DLVO theory is contributed by two independent groups: Derjaguin and Landau [18] and Verwey and Overbeek [19, 20, 21]. DLVO theory is able to predict the stability of colloids in polar liquids by considering the balance between electrical double-layer repulsions and van der Waals attractions. If particles dispersed in a liquid attract each other, they will stick together whenever they collide, form aggregates which grow heavy and sink: they do not form a stable colloid. On the other hand, if the repulsive forces between the particles are sufficiently high, they stay apart, and (if they are reasonably small) Brownian motion will keep them in a state of animated suspension for a much longer time.

The van der Waals force is ubiquitous, and is always attractive between like particles. It arises from the interaction of atomic and molecular electric dipoles whose orientations are correlated in such a way that they attract each other. The van der Waals force between two bodies depends on their surface separation h. For example, the force between two spheres of radius R_S is given by [22]

$$F(D) = \frac{A_H \bullet R_S}{12h^2} \qquad (1\text{-}4)$$

where A_H, the Hamaker constant, depends on the polarizabilities and number densities of the atoms in the two bodies under consideration.

When a body is immersed in a polar solvent such as water, the interface will, in general, acquire a charge, by either adsorbing or desorbing ions according to some chemical equilibrium with the surrounding solution. Ions of opposite charge dissolved in the polar medium, known as counterions, are attracted toward the surface of the particle, although for entropic reasons they remain in solution, forming a diffuse layer of charge adjacent to the particle. The surface charged layer (stern layer) plus the diffuse layer of opposite charge constitute an electrical double layer (Fig. 8) and electrostatic forces will be generated between the surfaces of the body in a polar environment.

The thickness of the double layer depends on the concentration of ions in solution: more ions available in the solution leads to a thinner double layer. A measure of the thickness is given by the Debye length Λ, which is the inverse of the Debye constant κ:

$$\Lambda = \kappa^{-1} = \left(\frac{e^2 \sum \rho_i z_i^2}{\varepsilon_0 \varepsilon_r kT} \right)^{-1/2} \qquad (1\text{-}5)$$

where e is the electronic charge, ρ_i is the number density and z_i is the valence of ion species i, ε_0 is the dielectric permittivity of vacuum, ε_r is the relative permittivity (or dielectric constant) of the solvent. For example, in a 0.01 M aqueous solution of a 1:1 electrolyte, the double layer "thickness", κ^{-1}, equals 30.4 $\mathring{A}$ [23]. As shown in equation (1-5), the "thickness" of the double layer varies inversely with z and inversely with $\rho^{1/2}$ for a symmetrical z:z electrolyte. Therefore, κ^{-1} equals 15 $\mathring{A}$ for a 0.01 M solution of a 2:2 electrolyte and is about 96 $\mathring{A}$ for a 0.001 M solution of 1:1 electrolyte.

Like bodies acquire the same charge and consequently repel each other, and the counterions screen that interaction. The complete expression for the repulsion is complicated and an approximate linearized expression valid for symmetrical z:z electrolytes and large separations (D>Λ) is [20]

$$F(D) = \frac{64 \rho kT}{\kappa} \cdot (\tanh \frac{ze\Psi_0}{4kT})^2 \cdot \exp(-\kappa D) \qquad (1\text{-}6)$$

where $\rho = \sum \rho_i$ and the surface potential ψ_0 is related to the surface charge density σ_0 by

$$\sigma_0 = -\frac{4 \rho ze}{\kappa} \sinh(ze\Psi_0 / 2kT) \qquad (1\text{-}7)$$

DLVO Theory of colloidal stability is based on the assumption that the net force between particles immersed in a polar liquid is given by the algebraic sum of the electrical double-layer repulsion and the dispersion attraction (van der Waals). This combination of a positive (repulsive) exponential function of separation, whose range depends on ionic strength (Eqs.(1-5) and (1-6)), with a negative (attractive) power law function which is insensitive to ionic strength (Eq. (1-4)), gives rise to some interesting behavior, as illustrated in Fig. 9. Electrical double-layer repulsion gives a positive contribution which decreases exponentially as surface separation increases (dash line in figure 9). van der Waals attraction gives a negative term which is an inverse power law function of separation (dash-dot line in figure 9). The net energy (solid line in Figure 9) is given by the sum of these two. At low electrolyte concentration (a) the double-layer term dominates at most separations, giving a maximum in

the energy. The height of this energy barrier depends on the surface charge density and the electrolyte concentration. If the energy maximum greatly exceeds typical values for the kinetic energy of dispersed particles (~kT) then particles remain dispersed; if it does not, then colliding particles may surmount the barrier and fall into the primary minimum at contact (i.e. zero separation), from which they are unlikely to escape: they coagulate. At high concentration (b) the double-layer term may decay so rapidly (within a few nanometers) that the van der Waals attraction is still significant at a separation beyond the range of the repulsion, and the particles can reside in a secondary minimum (arrow). This gives a much weaker adhesion, which could easily be overcome by sheer, or effectively removed by reducing the salt concentration [20].

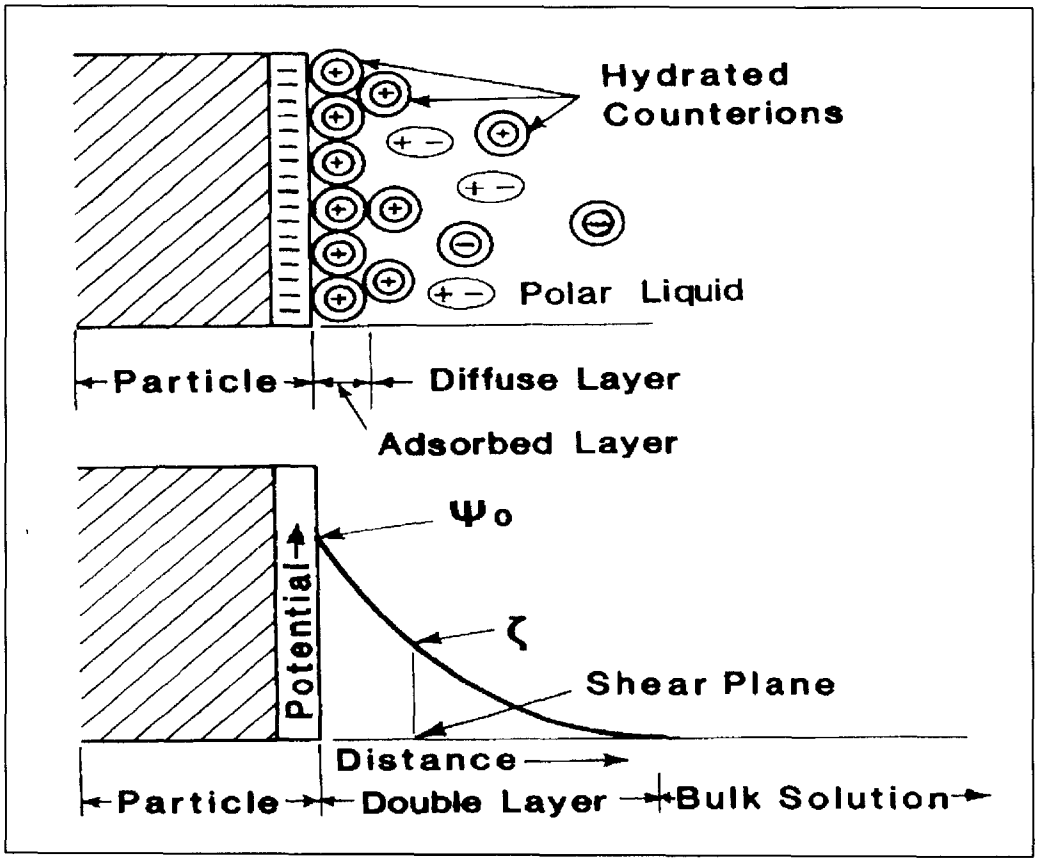

Fig. 8 Electrical double layer model for charged particle in a polar liquid and the profile of the electrical potential. [24]

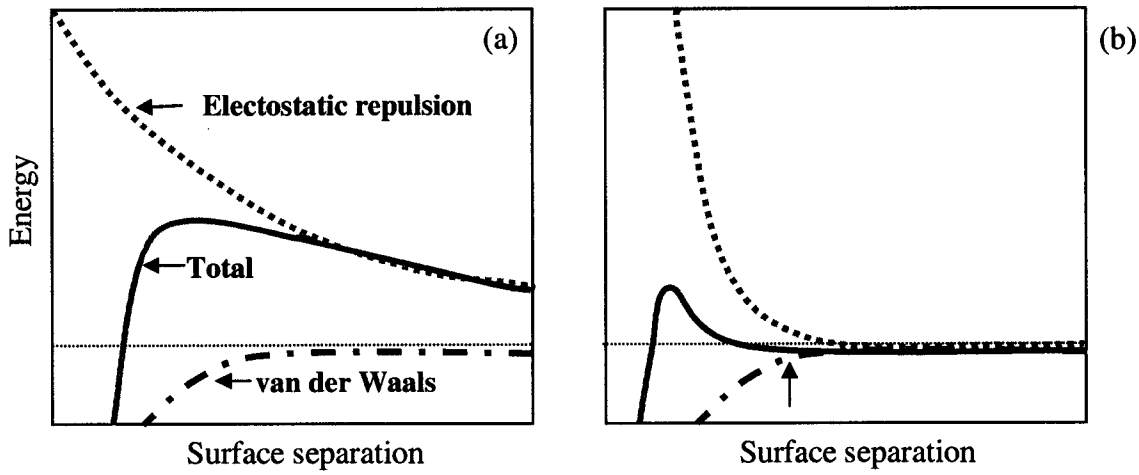

Fig. 9 Schematic plots of the energy of interaction between two surfaces across a polar liquid.

Previous research shows that the viscosity of the slurry varies inversely with the zeta potential on adding a polyelectrolyte deflocculant [24]. In suspensions of oxides deflocculated using simple electrolytes, the viscosity also varies inversely with the zeta potential. The viscosity of a slurry is very sensitive to the coagulation forces and the coagulated structure. Slurry that is only partially coagulated may be of lower viscosity, but exhibit shear-thickening behavior owing to the interaction of agglomerates when sufficiently concentrated. The minimum viscosity occurs when the zeta potential is high and the agglomerates are dispersed.

The DLVO theory has enjoyed considerable success in the years since then, although it is clear that it has its limitations, for reasons which will be discussed below. Nevertheless, it remains a cornerstone of modern colloid science.

This theory describes experimental results reasonably well for large separations but breaks down for the treatment of short range interactions between surfaces. The discrete nature of the solvent, which is neglected by DLVO theory, is essential for the description at small separation in nano-sized particle suspension [25].

Moreover, there are many forces in colloidal suspensions which are not indicated by DLVO theory (called non-DLVO forces). For example, steric forces, solvation forces (hydration forces), hydrodynamic forces, hydrophobic forces, and capillary forces exist in

colloidal suspensions [20]. All of these forces will affect the rheology of suspensions. In addition of these mentioned above, the DLVO theory is only able to predict the stability of colloidal suspension based on the interaction between particles. However, the influences of these interactions on the viscosity are still unknown. The question of predicting the rheology of a colloid from the knowledge of particle size, shape, volume fraction, and the surface forces, is far beyond the scope of DLVO theory. The problem becomes more complicated as the particle size gets smaller. Further research to understand the rheological behavior of concentrated suspensions with nanoparticles is needed.

1.4 Controlling Rheology by Using Electrolytes and Polymers (or Polyelectrolytes) to Modify Particle Surfaces

The rheology of colloidal suspensions can be simply changed by adding electrolytes or polymers. Many studies have shown that the rheology of suspensions can be modified by manipulation and tuning of particle interactions [26-29].

Low viscosity aqueous suspensions of various ceramic powders can be obtained by creating a high charge on the particle surface, which results in a strong double-layer repulsion. Such high surface charge densities can be created by working far away from the point of zero charge (pH_{pzc}) of powder. However, because this often means working at high or low pH, colloidal stability and low viscosity can be affected by other undesirable effects, such as dissolution and high ionic strength. To avoid the problems of working with pH values far from the neutral range, repulsive particle interactions are commonly produced by the addition of suitable dispersants (sometimes called deflocculants). Such additives will adsorb at the particle surface and generate a repulsive interaction caused by electrostatic or polymeric (steric) effects. When surfactants adsorb, they "paint" the surfaces and give them a different chemical "color," which can have a major effect on the forces between them. It is important to know whether or not polymer molecules adsorb to the surfaces, which depends on whether segments of the polymer molecule prefer to be in contact with the surface or with the solvent. The changes in surface force and rheology caused by surfactant adsorption are fairly straight forward to rationalize, although it is not always easy to predict the quantity and configuration of a given surfactant adsorbed to a given surface. Typically there will be a certain range of concentration over which a monolayer of surfactant adsorbs, at a density

from which it can be construed that the elongated molecules are oriented perpendicular to the surface. At lower concentrations there will be sub-monolayer coverage, with the possibility of having surfactant molecules lying parallel to the surface. At high concentrations it is possible to get a second monolayer adsorbed on the first, generally in the opposite orientation and more monolayers may adsorb on the surface [30].

Surfactant adsorption can affect other forces between surfaces, in particular the van der Waals attraction. If, as is often the case, the refractive index of the surfactant is intermediate between that of the particle and that of the solvent, its presence will weaken the attraction, and in turn will reduce viscosity.

1.5 Viscosity of Colloidal Suspensions

The viscosity of a suspension η_S is greater than the viscosity of the liquid medium η_L, and the ratio is referred to as the relative viscosity η_r. For a very dilute suspension of non-interacting spheres in a Newtonian liquid, the viscosity is described by the Einstein equation [31]:

$$\eta_r = \eta_S/\eta_L = 1 + 2.5\phi_P \qquad (1\text{-}8)$$

where ϕ_P is the volume fraction of dispersed spheres. The higher viscosity is caused by the dissipation of energy as liquid flows around the particles. A more general equation for the viscosity of a suspension of nonspherical particles is [32]:

$$\eta_r = 1 + K_H\phi_P \qquad (1\text{-}9)$$

where K_H is the apparent hydrodynamic shape factor of the particles, and $K_H>2.5$.

As the concentration of the dispersed phase increases, the viscosity of a suspension is increased due to the interaction between the dispersed particles and does not obey the Einstein equation. The rheological behavior of concentrated suspensions is much more difficult to work out [20]. Since the publication of Einstein's basic analysis of the viscosity of a dilute suspension of rigid spheres, many investigations have attempted to predict the rheology of hard-sphere colloidal dispersions. Much of the effort has focused on extending theoretical models for dilute dispersions to concentrated dispersions of hard spheres [33-36]. Commensurate with these theoretical developments, experimentalists have worked toward developing real colloidal dispersions that approximate hard spheres [37-39]. Computational

techniques that include many body hydrodynamic interactions have also been developed to enable direct numerical calculation of hard-sphere colloidal behavior [40, 41].

As the volume fraction of particles increases, the interaction between particles during flow causes the viscosity to increase greatly. Rheological data for suspensions of uniform spherical colloidal particles are often approximated by the Dougherty-Krieger equation [37].

$$\eta_r = \frac{\eta_S}{\eta_L} = \left(1 - \frac{\phi_P}{\phi_{cr}}\right)^{-K_H \phi_{cr}} \qquad (1\text{-}10)$$

where ϕ_{cr} is the packing factor at which flow is blocked. Effects of both the liquid viscosity and the particle loading are shown in the figure of apparent viscosity η_S with powder loading (Fig. 10) [32]. In suspensions of particles of anisometric shape both K_H and ϕ_{cr} depend on particle orientation produced during laminar flow. Brownian motion somewhat randomizes colloidal particles and increases the effective hydrodynamic shape factor. Woods and Krieger [42] obtained values of K_H=2.7 and ϕ_{cr}=0.57-0.68 for aqueous suspensions of dispersed monosize latex sphere finer than 0.7 μm. The effective volume fraction of dispersed particles ϕ_P was calculated from the volume fraction of spheres ϕ_S, their mean size $\bar{a}$, and the effective thickness of the adsorbed surfactant Δ. The effective volume fraction of the particles with adsorbed additive is calculated form the equation

$$\phi_P = \phi_S \left(1 + \frac{2\Delta}{\bar{a}}\right)^3 \qquad (1\text{-}11)$$

This correction becomes increasingly significant when the particle size decreases below 1 μm. Agglomeration reduces the effective ϕ_{cr}.

The Mooney equation [43]

$$\eta_r = \exp\left[\frac{K_H \phi_P}{1 - k_1 \phi_P}\right] \qquad (1\text{-}12)$$

may sometimes approximate the effect of solids loading on the relative viscosity of deflocculated casting slurries and slips of fine powders. In the equation, k_1 is a constant, the self-crowding factor, higher than unity. Equation (1-12) takes account of a proportion of immobilized liquid associated with the flow units.

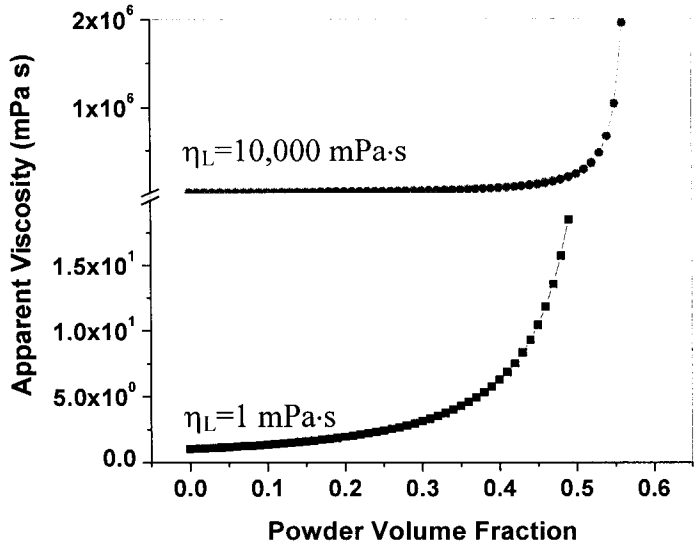

Fig. 10 The apparent viscosity depends on viscosity of the liquid medium and particle parameters described by the Dougherty-Krieger equation. (K_H=2.5, and ϕ_{cr}=0.58)

The equation of Chong et al.[44] in general form is

$$\eta_r = \left[\frac{(\phi_{cr} - k_2\phi_P)}{(\phi_{cr} - \phi_P)}\right]^2 \qquad (1\text{-}13)$$

and has been shown to approximate the viscous behavior of injection molding material containing a highly viscous polymer liquid [45], where, k_2 is a constant for a given suspension (k_2=0.25-0.7). These equations predict a viscosity increase similar to that of Dougherty-Krieger equation. The viscosity of suspensions varies for different particles and media even at the same particle volume fraction. A viscosity sensitivity index S calculated as [32]

$$S = \frac{d\ln\eta_s}{d\phi_P} \qquad (1\text{-}14)$$

will indicate the viscosity effect at some constant powder loading ϕ_P on substituting an alternative material. For the Mooney description,

$$S = \frac{K_H}{(1 - k_1 \phi_P)^2} \tag{1-15}$$

All the models were established based on interactions between the suspended particles, but treated the media as a continuum hydrodynamics (the viscosity of the liquid in the thin film around the particle surface was the same as it is in the bulk). For example, Batchelor and Green [33] gave an exact description of the viscosity of a semi-dilute suspension of hard spheres in the limit of vanishing sheer rate. This theory was extended to higher particle concentrations by Russel and Gast [34] who took the mean thermodynamic force in a concentrated dispersion into account, and treated the hydrodynamic interactions at the pair level. Wagner and Russel [35] calculated the viscosity as a function of volume fraction taking the hydrodynamic interaction between an arbitrary number of spheres into account. They used a multipole expansion in the force density.

Even though many models have been established, there is still a discrepancy between the data and the prediction, apparently in part due to the incomplete treatment of the hydrodynamics. Further research is needed to understand the rheology of colloidal suspensions especially of high solids content and nanometric particles.

1.6 Effect of Adsorbed Solvent Layers on the Rheology of Aqueous Suspensions

It is known that the nature of water in the vicinity of a surface or an interface is different from that of bulk water and that is important for the rheology of dense aqueous suspensions, especially for the suspensions containing nanosized particles, which will be discussed below. Water coming in contact with solid surfaces induces several changes, such as dissolution of solids, changes in surface conductivity, and adhesive force between particle surfaces [46].

However, many researchers ignored the influences of the adsorbed layers around particle surfaces [20, 47, 48]. They addressed that the continuum hydrodynamics can be employed for any computations concerning the approach of colloidal particles. These incomplete treatments of the hydrodynamics led to a discrepancy between the data and the prediction. In the suspension of large colloidal particles (e.g. microsized particles), the influences of the adsorbed layers may not be significant, but they are critical in the nanoparticle suspension, which will be discussed in the next section.

Forster [49, 50] found that the bound water content of the sludge was related to the yield stress, filtration characteristics and viscosity. As the bound water content of the sludge decreases, so does its viscosity. Katsiris and Kouzeli-Katsiri [51] have shown that any treatment which reduces the bound water content of sludges will reduce viscosity and the specific resistance to filtration. Therefore, the bound water content of slurries should be another parameter in describing viscosity.

In Takei's work [46] of water in silica pores, the result suggests that physisorbed water molecules are localized on the silica surfaces because of strong interactions with the surface hydroxyl groups. The second adsorbed layer is formed on the first adsorbed layer through the formation of hydrogen bonds, so the structure of the second adsorbed layer is affected by the configuration and orientation of the water molecules in the first adsorbed layer. The interaction effects of solid surfaces on adsorbed layers are gradually reduced with an increase in the thickness of the adsorbed layer. The results obtained [46] show that the structure of water is affected up to at least 4 nm from the solid surface. If the thickness of a single adsorbed layer of water is 0.29 nm [52, 53], the effects of solid surfaces extend to 11-14 molecular layers in small pores. Etzler and Fagundus [54] also reported that water is structurally modified up to 3-5 nm from the solid surface in silica pores. These long scales of

adsorbed solvent (water) layer may play a significant role in determining the rheology of dense aqueous suspensions containing nanoparticles.

Viscosity sensitivity index, S (see the equation (1-14)), was introduced in order to determine the extent of the viscosity change with the particle volume fraction. Suspensions with similar particle volume fractions, but different particles or media have different viscosities, which was attributed to the difference in particle-particle interactions by most researchers. Actually, in the aqueous suspension with low ionic strength, particle-particle interactions are, usually, established through the media (except for the strongly agglomerated particles). Therefore, the interactions between particle and media, and the adsorption layers around particle surface are more important in determining the particle-particle interactions and viscosity of this kind of suspension.

1.7 Suspension Containing Nanosized Particles: size effects

When hygroscopic oxide nanoparticles added to water, they react with water molecules to form hydroxyl groups which remain attached to the surfaces, and release or bind protons, resulting in a change of suspension pH. The unique feature of oxide nanoparticles is that they possess larger specific surface area than microparticles. Because of this, a large fraction of water content is bound to nanoparticle surfaces, and only small fraction of the water content remains as "free" water to provide fluidity to the suspension. In the following sections, a simple derivation is given to show how the surface area and particle separation change with the reduction of particle radius in suspension. These parameters will significantly influence the adsorption properties and interactions in suspensions, and consequently affect the viscosity.

1.7.1 Relationship between volume fraction, surface area and particle size

For a suspension of total volume V with solid volume fraction of ϕ consisting of n particles with a radius of R, the total solid surface area and volume are given by

$$A_S = n \cdot 4\pi R^2 \text{ and } V_S = n \cdot (4/3)\pi \cdot R^3 \text{ respectively} \qquad (1\text{-}16)$$

By definition:

$$\phi = \frac{V_S}{V} \tag{1-17}$$

From Eqn. (1-16) and (1-17), we know that

$$V_S = n\cdot(4/3)\pi\cdot R^3 = A_S\cdot(R/3) \tag{1-18}$$

According to Eqn. (1-17) and (1-18), Surface area can be expressed as a function of suspension volume, V, particle radius, R, and volume fraction, ϕ;

$$\frac{A_S}{V} = \frac{3\cdot\phi}{R} \tag{1-19}$$

From Eqn. (1-19), it can be easily seen that the total solid surface area per unit volume, A_S/V, proportional to volume fraction, ϕ, and inversely proportional to particle size. One of the unique features of nano-sized particles is the fact that a large portion of the atoms in the particle are at the surface. Because of this, the particles tend to be more reactive—more surfaces contribute to contact with solutes/solvent in the suspensions.

1.7.2 Particle separation in suspension

In the previous paragraph the significance of particle size and volume fraction of solids on the surface area was established. It may also be prudent to estimate particle-particle separation as a function of particle radius of solids volume fraction.

Knowing that highest volume fraction of randomly packed uniform spheres is equal to 0.64 (ϕ_{CR}), and volume fraction of solids in a suspension is ϕ (where $\phi < \phi_{CR}$), surface separation distance, $2a$, between the particles in a suspension can be related to particle radius and solids volume fraction as:

$$(\frac{\phi}{\phi_{cr}} = \frac{V_S/V}{V_{cr}/V} = \frac{V_S}{V_{cr}} =) \frac{n\cdot\frac{4}{3}\pi R^3}{n\cdot\frac{4}{3}\pi(R+a)^3} = \frac{\phi}{0.64}$$

(1-22)

So, the surface separation for adjacent particles,

$$2a = 2R\left(\sqrt[3]{\frac{0.64}{\phi}} - 1\right) \tag{1-23}$$

Eq. (1-23) indicates that the surface separation is proportional to the particle radius at a constant volume fraction. Conversely, surface separation, a weak function of volume fraction of solids, decreases with increasing solids volume fraction.

According to Eq. (1-23), the surface separation of adjacent particles is as low as 11.2 nm in the 30 vol.% suspension of nanosized particles with diameter of 40 nm, but the surface separation is about 112 nm for the same volume fraction of 0.4 μm particles. In a previous section, it was discussed that the thickness of double-layer around the particle is 9.6 nm for a 0.001 M solution of a 1:1 electrolyte. So, in the 30 vol.% suspension of nanosized particles with diameter of 40 nm in this kind of solution, the surface separation of particles is within the range of the electrical double-layer field of influence (11.2 nm < 2×9.6 nm). Therefore, this "bound layer" around the particles will affect the relative motion between particles in the suspension, which in turn influence the viscosity of the suspension. On the other hand, for the suspension of the same solid volume fraction (30 vol.%) with 2R = 0.4μm particles, the surface separation of neighboring particles is much larger than the range of the electrical double-layer potential. Hence, particles more-or-less flow independent of each other.

Therefore, more attention should be paid on the bound water for nanosized particles when dealing with the rheological properties of their suspensions.

Foregoing discussion shows that the viscosity of colloid suspensions is strongly influenced by particle volume fraction and interactions between particles/media. Nanometric particles possess larger surface area and shorter inter-particle separation than micrometric particles in the suspensions at the same solid volume fraction.

1.8 Motivation and approach of the research work

It was pointed out that the rheological properties of colloidal particle suspensions are not only determined by the solid phase (e.g. particle size, volume fraction, etc.), but also determined by the media in which the particles are suspended and the interactions of particle-media which in turn will influence interaction between particles.

The reason that saccharides greatly reduce the viscosity of nanoparticle alumina suspension could be attributed to 1) the change in the behavior of adsorption of water molecules which leads to higher fraction of water remain in the "free" state with higher

mobility; 2) the reduction in the interactions of particle-media which in turn will reduce the particle-particle interactions.

Therefore, the present research focused on the adsorption of water and fructose and the effect of interactions of particle-media on the rheology in order to develop scientific understanding of the influence on the viscosity of colloidal nanoparticle suspensions by the solid volume fractions, the adsorption of water and saccharide on particle surface, and particle-particle interaction, and to achieve a fundamental understanding on rheology of nanoparticle suspensions in aqueous media by answering the following questions: (i)How does the viscosity of the suspension change with the nanoparticle volume fraction? (ii) How do the adsorbed layers of water around the particle surface influence the viscosity of the suspension? (iii) How does the mobility of the water in the suspension changes with the addition of mono-saccharides and how does this influence the viscosity? (iv) How does the saccharide concentration influence the inter-particle forces? (v) How the interaction between particles affect the suspension rheology?

Series of experiments were conducted using rheometry, nature of water around particles by sub-zero temperature differential scanning calorimetry (SZT-DSC), chemically bound water analysis by thermo-gravimetry analysis (TGA), determination of adsorbed fructose on particle surfaces by nuclear magnetic resonance (NMR), measurement of the water mobility in the suspensions by (NMR), and the interactions between nanoparticles in fructose solutions by atomic force microscopy (AFM).

Nanometer-sized powders of alumina (γ phase, rigid and spherical particles with average particle size of 40 nm in diameter) were chosen as the model particulate systems for the research. Because of its common use in the ceramics industry and has been rigorously characterized (Kelso and Ferrazoli 1988 [55]; James 1984 [56]). D-fructose was chosen as the primary saccharide because of its well defined chemical composition and configurational simplicity, and its strong effect in reducing the suspension viscosity.

The goal of this research is to develop scientific guidelines for achieving the dense aqueous suspensions of ceramic nanoparticles with low viscosities by adding non-toxic additives derived from renewable agricultural resources.

Reference:

1. F. F. Lange, "Powder processing science and technology for increased reliability," *J. Am. Ceram. Soc.*, **72** (1), 3-15, 1989.

2. W. A. Ducker, Z. Xu, D. R. Clarke, and J. N. Israelachvili, "Forces between alumina surfaces in salt solutions: Non-DLVO Forces and the implications for colloidal processing," *J. Am. Ceram. Soc.*, **77**(2), 437-43, 1994.

3. D. M. Liu, "Rheology of aqueous suspensions containing highly concentrated nano-sized zirconia powders", *Journal of Materials Science Letters*, 17, 1883-1885, 1998.

4. J. C. Chang, F.F. Lange and D. S. Pearson, "Viscosity and yield stress of alumina slurries containing large concentrations of electrolyte," *Journal of the American Ceramic Society*, **77**(1), 19-26, 1994.

5. Q. D. Nguyen, D. V. Boger, "Yield stress measurement for concentrated suspensions," *Journal of Rheology*, **27**(4), 321-349, 1983.

6. V. K. Pujari and D. M. Tracey, "Processing methods for high reliability silicon nitride heat engine components," in *ASME Trans.*, Proc. Int. Gas Turbine and Aeroengine Congr., ASME 93-GT-319, Cincinnati, Ohio, 1993.

7. G. V. Franks and F. F. Lange, " Plastic to brittle transition of saturated, alumina powder compacts," *J. Am. Ceram. Soc.*, **79**(12), 3161-68, 1996.

8. C. H. Schilling, R. A. Bellman, R. M. Smith, H. Goel, "Plasticizing aqueous suspensions of concentrated alumina with maltodextrin sugar," *Journal of the American Ceramic Society,* **82**(1), 57-66, 1999.

9. C. H. Schilling, C. Li, P. Tomasik, J. Kim, "The rheology of alumina suspensions: influence of polysaccharides," *Journal of the European Ceramic Society,* **22**(6), 923-931, 2002.

10. M. Sikora, C. H. Schilling, P. Tomasik, C. Li, "Dextrin plasticizers for aqueous colloidal processing of alumina," *Journal of the European Ceramic Society*, **22**(5), 625-628, 2002.

11. C. H. Schilling, P. Tomasik, C. Li, Marek Sikora, "Protein plasticizers for aqueous suspensions of micrometric- and nanometric-alumina powder," *Materials Science & Engineering, A: Structural Materials: Properties, Microstructure and Processing*, A336 (1-2), 219-224, 2002.

12. C. H. Schilling, M. Sikora, P. Tomasik, C. Li, V. Garcia, "Rheology of alumina-nanoparticle suspensions: effects of lower saccharides and sugar alcohols," *Journal of the European Ceramic Society* , **22**(6), 917-921, 2002.
13. C. Kleijn, K. Kuijlaars and H. Akker, "Design and scale-up of chemical vapour deposition reactors for semiconductor processing," Chemical Engineering Science, 51(10), 2119-2128, 1996.

14. R.W. Whorlow, *Rheological Techniques*, Ellis Horwood Limited, John Wiley & Sons, New York, 1980.

15. E.C. Bingham, *Fluidity and Plasticity*, McGraw Hill, New York, p.228, 1922.

16. G.D. Parfitt, *Dispersion of Powders in Liquids with special reference to pigments*, Third edition, Applied Science Publishers LTD 1981.

17. I. M. Krieger, "Rheology principles, measurements, and applications," Journal of Colloid and Interface Science, 178(1), 382, 1996.

18. B. V. Derjaguin and L. D. Landau, "Theory of stability of highly charged lyophobic sols and adhesion of highly charged particles in solutions of electrolytes," *Acta Physicochim.* URSS., 14, 633-52, 1941.

19. E. J. W. Verwey and J. Th. G. Overbeek, *Theory of stability of lyophobic colloids*, Elsevier, Amsterdam, Netheriands, 1948.

20. R. G. Horn, "Surface forces and their action in ceramic materials," *J. Am. Ceram. Soc.*, **73**(5), 1117-1135, 1990.

21. T. G. M. Van de Ven, *Colloidal Hydrodynamics*. Academic Press, New York, 1989.

22. H. C. Hamaker, "The London-van der Waals attraction between spherical particles," *Physica (Amsterdam)*, 4, 1058-72, 1937.

23. P. C. Hiemenz, *Principles of Colloid and Surface Chemistry*, 3rd edition, Marcel Dekker, INC. p 369, 1997.

24. J. S. Reed, *Principles of ceramics processing*, second edition, 158, 161, 297-298, Wiley & Sons, New York, 1995.

25. J.N. Israelachvili, *Intermolecular and Surface Forces*, Academic Press, New York, 1985.

26. F. F. Lange, "Powder processing science and technology for increased reliability," *J. Am. Ceram. Soc.*, 72, 3-15, 1989.

27. R. J. Pugh and L. Bergstrom, *Surface and Colloid Chemistry in Advanced Ceramics Processing*. Marcel Dekker, New York, 1994.

28. T. A. Ring, *Fundamentals of Ceramic Powder Processing and Synthesis*. Academic Press, San Diego, CA, 1996.

29. M. E. Woods and I. M. Krieger, "Rheological studies on dispersions of uniform colloidal spheres," *Journal of Colloid and Interface Science*, 34(1), September 1970.

30 K. Shinoda, T. Nakagawa, B. Tamamushi, and T. Isemura, *Colloidal Surfactants*, Academic Press, New Youk, 216-247,1963.

31 A. Einstein, "A new determination of molecular dimensions," *Annalen der Physik* 19, 289-306 (1906); Corrections, ibid. 34, 591-592 (1911).

32. J. S. Reed, *Principles of ceramics processing*, second edition, 294, Wiley & Sons, New York, 1995.

33. G. K. Batchelor and J. T. Green, "The determination of the bulk stress in a suspension of spherical particles to order," *J. Fluid mech.* 56, 401-472, 1972.

34. W. B. Russel and A. P. Gast, "Nonequilibrium statistical-mechanics of concentrated colloidal dispersions—hard-spheres in weak flows," *J. Chem. Phys.* 84, 1815-1826, 1986.

35. N. J. Wagner, and W. B. Russel, "Nonequilibrium statictical-mechanics of concentrated colloidal dispersions—hard-spheres in weak flows with many-body thermodynamic interactions, *Physica A,* 155, 475-518, 1989.

36. J. F. Brady and J. Morris, "Microstructure of strongly sheared suspensions and its impact on rheology and diffusion," J. Fluid Mech. 348, 193-139 (1997).

37. I. M. Krieger and T. J. Dougherty, "A mechanism for non-newtonian flow in suspensions of rigid spheres," *Trans. Soc. Rheol.*, 3, 137-152, 1959.

38. J. C. van der Werff and C. G. de Kruif, "The scaling of rheological properties with particle size, volume fraction and shear rate," *J. Rheol.*, 33, 421-454, 1989.

39. P. N. Segre, and P. N. Pusey, "Dynamics and scaling in hard-sphere colloidal suspensions," *Physica A,* 235, 9-18, 1997.

40. J. F. Brady, and G. Bossis, "Stokesian dynamics," *Annu. Rev. Fluid Mech.* 20, 111-157, 1988.

41. D. Foss and J. Brady, "Structure, diffusion and rheology of Brownian suspensions by stokesian dynamics simulation," *J. Fluid Mech.* 407, 167-200, 2000.

42. M. E. Woods and I. M. Krieger, " Rheological studies on dispersions of uniform colloidal spheres I. Aqueous dispersions in steady shear flow," *J. Colloid Interface Sci.* 34, 91-99, 1970.

43. M. Mooney, "The viscosity of a concentrated suspension of spherical particles," *Journal of Colloid Science*, 6, 162-170, 1951.

44. J. S. Chong, E. B. Christiansen, and A. D. Baer, "Rheology of concentrated suspensions," *Journal of Applied Polymer Science*, **15**(8), 2007-2021, 1971.

45. T. Zhang and J. R. G. Evans, "Predicting the viscosity of ceramic injection molding suspensions," *Journal of the European Ceramic Society*, **5**(3), 165-172, 1989.

46. T. Takei, K. Mukasa, M. Kofuji, M. Fuji, T. Watanabe, M. Chikazawa, and T. Kanazawa, "Changes in density and surface tension of water in silica pores," *Colloid Polym. Sci.* 278: 475-480, 2000.

47. D. Y. C. Chan and R. G. Horn, "The drainage of thin liquid films between solid surfaces," *J. Chem. Phys.*, 83, 5311-24, 1985.

48. J. N. Israelachvili, "Measurement of the viscosity of liquids in very thin films," *J. Colloid Interface Sci.*, 110, 263-271, 1986.

49. C. F. Forster, "The rheological and physico-chemical characteristics of sewage sludges," *Enzyme and Microbial Technology*, **30**(3), 340-345, 2002.

50. C. F. Forster, "Bound water in sewage sludges and its relationship to sludge surfaces and sludge viscosities," *Journal of Chemical Technology and Biotechnology*, 33B, 76-84, 1983.

51. N. Katsiris, A. Kouzeli-Katsiri. "Bound water content of biological sludges in relation to filtration and dewatering," *Water Res.* 21: 1319-1327, 1987.

52. Gregg SJ, Sing KSW, *Adsorption, Surface Area and Porosity*, Academic, New York, pp 157-158, 1967.

53. J. Jr. Hagymassy , S. Brunauer, R. S. Mikhail, "Pore structure analysis by water vapor adsorption. I. t-Curves for water vapor," *Journal of Colloid and Interface Scence,* **29**(3), 485-491, 1969.

54. F. M. Etzler, D. M. Fagundus, "The extent of vicinal water. Implications from the density of water in silica pores," *J. Colloid Interface Sci.* **115**(2): 513-519, 1987.

55. J. F. Kelso and T. A. Ferrazzoli, "Surface Chemistry Effects in Concentrated Aqueous Dispersions of Bayer Process Calcined Alumina," in *Ceramic Transactions Volume 1,*

Ceramic Powder Science II, edited by G. L. Messing, E. R. Fuller, and H. Hausner (American Ceramic Society, Westerville, Ohio, 1988), pp. 433-439.

56. R. O. James, "Characterization of Colloids in Aqueous Systems," in *Advances in Ceramics, Volume 21, Ceramic Powder Science*, editors G. L. Messing, K. S. Mazdiyasni, J. W. Cauley, and R. A. Haber (American Ceramic Society, Westerville, Ohio, 1984), pp. 349-410.

Chapter 2:

Role of Bound Water on the Viscosity of Nanometric Alumina Suspensions

(A paper submitted to Journal of the American Ceramic Society)

Chuanping Li and Mufit Akinc

Department of Materials Science and Engineering and Ames Laboratory
Iowa State University, Ames, IA 50011, U.S.A.

Abstract

Successful colloidal processing of fine ceramic powders requires accurate control of the rheological properties, which are determined by the colloidal parameters. Characteristics of adsorbed water layers on the surfaces of nanometric alumina particles were studied by differential scanning calorimetry (DSC) and thermogravimetry (TGA). The experiments indicated that a large number of water layers were physically bound on the particles' surfaces. These bound water layers increased the viscosity of the suspensions. It was also shown that the addition of monosaccharides, fructose in particular, reduced the viscosity of the suspensions dramatically. The reduction in the number of water layers bound to the particle surface could be attributed to the fructose present in the solution. NMR experiments indicated that only a fraction of a monolayer (0.22-0.24) of fructose was adsorbed on the particle surfaces.

1. Introduction

Nanometric ceramic powders are widely used in the production of ultra-thin dielectrics, solid-oxide fuel cells, and oxygen separation systems for medical and aerospace applications [1-4]. An aqueous ceramic suspension is commonly used in forming ceramic parts because it is safe, inexpensive and is an excellent solvent for many processing additives. Water, as a vehicle, plays a very important role in the viscosity of the suspensions. Water may be adsorbed on the particle surfaces or react with additives. The reaction, or adsorption, between

water and powders, water and additives, as well as between powders and additives will affect the rheological behavior of the suspension. The nature of water in suspensions varies greatly, depending on whether it is hydrogen bonded to the surface or associated with additives or simply bulk (free) water. It is believed that it is the "availability" of water, not the water content alone, that governs the rheology of aqueous suspensions. The higher the fraction of "free" water, the lower the viscosity of the suspension.

However, previous research [5-8] on the rheology of aqueous suspensions, for the most part, neglected the influence of the bound water, which exhibits lower degrees of freedom than bulk water. The influence of bound water on the rheology of suspensions containing micron-sized particles may be negligible, but in nano-sized particle suspensions the effect of bound water layers needs to be taken into account, as nanometric particles possess a higher fraction of surface atoms and are more reactive. Interactions of the particle surface with water and processing additives influences the rheological properties of the suspension, especially for dense suspensions containing nano-sized particles.

Forster [9,10] found that the yield stress, filtration characteristics, and viscosity of the sludge was related to the bound water content. As the bound water content of a sludge decreases, so does its viscosity. Katsiris and Kouzeli-Katsiri [11] have shown that any treatment which reduces the bound water content of sludges also reduces the viscosity and the specific resistance to filtration. Therefore, the bound water content of a slurry should be an important parameter in describing its viscosity.

Recent work [12] has shown that a small amount of mono- or di-saccharides, such as D-fructose or sucrose, are very effective on reducing the viscosity of aqueous suspensions of nanometric alumina. Use of saccharides as processing additives offers a number of advantages over other organic additives. Saccharides are nontoxic, readily available, and they are soluble in water. If they improve the rheological properties of aqueous suspensions, they will be additive of choice in forming ceramics. The majority of current processing additives are either ionic surfactants or non-ionic polymers. However, mono- and di- saccharides are neither electrolytes nor polymers. The question as to how they affect the rheology of the suspension remains to be answered. The adsorption characteristics of fructose on the particle surfaces and the role of mono saccharides on the bound water content need to be explored.

In the present work, the nature (and hence mobility) of water in aqueous suspensions of nanometric alumina particles in varying solids content and fructose concentrations as it affects the rheological properties was investigated. The primary purpose of the investigation was to have a better understanding of the role mono- and di-saccharides play in altering the rheology of nanoparticle suspensions. Fructose was chosen as a model saccharide because of its simple structure and well-known properties.

2. Experimental procedure

2.1. Materials.

The nanometric alumina powders (99.99% alumina) were purchased from Nanophase Technologies Corporation (Burr Ridge, Illinois). The surface area of the nanometric alumina particles was measured to be 37.9±0.2 m^2/g by the BET method, corresponding to an equivalent spherical diameter of 40 nm. TEM micrograph shows that the particles are spherical, with considerable size distribution and agglomeration (Figure 1). The nanosized alumina used in this investigation is pure γ-phase alumina, as stated by the manufacturer and confirmed by XRD. The specific gravity of the nanometric alumina was 3.6 g/m^3.

D-Fructose was purchased from SIGMA Corporation (St. Louis, Missouri). Chemical analysis, as provided by the manufacturer, is 99.9% pure. Deuterated water (D_2O) was purchased from Aldrich Chemical Company, Inc. (Milwaukee, WI), with 99.9 atomic percent deuterium. Reagent grade methanol was purchased from Fisher Scientific Company (Fair Lawn, New Jersey)). All materials were used as received without further purification.

2.2. Experiments.

The nanometric alumina powders were dried at 110 °C before use. Suspensions were equilibrated by shaking for three days in sealed plastic bottles before any measurements were made.

The objective of the rheological measurements was to determine the dependence of solid content and fructose concentration on the viscosity of the suspensions. Rheological properties of aqueous nanometric alumina suspensions with various solid contents and fructose concentrations were examined at 25 °C using a RheoStress RS75 rheometer (Gebrueder

Haake GmbH, Karlsruhe, Germany). The cylinder sensor system, Z40, was used, and the flow stress was measured as a function of shear rate from 1 to 300 s^{-1}, and back to 1 s^{-1}. All measurements were duplicated.

The adsorption of fructose on the particle surfaces was measured by pyrogenation and nuclear magnetic resonance (NMR) spectroscopy. In the pyrogenation method, aqueous suspensions of 30 vol.% alumina with 1, 3, 5, 7, 10, 15, and 20 wt.% fructose (based on alumina) were centrifuged at 10,000 rpm for one hour. Clear aliquots were carefully taken out of centrifuged suspensions. The concentration of fructose in each supernatant was measured by the pyrogenation method. The supernatants were heated up to 140 °C and held at this temperature for six hours to drive off the water, leaving molten fructose and a trace amount of alumina powders as residue. The residue was then heated up to 1100 °C to decompose the fructose completely, leaving unhydrous alumina behind. During each step, the samples were weighed. The mass difference between the two corresponds to fructose in the solution. The fructose adsorbed on the powder surface is calculated by subtracting the fructose in solution from the total fructose in the suspension.

Adsorption of fructose was also determined by NMR spectroscopy. Suspensions of 20 vol.% alumina in D_2O with 1, 3, 5, 7, 10, 15, 20, and 25 wt.% fructose were centrifuged at 4,500 rpm for two hours. One milliliter of supernatant was mixed with 0.06 mL of methanol. The solution was then scanned using VXR-300 NMR (Varian, Inc. Palo Alto, CA) in a 5 mm tube to determine the integrated peak intensity ratio of the $-CH_2$ groups of fructose to the $-CH_3$ group of methanol. The concentration of fructose in the supernatant was determined from a calibration plot obtained using known concentrations of fructose and methanol in D_2O. The amount of fructose adsorbed on the powder surface was determined by subtracting the fructose in the supernatant from the total fructose added to the suspension.

The fraction of chemically bound water was determined by a thermogravimetric analyzer (TGA). Alumina powders or suspensions were heated to 130 °C at a heating rate of 30 °C/min and held until the weight was stabilized. At the end of this step, it was assumed that the physically bound water was completely removed. Then the sample was heated to 800 °C at the same heating rate to drive off the chemically bound water. The mass difference between the two steps was attributed to chemically bound water.

Physically bound water in suspension was studied by sub-zero temperature differential scanning calorimetry (SZT-DSC), employing a commercial instrument (Pyris I, Perkin Elmer, Shelton, CT). Four drops of suspension with known solids content was placed in DSC pans and sealed. The sample was first cooled to –35 °C, and equilibrated at this temperature for five minutes. Then it was heated to 10 °C at a rate of 1 °C/min. The experiment was repeated for different solids content suspensions. Similar experiments were carried out at constant solid content of 30 vol.% but varying fructose concentrations. The plot of heat absorbed versus temperature indicates two melting events: one for bulk (or free) water, the other "bound" water. By comparing the relative integrated intensities of these peaks and known values of latent heat values, relative amounts of "free" and "bound" water were determined.

3. Results and Discussion

3.1. Rheology.

Figure 2 shows the viscosity of the suspension with and without fructose (18wt% by weight of alumina) as a function of solids content at a shear rate of 100 s^{-1}. At low solids loadings (i.e. up to 25 vol.%) the viscosity remains low for both cases. However, when the particle volume fraction reaches 28 vol.%, the viscosity of the suspension starts to increase. Above 30%, the rate of increase was much slower for the suspension with fructose than without. Above 35% solids content, the viscosity of the suspension without fructose rose very sharply, and it does not flow above 40%. The major change in the flow behavior of the suspension occurs between 28 and 32 % solids content, indicating onset of strong particle-particle interactions. The effect of fructose addition on the viscosity of 30 and 40 vol.% suspensions is shown in Figure 3. The results show that viscosity decreases steadily with the increase of fructose concentration up to 15 wt.%. It is clear from Figures 2 and 3 that the addition of fructose decreases the viscosity dramatically. Obviously, the addition of fructose to water alone was not responsible for the reduction in the suspension viscosity, as it is well known that the viscosity of an aqueous solution increases with fructose concentration.

In order to understand the cause of viscosity reduction with fructose addition, the collective interactions of water, fructose, and solid surfaces must be taken into account.

3.2. Fructose Adsorption on alumina surfaces.

Since complete separation of nanosize particles from the suspension poses a significant challenge, measuring fructose concentration in solution by UV-VIS spectroscopy was deemed inaccurate. Therefore, the fructose concentration in the supernatant was determined by pyrogenation and NMR spectroscopy.

The amount of fructose in the supernatant was calculated using the following expressions:

$$W_{H2O} = \frac{1-\phi}{\phi} \cdot \frac{W_{Al2O3}}{\rho_{Al2O3}} \cdot \rho_{H2O}$$

$$or \qquad (1)$$

$$W_{Al2O3} = \frac{\phi}{1-\phi} \cdot \frac{W_{H2O}}{\rho_{H2O}} \cdot \rho_{Al2O3}$$

where W_{H2O}, ρ_{H2O} and W_{Al2O3}, ρ_{Al2O3} are the weight and specific gravity of the water and alumina in the suspension respectively (ρ_{H2O} = 1 g/cm^3, and ρ_{Al2O3}=3.6 g/cm^3 for γ-alumina were used); ϕ is the solids volume fraction.

For ϕ = 0.30, the fructose concentration in the suspensions, C, is given by:

$$C = C_f \frac{W_{Al2O3}}{W_{H2O}} = 1.54 \cdot C_f \qquad (2)$$

where C_f is the fructose concentration based on dry alumina. Then the concentration of adsorbed fructose, C_a, is obtained by subtracting the concentration of fructose, C_m, in the supernatant from that of suspension, C:

$$C_a = C - C_m \qquad (3)$$

If one makes the assumption that the "effective" cross-section of the fructose molecule is simply square of its molecular length, l (~0.49 nm) [14], surface coverage of the alumina particles by fructose molecules can be calculated by:

$$N_f = \frac{\frac{C_a}{M_f} \cdot N_a \cdot \ell^2 (nm)^2}{154 \cdot 38 \cdot (10^9)^2 (nm)^2} = \frac{\frac{C_a}{180} \cdot 6.023 \cdot 10^{23} \cdot 0.49^2}{154 \cdot 38 \cdot (10^9)^2}$$

The results are shown in Table 1, and indicate that only a fraction of the surface was covered by fructose.

Adsorption of fructose was also determined by the NMR method. The integrated intensity ratio of $-CH_2$ of fructose to $-CH_3$ for known methanol additions in D_2O containing suspension was used for determining fructose concentration in the supernatant solution. The calibration line constructed using the known concentration of fructose and methanol in the D_2O solution. The results are shown in Table 2. Comparison of Table 2 and Table 1 shows that the agreement between the results obtained by the two independent techniques is remarkable, and confirms that only a fraction of fructose was adsorbed on the alumina surface. It is plausible that the "effective" cross-sectional area of the fructose is significantly higher than what we assumed here due to association of water with fructose, leading to only one-fourth of the surface being occupied by actual fructose molecules. The sorption of fructose based on NMR data is shown in Figure 4.

Table 1. Fructose adsorption on alumina surface as determined by pyrogenation.

C_f	C	C_m	C_a	(C_a/C)	N_f
1	1.54	1.08	0.46	0.30	0.06
3	4.63	3.33	1.30	0.28	0.18
5	7.71	6.23	1.48	0.19	0.20
7	10.8	9.22	1.58	0.15	0.22
10	15.43	13.55	1.88	0.12	0.26
15	23.14	21.14	2.00	0.09	0.27
20	30.86	28.94	1.92	0.06	0.26

C_f- fructose concentration in the suspension, (g/100g Al_2O3),
C, C_m, C_a -fructose concentration in the suspension, supernatant, and adsorbed on alumina surface (g/ 100 g water).
C_a/C-fraction of fructose adsorbed on the alumina particle surfaces
N_f-number of adsorbed layers of fructose on the alumina surface
A small amount of chemically bound water ($\approx 0.3 \times 0.01 = 0.003$g) was assumed to be negligible.

Table 2. Fructose adsorbed on nanometric alumina surface as determined by NMR.

C_f	C_a (g)	$C_{Al2O3,*}$ (g)	C_a/C	N_f
1	0.0033	0.8906	0.36	0.08
3	0.0051	0.9038	0.19	0.12
5	0.0065	0.8449	0.15	0.16
7	0.0088	0.8995	0.14	0.21
10	0.0098	0.8551	0.11	0.24
15	0.0100	0.8585	0.07	0.25
20	0.0096	0.7860	0.06	0.26
25	0.0093	0.7722	0.05	0.26

*C_{Al2O3} is the weight of alumina in 20 vol.% suspension

3.3. Chemically bound water

Chemically bound water was measured for both dried and wet powders by TGA. The majority of chemically bound water was evolved between 150°C and 530°C. The total amount of chemically bound water was estimated to be 1.1%, based on the dry weight of alumina. If the cross section of a water molecule, A_{H2O}, is taken as 10.8 $^{\prime 2}$ [15], and the specific surface area of nanometric alumina powders, S_{Al2O3}, as 38 m^2/g, the amount of chemically bound water (1.1 wt.%), corresponds to one monolayer of coverage. This is in good agreement with fully hydroxylated alumina surface, as expected for nanometric powders.

3.4. Physically bound water

The hydroxyl groups on the oxide particle surfaces interact with the water molecules near the surfaces through hydrogen bonds, which localize the water molecules on the particle surface. Hence, the bound water is expected to freeze at a lower temperature than the bulk water does (& vice versa). The integrated intensity of the melting peaks is indicative of the relative amounts of bound and free water. Kodama and Aoki [16] estimated the number of bound water layers from DSC melting data. They showed that the fraction of the interlamellar/bound water vary with the total water content. A maximum amount of bound water was observed when the water content exceeded 22 wt% corresponding to six bound water molecules per lipid molecule.

Figure 5 shows the DSC plot of aqueous suspensions of various solid volume fractions of nanometric alumina particles. The DSC curves indicate two distinct peaks. The smaller peak (peak1) starts at about –10 to -7 °C, and is completed below 0 °C corresponding to "bound" water. The larger peak (peak2) starts at 0 °C, corresponding to melting of free/bulk water. The ratio of peak1 to peak2 area increases with the solids volume content.

Relative amounts of free and "bound" water can be estimated if the heat of fusion for the bound water is known. The DSC plot for 60 vol.% solids indicates that practically all the water in the suspension is bound, i.e. there is no measurable bulk water peak (see Figure. 6). The area under the peak1, A_1 was used to determine an average heat of fusion for the physically bound water, ΔH_{Bound} :

$$W_{Total} = W_{Free} + W_{bound} = \frac{A_1}{\Delta H_{bound}} + \frac{A_2}{\Delta H_{Free}}$$

or for $W_{Free} \approx 0$ for 60 vol.% solids:

$$\Delta H_{Bound} = \frac{A_1}{W_{bound}} \approx \frac{A_1}{W_{H2O}^{total}}$$

For this particular test with 4.39 mg water and measured peak area of 754 mJ, the heat of fusion for bound water was determined to be 172 J/g, which is approximately half that of bulk water.

Using this value, the fraction of bound water was calculated for each suspension and summarized in Table 3. The weight of total water content in suspensions, W_{H2O}^{total} is given by

$$W_{H2O}^{total} = \frac{W_S}{\left(1 + \frac{\phi}{1-\phi} \cdot \frac{\rho_{Al2O3}}{\rho_{H2O}}\right)} \qquad (4)$$

where W_S is the weight of suspension. The results indicate that the bound water fraction increases more or less linearly with the solids content, approaching a limiting value of 99% at 60% solids content. These findings are in agreement with the rheological measurements.

Table 3 also shows that the sum of bound and free water differs from the total water by less than 7.5%, in many cases less than a few percent, providing an independent check on the method employed.

Table 3. Determination of Bound water content of the suspensions by SZT-DSC.

ϕ (%)	W_S (mg)	W_{H2O}^{total} (mg)	W_f (mg)	W_b (mg)	W_f+W_b (mg)	W_b/W_{H2O}^{total} (%)	Δ* (%)	n	L (nm)
5	21.1	17.7	17.4	0.5	17.9	2.9	1.1	11	3.2
25	27.5	12.5	8.3	4.1	12.4	32.7	0.8	19	5.5
30	23.5	9.2	5.6	4.0	9.7	43.7	4.8	20	5.8
32	28.8	10.7	6.2	5.2	11.5	49.1	7.3	20	5.8
35	30.7	10.4	5.5	5.7	11.2	54.3	6.7	19	5.5
40	25.8	7.6	2.9	4.7	7.6	62.5	0.4	18	5.2
50	39.4	8.6	2.7	6.2	8.9	72.1	3.6	14	4.1
60	28.1	4.4	0.01	4.35	4.36	99.0	0.9	13	3.8

* $\Delta = \left|W_{H2O}^{total} - (W_f + W_b)\right| / W_{H2O}^{total} * 100\%$ L = thickness of bound layer

Using the bound water content, W_b, the specific surface area of the nanometric alumina particles, S_{Al2O3}, the thickness of water mono-layer, t = 0.29 nm [17] and taking into consideration the increase in effective surface area due to adsorbed water layers, the number of adsorbed water layers, n, was estimated by the following equations:

$$\frac{W_b}{W_{Al2O3} \cdot S_{Al2O3} \cdot \rho_{H2O} \cdot t} = \sum_{m=0}^{n-1}\left[1+\frac{mt}{R}\right]^2 \tag{6}$$

$$W_{Al2O3} = \frac{W_S}{\left(1+\frac{1-\phi}{\phi}\cdot\frac{\rho_{H2O}}{\rho_{Al2O3}}\right)} \tag{7}$$

where, W_{Al2O3} is the weight of alumina; S_{Al2O3} is the specific surface area of alumina as measured by BET method (37.94 m^2/g.). Results are shown in Table 3. It shows that the number of bound water layers on the particle surface is quite large, meaning the surface forces extend a long distance from the particle surface. For the 30 vol.% aqueous suspension, it reaches to 20 layers corresponding to a bound layer thickness of 5.8 nm. The number of adsorbed layers goes through a maximum around a 32 vol.% suspension above which bound layers will overlap due to confined space between the particles.

Of these bound layers, the first couple of water layers may have reacted with the surface to form a hydroxylated surface and releasing protons into the suspension. This is consistent with the observed decrease of water pH to 4.8 with the addition of nanometric alumina

particles to form the suspension. Takei [18] suggested that physisorbed water molecules were localized on the silica surfaces because of strong interactions with the surface hydroxyl groups. The structure of second and subsequent layers was affected by the configuration and orientation of the first adsorbed layer. The effect of surface on the adsorbed layers decreases gradually with the thickness of the adsorbed layer. It was claimed that the structure of water was affected up to at least 4 nm from the solid surface. Considering the thickness of water molecule (t = 0.29 nm [17, 19]), the solid surface influences 11-14 layers of water in silica pores. Etzler and Fagundus [20] also reported that water is structurally modified up to 3-5 nm from the solid surface in silica pores. These long scales of adsorbed solvent (water) layer will play a significant role in determining the rheology of dense aqueous suspensions containing nano particles.

One of the unique features of nano-sized particles is the fact that a large fraction of the atoms is at the surface. These particles are more reactive than the powders used in typical ceramic processing operations (e.g. micron-sized particles). In colloidal suspensions, the ratio of the total surface area of particles, A, to the volume of the suspension, V, can be expressed as:

$$\frac{A}{V} = \frac{3\phi}{R} \tag{8}$$

where, R is the radius of the particle. As the above expression clearly indicates, the interfacial area for a constant volume of suspension increases with the solid volume fraction and decrease with particle radius.

Influence of water adsorption on rheology of suspensions is two-fold. First, it restricts the mobility of water molecules and reduces the fraction of free water contributing to the flow. Secondly, the overlap of the bound water layers lead to dipole interaction between particles, hence increased resistance to flow.

For the same solid volume fraction, the distance between adjacent particle surfaces is shorter in nanometric suspensions compared to large-particle slurries.

If the spherical particles were packed uniformly and randomly, and the surface separation between two neighbor particles, 2a can be related to the solid volume fraction, ϕ,:

$$2a = 2R\left(\sqrt[3]{\frac{0.64}{\phi}} - 1\right) \tag{9}$$

where, the value of 0.64 is the maximum packing fraction of the volume for the random dense packing of monosize particles having a radius of R [21].

For 30 vol.% suspension of nanosized particles with a radius of 20 nm, the surface separation between two adjacent particles is calculated to be 11.5 nm, compared to 115 nm for the same volume fraction sub-micron size (R=200 nm) particles. Therefore, for a nanoparticle (R = 20 nm) suspension, adsorbed/bound layers will overlap at 2a< 5.75 nm. The overlapped "adsorbed layer" associated with the particles will affect the mobility of the particles relative to each other, and hence increase the viscosity of the suspension. On the other hand, for the suspension of the same solid volume fraction (30 vol.%) containing micron-sized particles (say, R = 200 nm), the surface separation of adjacent particles is much larger than the range of the bound-layer thickness.

In the treatment of colloidal suspensions of micron sized particles, the influence of the adsorbed layers on the flow characteristics of the suspension is considered negligible, but when the particle size approaches nanoscale, the role of adsorbed layers become quite significant.

The analysis of the SZT-DSC measurements indicated that as much as 20 layers of water (~5.8 nm) were affected by the particle surface forces. Simple calculation shows that at 30 vol.% solids, the bound water layers would overlap leading to an increase in the viscosity of the suspension. Indeed, the viscosity increased as the solids content reaches 28 vol.% (see Fig. 1). Therefore, it is plausible to assume that the overlap of the bound water layers was responsible from the observed viscosity increase.

3.5 Effective particle volume fraction and critical thickness.

Since a fraction of the water and/or solute molecules are bound to the particle surface, one might introduce "*effective particle radius*" and "*effective particle volume fraction*" in order to describe the rheological properties of suspensions more accurately. Figure 8 is a schematic representation of particles having a bound layer around them. When dealing with

the flow properties of an aqueous suspension, a "*hydrodynamic radius*", (R + *l*), should be considered, where R is the particle radius and *l* is the thickness of the bound layer. For a spherical particle, the effective particle radius is taken as the same as its hydrodynamic radius, (R + *l*). The effective particle volume fraction is then calculated using effective particle radius.

The effective particle volume fraction, ϕ_{eff}, for spherical particles is then given by,

$$\phi_{eff} = \phi \times (1 + l/R)^3 \qquad (10)$$

where ϕ is the solid particle volume fraction.

Figure 9 shows variation of the effective particle volume fraction as a function of thickness of adsorbed layers for a nanosized particle (R=20 nm) for several solid particle volume fraction. For a suspension of any particle volume fraction, the effective volume fraction increases with the thickness of bound layers. Thus, for any given solids loading, the effective particle volume fraction is calculated as a function of bound layer thickness. Conversely, the critical bound layer thickness can be calculated using equation (10). Assuming random packing of equal-spherical particles and setting the maximum packing factor at 0.64 for the random dense packing [21], the critical bound layer thickness can be calculated for any given solids loading. For example, for 30 vol.% solids loading, the critical thickness is 5.75 nm. As discussed before, this value corresponds to about 20 monolayers of water molecules. Therefore, for 30 vol.% solids loading, if the number of adsorbed water layers is greater than 20, the bound water layers will overlap.

3.6 Effect of fructose in reducing the viscosity.

SZT-DSC measurements were performed on the aqueous suspension of nanometric alumina particles with various concentrations of fructose in order to determine the effect of fructose addition on the bound water content of the suspensions.

Figure 10 shows the results for the 30 vol.% suspensions at several fructose concentrations. It is clear that the area under peak1 decreases with fructose concentration indicating that the bound water content is decreased with fructose addition.

One plausible mechanism by which fructose decreased the viscosity of the nanometric alumina suspensions is that fructose might adsorb on the surface displacing water molecules. It also conceivable that fructose molecules might have disturbed the long range ordering of water molecules that are adsorbed on the surface, thus making water molecules more "mobile". As mentioned earlier, the adsorbed layers are formed through layer-by-layer hydrogen bonds extending from the particle surface. D-fructose has both hydrophilic and hydrophobic sites. When added to the suspension, there is a competition for hydrophilic sites of fructose between water molecules and alumina particles. The competition disturbs the hydrogen bonds between water layers, which weakens the interaction between the solid surface and water molecules.

The fraction of bulk and bound water may be estimated from Figure 10, provided that the heat of fusion for peak1, ΔH_{peak1}, and the heat of fusion for peak2, ΔH_{peak2}, are known. In Figure 10, the first peak corresponds to the melting of "bound-ice," and the second peak occurs at a higher temperature, corresponding to melting of "bulk-ice," which is only perturbed by fructose molecules. Since the peak2 for the suspension without fructose occurs at 0 °C, (i.e., it does not shift by the presence of nanometric alumina particles), ΔH_{peak2} should be taken as the fusion heat of fructose solution, that is $\Delta H_{peak2} = \Delta H_{fs}$, which can be measured by DSC. Generally, the heat of fusion of the fructose solution, ΔH_{fs}, changes with the concentration of fructose in the solution. Figure 11 shows DSC plots of fructose solutions at several fructose concentrations. The heat of fusion for different fructose concentrations was measured and calculated, and is given in Table 4.

Table 5 summarizes the amount of bound water as a function of fructose concentration for a 30 vol.% alumina suspension. The table shows that as the concentration of fructose increased, the fraction of the bound water decreased. The decrease in bound water content with fructose addition follows a similar trend observed for the viscosity decrease with fructose concentration (see Fig. 2).

Various experimental techniques point to a common observation that water molecules in nanometric particle suspensions are strongly bound to the surface and the surface forces extend long distances from the surface influencing the rheological properties of the suspensions. This effect is more pronounced at high solids contents. Addition of fructose

apparently either displaces the bound water molecules from the surface or disturbs the interaction of particles with water molecules causing a significant reduction in the viscosity.

Table 4. Variation of heat of fusion for water with fructose concentration.

C_f (g/ 100 g H_2O)	ΔH_f (J/g)
0	334
1	313
3	304
5	289
7	276
15	260
22	243
28	230

Table 5. Reduction in bound water by fructose addition for 30 vol.% suspension.

C_f' (1) (wt.%)	W_f (2) (mg)	W_b (3) (%)	W_{br} (%)
0	5.6	43.7	0.0
1	6.4	36.2	7.3
3	6.8	31.5	19.5
5	6.7	26.1	33.3
7	7.1	19.0	51.5
10	7.1	18.2	53.5
15	8.2	7.4	81.1

(1) C_f' is fructose concentration in the suspension, expressed as g fructose/100 g alumina powders.
(2) W_f is the bulk water content calculated from the area of the peak2 in the DSC curves.
(3) W_b is the bound water content expressed as % of total
(4) W_{br} is % of bound water reduced by fructose addition

4. Conclusions

The role of fructose addition on rheological behavior of nanometric alumina suspensions was investigated. Differential scanning calorimetry and thermogravimentry experiments showed that there were three types of water in nanometric suspensions: bulk (free) water, physically bound water, and chemically bound water. Bound water plays a major role in suspension viscosity. At high solids contents (ϕ > 30 vol.%), the number of bound water layers approached 20. At this level, bound water layers overlap, resulting in a dramatic increase in the viscosity of the nanometric alumina suspensions. A new term "effective particle volume" was defined, which takes into account adsorbed layers in determining the volume fraction of solids. Effective particle volume fraction was shown to better explain the observed flow behavior of the suspensions. The addition of fructose reduced the viscosity significantly, and is believed to either release some of the bound water from the nanometric alumina surfaces or alter the nature of the interaction between solid surface and water molecules, resulting in a significant reduction in viscosity. Further investigation in other nanometric powder suspensions is needed to establish the universality of the findings and the proposed mechanism offered in this work.

Acknowledgment

Ames Laboratory is operated for the U.S. Department of Energy by Iowa State University under Contract No. W-7405-ENG-82. This research was supported by the Office of Basic Energy Science, Materials Science Division. The authors also wish to thank C. Schilling, Andrew Thom, M. Kramer, K. Schmidt-Rohr, P. Tomasik, M. Sikora, and B. Mavis for valuable assistance and discussions.

References

1. M. N. Rittner, "Market analysis of nanostructured materials," *American Ceramic Society Bulletin*, 81 (3), 33-36 (2002).

2. C. Crabb, and G. Parkinson, "The nanosphere: A brave new world," *Chemical Engineering*, 109 (2), 27, 29-31, (2002)

3. T. Abraham, "Advanced ceramic powder and nano-sized ceramic powder: an industry and market overview," *Ceramic Trasactions* 62, 3-13, (1996).

4. I Roy, T. Y. Ohulchanskyy, H. E. Pudavar, E. J. Bergey, A. R. Oseroff, J. Morgan, T. J. Dougherty, and P. N. Prasad, "Ceramic-based nanoparticles entrapping water-insoluble photosensitizing anticancer drugs: a novel drug-carrier system for photodynamic therapy," *Journal of American Chemistry Society*, 125, 7860-7865, (2003).

5. J. F. Brady, "The rheological behavior of concentrated colloidal dispersions," *J. Chem. Phys.* 99, 567-581 (1993).

6. J. C. van der Werff and C. G. de Kruif, "The scaling of rheological properties with particle size, volume fraction and shear rate," *J. Rheol.* 33(3), 421-454 (1989).

7. I. M. Krieger and T. J. Dougherty, "Amechanism for non-newtonian flow in suspensions of rigid spheres," *Trans. Soc. Rheol.* 3, 137-152 (1959).

8. M. Mooney, "The viscosity of a concentrated suspension of spherical particles," *J. Colloid Sci.*, 6, 162-170 (1951).
9. C. F. Forster, "The rheological and physico-chemical characteristics of sewage sludges," *Emzyme and Microbial Technology*, 30 (3), 340-345, (2002).

10. C. F. Forster, "Bound water in sewage sludges and its relationship to sludge surfaces and sludge viscosities," *Journal of Chemical Technology and Biotechnology*, 33B, 76-84 (1983).

11. N. Katsiris and A. Kouzeli-Katsiri, "Bound water content of biological sludges in relation to filtration and dewatering," *Water Res.* 21: 1319-27, (1987).

12. C. H. Schilling, M. Sikora, P. Tomasik, C. Li, and V. Garcia, "Rheology of alumina-nanoparticle suspensions: effects of lower saccharides and sugar alcohols," *Journal of the European Ceramic Society* (2002), 22(6), 917-921.

13. P. Tomasik, "Thermolysis of Carbohydrates in Oxygen-free Aumosphere," *Starch* 39(3), 94-97 (1987).

14. H. J. M. Bowen, J. Donohue, O. Kennard, and D. H. Whiffen, "Tables of Interatomic Distances and configuration in Molecules and Ions," The Chemical Society Burlington House, W.1, London, (1958).

15. T. Morimoto, M. Nago, and F. Tokuda, "Relation between the amounts of chemisorbed and physisorbed water on metal oxides," *J. Phys. Chem.* 73(1), 243-8, (1969).

16. M. Kodama and H. Aoki, "Water behavior in phospholipid bi-layer systems," Surfactant Science Series Volume 93, Thermal Behavior of Dispersed Systems, edited by Nissim Garti, 247-294, (2001).

17. S.J. Gregg and K. S. W. Sing, "Adsorption, surface area and porosity," Academic Press, New York, pp 157-158, (1967).

18. T. Takei, K. Mukasa, M. Kofuji, M. Fuji, T. Watanabe, M. Chikazawa, and T. Kanazawa, "Changes in density and surface tension of water in silica pores," *Colloid Polym. Sci.* 278: 475-480 (2000).

19. J. Hagymassy Jr., S. Brunauer, and R. S. Mikhail, "Pore structure analysis by water vapor adsorption: I. t-curves for water vapor," *J. Colloid Interface Sci.* 29: 485-491, (1969).

20. F. M. Etzler and D. M. Fagundus, "The extent of vicinal water. Implications from the density of water in silica pores," *J. Colloid Interface Sci.* 115: 513-519, (1987).

21. D. I. Lee, "Packing of spheres and its effect on the viscosity of suspensions," *J. Paint Technol.,* 42(550), 579-587 (1970).

FIGURE CAPTIONS:

Figure 1. TEM image of nanometric alumina particles

Figure 2. Viscosity of the suspension of various alumina volume fractions with and without fructose additive

Figure 3. Variation of viscosity with fructose concentration

Figure 4. Adsorption of fructose on nanometric alumina as a function of fructose concentration in the suspension

Figure 5. SZT-DSC data showing melting of ice for the aqueous suspensions of nanometric alumina particles at various solids contents.

Figure 6. SZT-DSC plot for 60 vol.% aqueous suspension of the nanometric alumina particles. Note that bulk (free) water peak almost disappeared.

Figure 7. Plot of bound water fraction as a function of alumina solids content.

Figure 8. Schematic representation of "effective particles packing" in suspension by taking adsorbed layer thickness into consideration.

Figure 9. Variation of "effective volume fraction" at several solids content levels (for nanometric particles with R=20 nm)

Figure 10. SZT-DSC plots for 30 vol.% nanometric alumina suspensions at various fructose concentrations

Figure 11. SZT-DSC plots for melting of water in fructose solution at various fructose concentrations.

Figure 1.

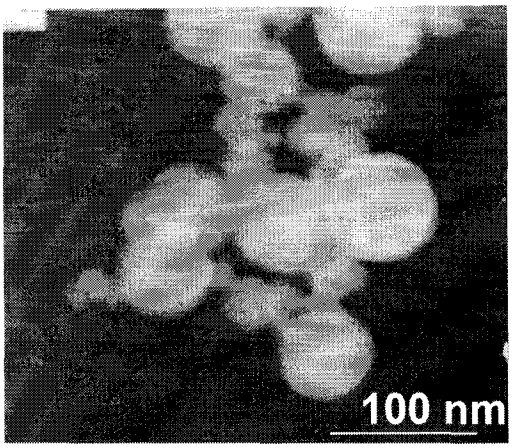

Figure 2.

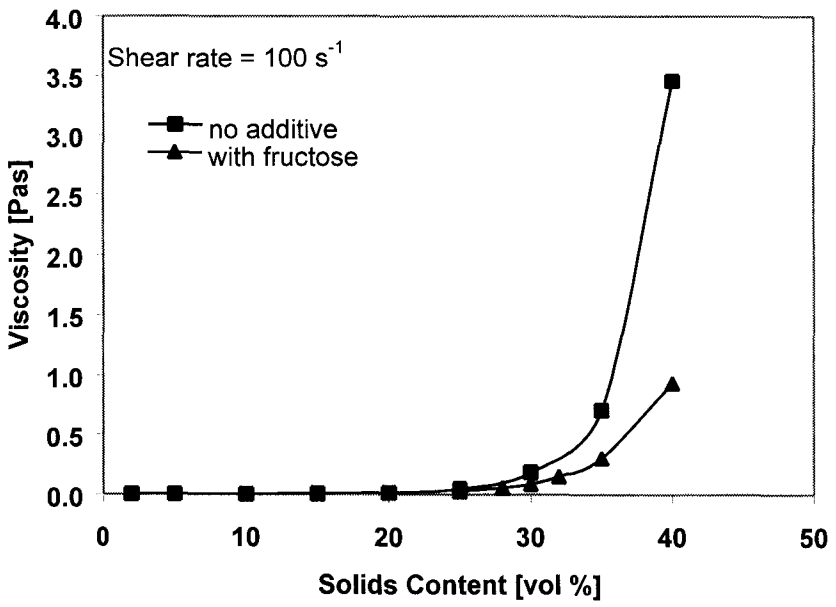

Figure 3.

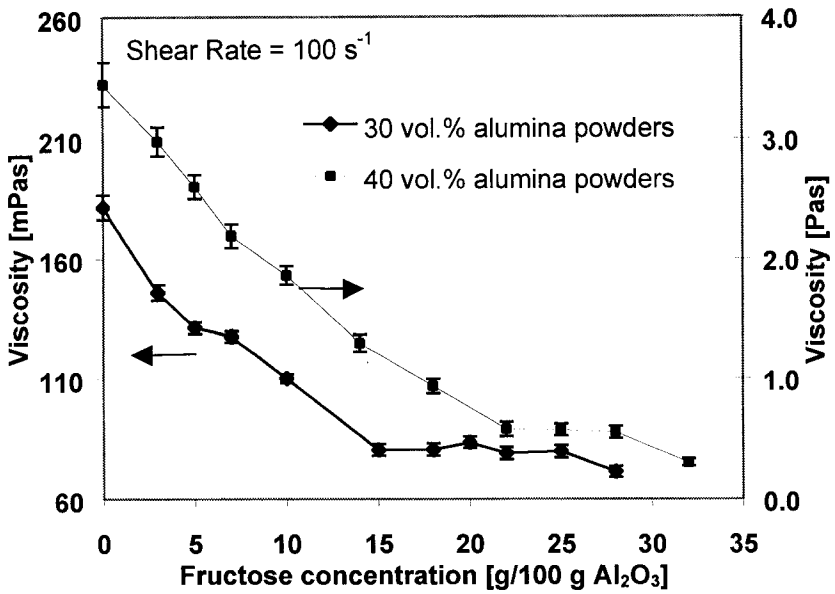

Figure 4.

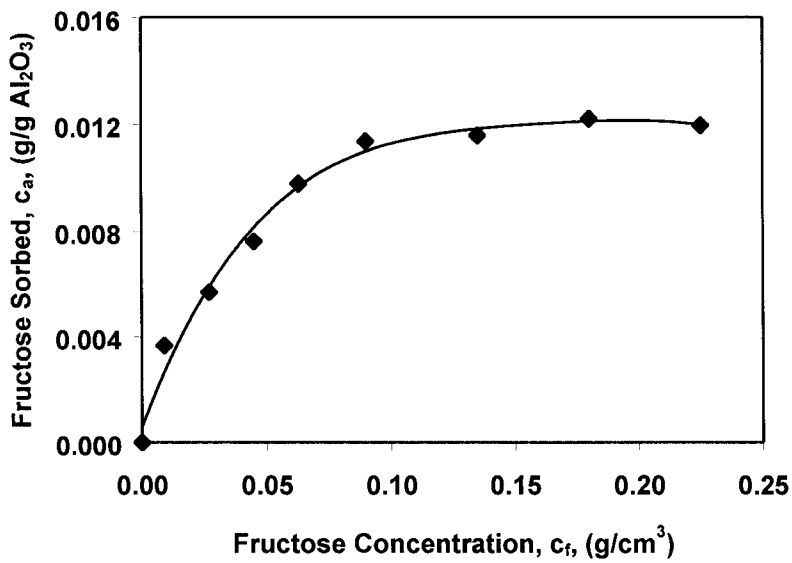

Figure 5.

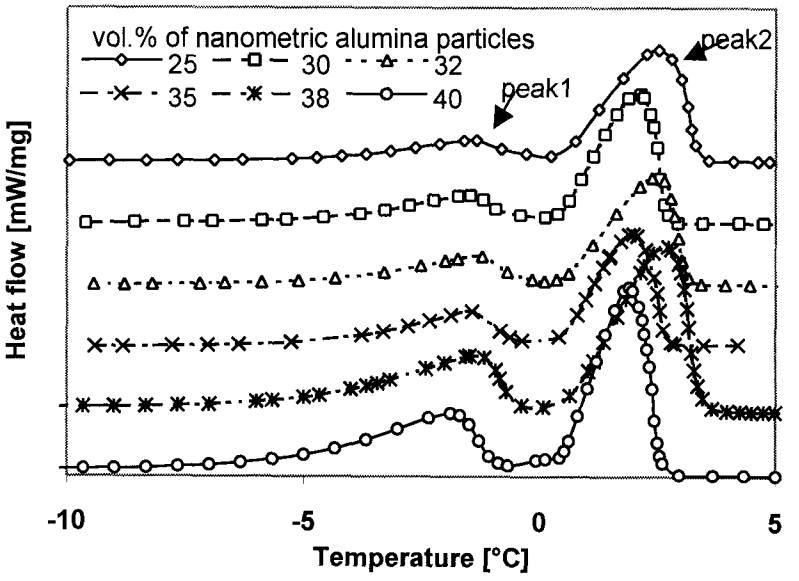

Figure 6.

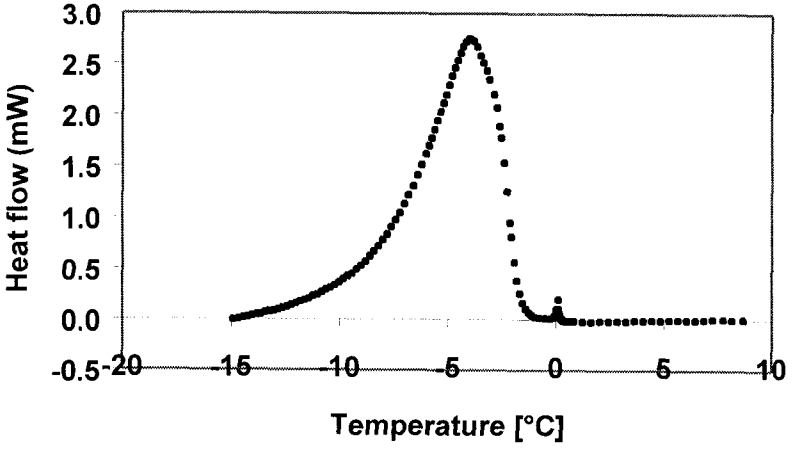

Figure 7.

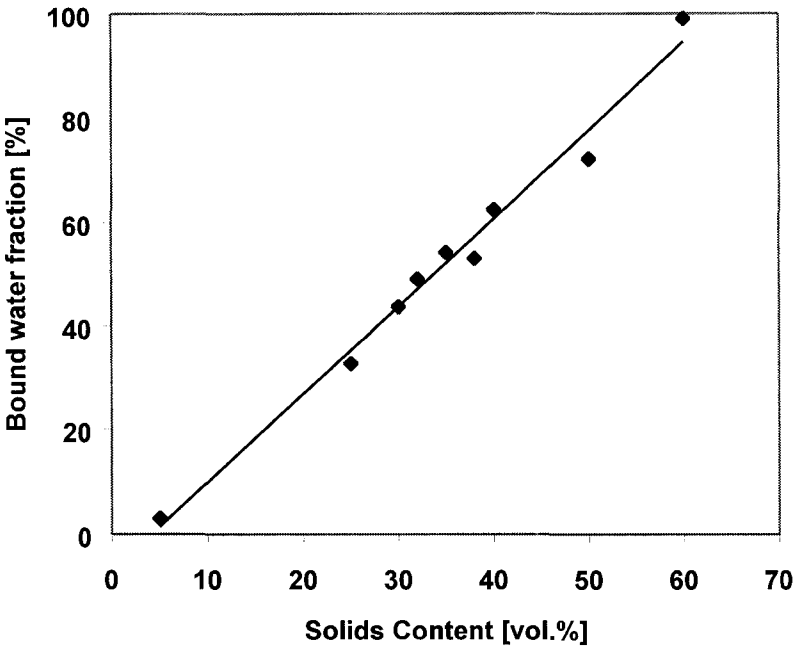

Figure 8.

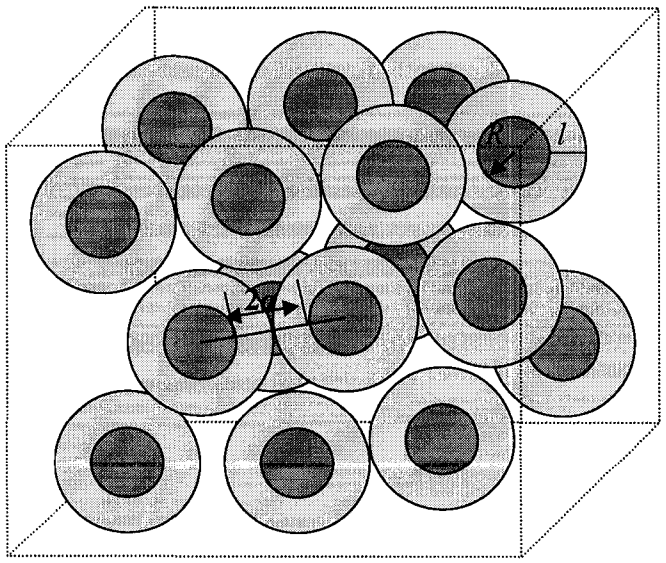

Figure 9.

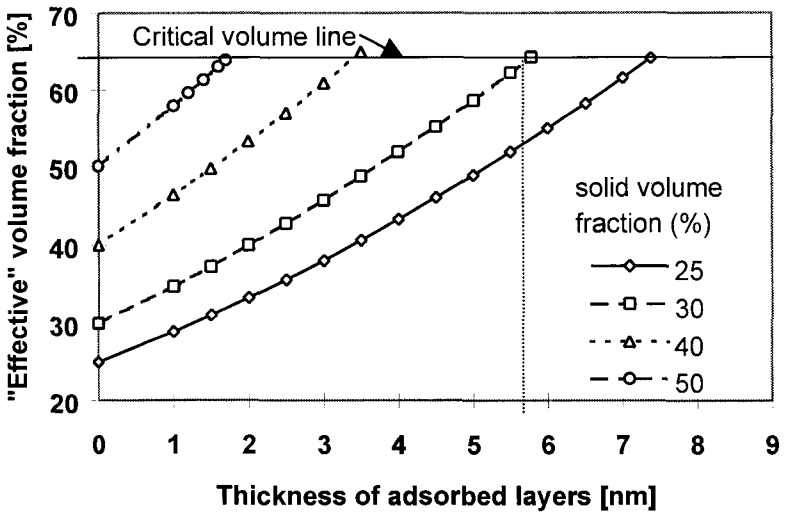

Figure 10

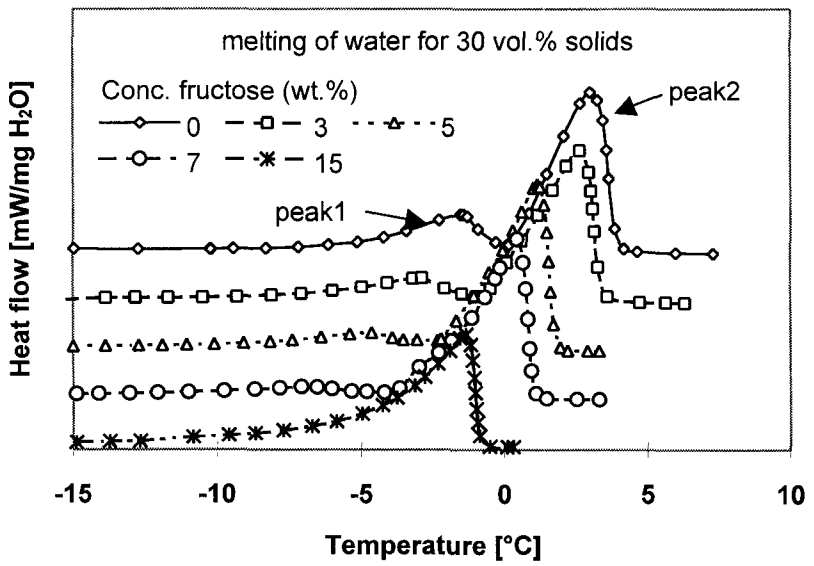

Figure 11.

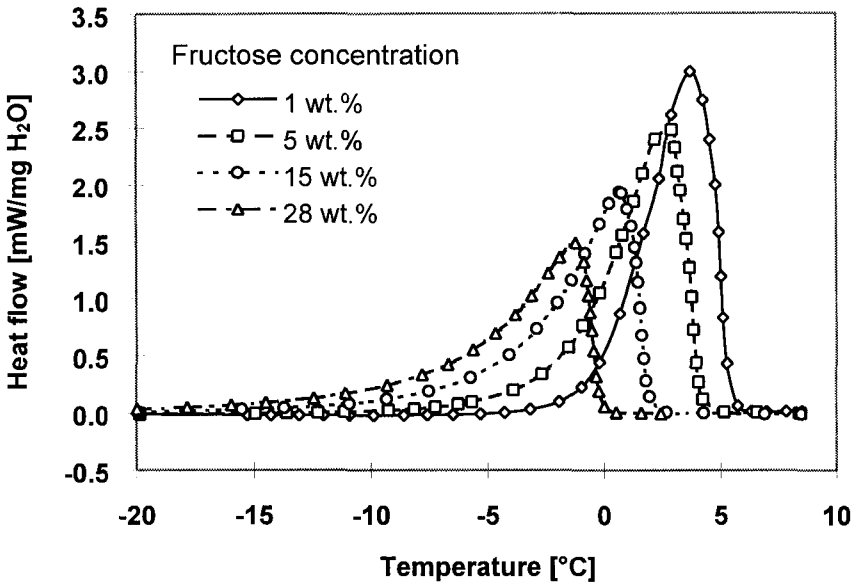
Fructose concentration
1 wt.%
5 wt.%
15 wt.%
28 wt.%
Heat flow [mW/mg H2O]
Temperature [°C]
3.5
3.0
2.5
2.0
1.5
1.0
0.5
0.0
-0.5
-20
-15
-10
-5
0
5
10

Chapter 3:
Relationship between Water Mobility and Viscosity of Nanometric Alumina Suspensions

(To be Submitted to the Journal of the American Ceramic Society, 2004.)

Chuanping Li[a], Jerzy Wiench[b], Christopher H. Schilling[c], Marek Pruski[b], Mufit Akinc[a]

[a] Ames Laboratory* and Department of Materials Science and Engineering,

[b] Ames Laboratory

Iowa State University, Ames, IA 50011, USA

[c] Saginaw Valley State University, University Park, Michigan 48710

Abstract

The addition of fructose has been shown to reduce the viscosity of aqueous suspensions of nanometric alumina powders. Highly concentrated and flowable aqueous nanometric alumina suspensions were achieved. Oxygen-17 nuclear magnetic resonance (NMR) spectroscopy was used to investigate the relaxation time and the molecular mobility of water in the suspensions with and without fructose. The results were related to rheological behavior of the suspensions. The study shows that there are fractions of bound water layers with lower molecule mobility and the viscosity decrease upon adding fructose is due to the increase of molecule mobility of water in the suspension.

1. Introduction

High solids loading in particle suspensions is desirable in forming ceramic components since it reduces the shrinkage during drying and firing, increases the wet and dry strength of the as cast components, and produces a superior green microstructure with good homogeneity and few defects. Unfortunately, the green density is often limited by the low concentration of solids needed to maintain acceptable flow properties during shape forming,

especially for the suspension containing nanoparticles. Flowability of the suspension expressed by low viscosity is necessary in order to achieve the highest possible concentration and uniformity of suspension. Moreover, dense, uniform and crack-free bulk or film ceramic components can be produced by this kind of suspensions.

The rheological measurements [1] showed that the aqueous nanometric alumina suspension system has an extraordinarily high viscosity in comparison with the aqueous micrometric alumina suspension. The rheological characteristics of the aqueous nanometric alumina suspension is primarily determined by a strong interaction between the particles and the aqueous solution used as vehicle. It was also shown that small amount of saccharides with low molecular weight, such as sucrose and fructose is very effective in reducing the viscosity of aqueous suspensions of nanometric alumina particles. The present research employs NMR spectroscopy as a probe to determine the mobility of water molecules in suspensions of various particle concentrations of Al_2O_3 nanoparticles with or without fructose and correlates this information with the flow properties of the suspensions.

Water, as a vehicle in aqueous suspension, therefore, plays a very important role on the viscosity of the aqueous suspension. Recent work in our lab [2] showed that the behavior of water in close proximity of particles distinctly differs from that of bulk water as manifested itself by lower melting temperature for a wide range of solids content in nanometric alumina suspensions. These two states of water in the suspension should have different contributions to the rheological properties of the suspension. Free water molecules have higher mobility than bound water molecules. Higher the fraction of the water is 'free', the lower viscosity of the suspension is expected to be. Although the difference between the physical characteristics of 'bound' and 'free' water has been established indirectly by means of melting characteristics of 'frozen' suspensions [2], a direct evidence that the mobility of water molecules changes by the presence of nano-particles is necessary to unequivocally relate the role that bound water plays in altering the viscosity of aqueous nanometric powder suspensions. Furthermore, if one can demonstrate the water mobility changes by the addition of mono-saccharides (i.e. fructose), a better understanding for the role of saccharide addition on the rheological behavior of nanometric powder suspensions may be gained. Nuclear magnetic resonance (NMR) spectroscopy has become an increasingly important tool in

probing the chemical and physical characteristics of various materials and processes. Differences in relaxation behavior of water in nanometric powder suspensions may be investigated by NMR spectroscopy.

Proton, deuteron, and oxygen-17 NMR of water has been applied to the study the interaction of water with glass, [3, 4, 5] clay, [6, 7] protein, [8] hydrated alumina, [9, 10] and silica, [11]. A marked decrease in the longitudinal and transverse relaxation times, T_1 and T_2, as well as an increase in the T_1/T_2 ratio were observed compared to the values for 'bulk' water. The results were interpreted in terms of layers of water molecules with restricted mobility in the vicinity of an interface. Water molecules are dynamically exchanged between an environment in which they relax slowly (free water) and one in which they relax rapidly (bound water). Under conditions of rapid exchange on the NMR time scale, a single relaxation rate is observed and is the weighted average of the individual rate for each environment [12]. Accordingly, the signal is broader for a higher ratio of bound- to bulk-water. When the exchange of molecules between sites corresponding to different resonances is slow on the NMR time scale, multiple peaks can be observed. [13]

Somasundaran and Turro [14] investigated zeolite-water systems with particle sizes varying by a factor of 10. They found that the proton NMR peak ratio of the bound water to bulk water increases with decreasing particle size, indicating a greater fraction of bound water for smaller particles. They also investigated the hydrophilic alumina particles, and found that the bound water peak decreases markedly with an increase in temperature.

Compared to proton and deuteron magnetic relaxation, ^{17}O relaxation has the major advantage that exchange processes between solvent and solute are generally slow, so that the relaxation processes of the different species can be separated; in contrast, proton or deuteron relaxation studies always have to contend with the problem of exchange between solvent and solute. [15] In addition, ^{17}O nuclear magnetic relaxation is unaffected by either cross-relaxation or chemical exchange and provides, a more direct means for probing hydration. [16] Therefore, we used ^{17}O nuclear magnetic relaxation to measure the mobility of water molecules in the aqueous suspensions of various solid loading of nanometric alumina particles with and without presence of D-fructose. The purpose of this work is to employ nuclear magnetic resonance (NMR) spectroscopy to study relaxation characteristics of water

in nanometric alumina suspensions with or without fructose additive, and thereby obtain information on binding state of water molecules and its relation with viscosity of the suspensions.

2. Experimental

2.1. Materials

γ-alumina powders with an average particle size of 40 nm, were purchased from Nanophase Technologies Corporation (Burr Ridge, Illinois). Specific surface area of powders was measured to be 37.94 m^2g^{-1}. Chemical analysis of the powder was provided by the manufacturer and given in Table 1. The specific gravity of the nanometric alumina particles is 3.6 g/m^3. SEM micrograph of the as-received powders is shown in Figure 1. The particles are spherical in shape with particle size ranging from 10 to 100 nm.

Table 1. Elemental analysis of nanometric alumina used in this study

Element	Conc. (ppm wt.)	Element	Conc. (ppm wt.)	Element	Conc. (ppm wt.)	Element	Conc. (ppm wt.)
B	7	Zn	2	Mg	15	Si	14
P	2	S	3.5	Ce	2	Y	2.3
W	<5	Nb	<10	Cr	2.5	Fe	7
Note: Alumina is 99.99%; All the others are less than 1 ppm.							

D-fructose was obtained from Sigma Corporation (St. Louis, Missouri). Formula: $C_6H_{12}O_6$. Formula weight: 180.2. Elemental analysis of the fructose was given in Table 2. ^{17}O enriched water (40.2 atom % ^{17}O, and 7.4 atom % ^{18}O), was purchased from ISOTEC, Inc. (Miamisburg, Ohio).

Table 2. Elemental analysis of the D-fructose (supplied by manufacturer)

Element	Conc. (ppm wt.)	Element	Conc. (ppm wt.)	Element	Conc. (ppm wt.)
Ammonia content	<500	Aluminum	<5	Magnesium	<5
Residue on ignition	<1000	Calcium	<5	Phosphorus	<5
Chloride	<500	Copper	<5	Sodium	<50
Sulfate	<500	Iron	<5	Zinc	<5
Insoluble matter	<1000	Lead	<10	Potassium	<50

2.2. Methods

Rheology:

Two series of alumina aqueous suspensions with and without fructose additive were prepared in deionized water. For each series, the solids contents of the suspensions were: 25, 28, 30, 32, 35, and 40 vol. %. The concentration of fructose was kept constant at 18 wt.% (based on the alumina powder, g/100g Al_2O_3). So, a 1000 ml, 35 vol% nanometric alumina suspension with fructose was prepared by mixing: 650 g H_2O, 1260 g alumina, and 226 g fructose.

Suspensions were sealed in plastic bottles and shaken for 72 hours at room temperature. Rheological properties were measured at room temperature by the use of RheoStress RS75 rheometer (Gebrueder Haake GmbH, Karlsruhe, Germany). The cylinder sensor system, Z40, was used, and the suspensions were subjected to increasing shear rate from 1 to 300 s^{-1}, and then decreasing from 300 to 1 s^{-1}. Each experiment was run in duplicate for reproducibility.

Relaxation/mobility Measurements

Two sets of suspensions with and without fructose additive with the solids content of 25, 28, 32, 35, 38, and 40 vol. %, using 1 atom % ^{17}O enriched water as the vehicle were prepared. The suspensions were sealed in NMR tubes and shaken for 72 hours at room temperature before measurement.

Oxygen-17 relaxation rates were measured for each of the suspensions at two frequencies: (i) at 27.1 MHz on Bruker AC 200 spectrometer (Bruker Instruments, Inc., Billerica, MA, USA), (ii) at 54.2 MHz on Varian VXR 400 or Chemagnetics spectrometer. The longitudinal relaxation time was measured by inversion recovery [17] (π-τ-$\pi/2$ pulse sequences; τ was varied from 30 μs to 30 ms with 11 data points. The 90° pulse width was determined separately for each spectrometer, 11 μs for AC200 and 22.3 μs for VXR400). The transverse relaxation time was obtained from the full width at half maximum (FWHM) of absorption ($\Delta\nu_{obsd}$) data according to $T_{2,\,obsd} = 1/(\pi\Delta\nu_{obsd})$.

3. Results and discussion

3.1. Rheological behavior

Figure 2 shows the variation of viscosity of suspensions with the solids content with and without fructose. The viscosity of the suspension without fructose increases dramatically with the solid volume fraction. As seen in the figure, highly concentrated suspensions (above 35 vol.% solids) are very viscous and as a consequence – does not easily flow. For the suspensions containing fructose, however, the increase in viscosity with solids content is much slower. Particularly, the difference between the viscosities of suspensions with and without fructose is much more pronounced at solids contents above 30 vol. %. Apparently, addition of fructose to the nanometric alumina suspension plays a profound role in reducing the viscosity of the suspensions, especially at high solids loadings. Suspensions containing even as much as 40 vol.% solids results in suspensions which can be poured.

Saccharides are recognized with their adsorbing properties onto the oxide surfaces in aqueous media [18]. This adsorption could occur by the hydrogen bonding between hydroxyl groups of the oxide surface and hydroxyl groups of the saccharide. Adsorption mechanism can be presented in two steps as described by Jucker et al [19]. In the first step, the fructose form hydrogen bonds with water molecules physisorbed on oxide surface. In the second step, the water molecules are displaced and the hydroxyl groups on the oxide surface are involved in the hydrogen bonding with fructose. Similar claims were made by Jones and Hockey [20] on sugar adsorption on titania surface.

Variation of the viscosities of fructose solutions at shear rate of 20 s^{-1} are shown in Figure 3. As expected, viscosity of fructose solution increases with the concentration of fructose in the solution, a clear demonstration of the fact that the addition of fructose alone does not bring about the reduction in viscosity of aqueous alumina suspensions. In order to understand the mechanism of viscosity reduction in nanometric alumina suspensions by fructose addition, interaction between alumina powder surface and fructose and water need to be elucidated. Changes brought up in the mobility of water molecules by fructose addition to the suspensions may shed light into the mechanism of viscosity reduction by fructose addition.

3.2. Water mobility

3.2.1. Water relaxation time in fructose aqueous solution

The relaxation of water interacting with solute molecules differs from that in the pure state. Water molecules interact with the solute via hydrogen bonds and/or electrostatic forces through their high dipole moments. At room temperature the correlation time, τ, of rotational and translational motion of water which is on the order of 10^{-11} to 10^{-12} s in pure state may increase to 10^{-8} or even 10^{-6} s in the hydration layer of macromolecules [21] giving rise to a drastic reduction in T_1 and T_2 relaxation times.

^{17}O relaxation measurements were carried out on water molecules in aqueous solutions containing fructose as solute. Variation of relaxation time with fructose concentration is shown in Figure 3. The longitudinal relaxation time, T_1, of water molecules in the solutions decreases with fructose concentration, indicating that more water molecules associate with fructose molecules via hydrogen bonds as the concentration increases. Consequently, the mobility of water decreases with fructose addition. Qualitatively, relaxation time and viscosity change with fructose concentration correlate well for aqueous fructose solution in the concentration range studied.

3.2.2. Water relaxation time in nanometric alumina suspensions

Ruan et al [22] in their study of water-starch interaction found that the nature of water molecules in this system can be considered in several categories according to their mobility. Using the curve-fitting model, three types of water were identified, free, partially free, and bound, each of which identified with a distinct relaxation time constant. Earlier, Chinachoti [23] showed that the presence of sucrose has a profound effect on the interaction of starch with water. The author mixed water with starch granules and the resultant blend was not fluid. Upon the addition of sucrose, however, the suspension became fluid. NMR results [24] showed that water mobility increased dramatically upon the addition of a small amount of sucrose. Since both starch granules and alumina particles are solids with very little solubility in water at room temperature, and their surfaces are hydroxylated, we assume similar behavior in aqueous suspensions. Starch granule consists of glucose mers with hydroxyl groups surrounding its ring. All these free hydroxyl groups can be involved in water adsorption. A similar behavior is expected in alumina particles, especially in nanometric alumina particles. Sucrose and fructose have strong affinity to water molecules and are highly soluble in water.

Figure 4 demonstrates the effect of fructose on the flow characteristics of nanometric alumina paste simply but elegantly. In this demonstration starch was replaced with nanometric alumina powder and sucrose with fructose. Water was added to nanometric alumina powder at 38 vol. % solids resulting a moist, viscous blend that was intractable. Upon an addition of fructose, however, the mixture became fluid. Apparently, before adding fructose, water was immobilized on the alumina particles surfaces. Addition of fructose appears to 'free' the water molecules from the 'bound' state which reduces the viscosity of the suspension to a level that it becomes fluid.

^{17}O NMR spectroscopy was employed to provide dynamic information about water interaction with Al_2O_3 surface. The results were shown in Figure 5. The plot of relaxation time as a function of solids content indicates that: (i) both longitudinal and transverse relaxation times, T_1 and T_2, decrease with the volume fraction of alumina particles with or without fructose, which indicates that more fraction of water interacts with particle surfaces or stronger the interactions while solid volume fraction increases as expected; (ii) T_1 and T_2 are higher for suspension without fructose than with fructose for the same solid volume

fraction, implying that more fraction of water interacts with either particle surfaces or fructose molecules. Figure 3 shows clearly that fructose influences the relaxation of water molecules. In the alumina particle suspension with fructose, both alumina particle surfaces and fructose molecules have influence on the relaxation of water molecules, which made the T_1 and T_2 values short compared with those of the suspension without fructose. The combination influences of particle surfaces and fructose on the relaxation of water molecules are complex. Short relaxation time in the suspension with fructose does mean the low mobility of water in the suspension with fructose. The mobility of water is determined by correlation time for ^{17}O of the water molecules. A suitable mode was used to calculate the correlation time for ^{17}O of the water molecules in the suspensions with and without fructose in the following section. In general, the addition of fructose in water decrease water mobility by creating fructose-bound water, which is liquid-like, [25] and therefore the mobility of this kind of water does not decrease much. However, the oxide surface-bound water is solid-like, and the mobility of this kind of water is significantly lower than the 'free' water.

3.2.3. Mobility of water in the aqueous suspension of nanometric alumina particles with and without fructose additive

Water mobility was determined by correlation time, τ_c, of the water in the suspension based on relaxation time of water. Higher water mobility is reflected by shorter correlation time which is associated with molecular motion. The simplest possible expressions for the relaxation time/relaxation rates that are compatible with these observations and with basic relaxation theory [17] are

$$R_1(\omega_0) = \frac{1}{T_1(\omega_0)} = \alpha + \beta\left(\frac{0.2}{1+(\omega_0\tau_c)^2} + \frac{0.8}{1+(2\omega_0\tau_c)^2}\right)$$
$$R_2(\omega_0) = \frac{1}{T_2(\omega_0)} = \alpha + \beta\left(0.3 + \frac{0.5}{1+(\omega_0\tau_c)^2} + \frac{0.2}{1+(2\omega_0\tau_c)^2}\right) \quad (1)$$

α and β are the parameters in terms of a two-state exchange model with two states ('free' and 'bound' water). For fast exchange regime, when $\omega^2 \cdot \tau_c^2 << 1$ (τ_c in ps range), the terms in brackets are reduced to one, and R_1 (or T_1) equals R_2 (or T_2). An example of this case is the presence of free water, which has τ_c of 3.3 ps (for ^{17}O NMR).

Water in the suspension is considered as free and bound, based on its mobility. Overall relaxation rate (R_1 or R_2) is then a sum of the weighted average of each contributed species. Therefore the following equations [26] can be written for alumina suspensions.

$$R_1 = P_f \cdot R_{1,f} + P_b \cdot R_{1,b}$$
$$R_2 = P_f \cdot R_{2,f} + P_b \cdot R_{2,b} \quad (2),$$

where P_f and P_b are the fractions of free and bound water in the sample respectively;

$R_{1,f} = R_{2,f} = A \cdot \left(1 + \frac{\eta^2}{3}\right) \cdot \tau_{c,f}$ is relaxation rate of free water;

$R_{1,b} = A \cdot S^2 \cdot \tau_C \cdot \left[\frac{0.2}{1 + \omega^2 {\tau_C}^2} + \frac{0.8}{1 + 4\omega^2 {\tau_C}^2}\right]$ is a spin-lattice (longitude) relaxation rate of bound water;

$R_{2,b} = A \cdot S^2 \cdot \tau_c \cdot \left[0.3 + \frac{0.5}{1 + \omega^2 {\tau_c}^2} + \frac{0.2}{1 + 4\omega^2 {\tau_c}^2}\right]$ is a spin-spin (transverse) relaxation rate of bound water; τ_c is the correlation time for the motion of bound water; $A = \frac{9}{125} \cdot \pi^2 \cdot C_Q^2$, ($C_Q$ is ^{17}O quadrupolar coupling constant (value of 6.67 MHz is used [27, 28])), η is asymmetry parameter (value of 0.93 is used), and S is the order parameter that describes the anisotropic orientation of water molecules in the vicinity of the alumina surface.

Relaxation rates of free water are equal ($R_{1,f}(\omega_1) = R_{2,f}(\omega_1) = R_{1,f}(\omega_2) = R_{2,f}(\omega_2)$) even if measured at different magnetic field of 400 MHz (VXR-400) or 200 MHz (Bruker Spectrometer, AC200). Therefore it is possible to calculate τ_c from the equation shown below, which was derived from equations 1 and 2:

$$\frac{R_1(\omega_2) - R_1(\omega_1)}{R_2(\omega_1) - R_1(\omega_1)} = \frac{\frac{0.2}{1+\omega_2^2\tau_c^2} + \frac{0.8}{1+4\omega_2^2\tau_c^2} - \frac{0.2}{1+\omega_1^2\tau_c^2} - \frac{0.8}{1+4\omega_1^2\tau_c^2}}{0.3 + \frac{0.3}{1+\omega_1^2\tau_c^2} - \frac{0.6}{1+4\omega_1^2\tau_c^2}}$$
$$= \frac{2(\omega_1^2 - \omega_2^2)[17 + 32\omega_1^2\omega_2^2\tau_c^4 + 20(\omega_1^2 + \omega_2^2)\tau_c^2]}{3\omega_1^2(7 + 4\omega_1^2\tau_c^2)(1 + \omega_2^2\tau_c^2)(1 + 4\omega_2^2\tau_c^2)} \quad (3)$$

The relaxation times and relaxation rates were recorded by two different spectrometers: VXR400 (T_1^V, R_1^V, T_2^V, R_2^V), and Bruker AC200 (T_1^B, R_1^B), operating at 54.2 and 27.1 MHz for ^{17}O, respectively. The data is given in Table 3.

Theoretically, the fraction of bound water, P_b, can be calculated from the following equation:

$$R_2(\omega_1) - R_1(\omega_1) = P_b \cdot A \cdot S^2 \cdot \tau_c \cdot (0.3 + \frac{0.3}{1+\omega_1^2\tau_c^2} - \frac{0.6}{1+4\omega_1^2\tau_c^2}) \quad (4)$$

However, the order parameter, S, is unknown. Previous work employed S=0.02-0.06 for water on the colloidal silica surface [27, 28], and S=0.12-0.15 for water molecules in the vicinity of the protein surface [16, 26]. There is not an accepted value for S which can be used for describing the water molecules on the nanometric alumina particle surface, and moreover, the order parameter of water in the alumina-water-fructose system is even more difficult to assign, due to the complexity of the interactions between water with alumina particle surfaces and fructose molecules.

Table 3. ^{17}O relaxation rates of nanometric alumina suspensions with and without addition of fructose

Solid volume fraction, %	Al_2O_3 suspensions			Al_2O_3-Fructose suspensions		
	R_1^{V*}	R_2^V	R_1^{B**}	R_1^V	R_2^V	R_1^B
25	238	368	254	322	586	353
28	244	376	256	353	701	394
32	251	415	260	398	727	437
35	256	462	265	467	834	500
38	259	470	268	481	1001	521
40	270	513	280	493	1038	532

* V stands for VXR400 spectroscopy; ** B stands for Bruker AC200 spectroscopy.

By the use of data from Table 3, τ_c was calculated based on the equations (3) [16, 26]. The results of these calculations are shown in Table 4 and Figure 6.

Table 4. Correlation times τ_C calculated for aqueous Al_2O_3 and Al_2O_3-Fructose suspensions

Solid volume fraction, %	Al_2O_3 suspensions	Al_2O_3-Fructose suspensions
	τ_C [ns]	τ_C [ns]
25	15.8	15.9
28	19.3	16.3
32	23.5	16.2
35	26.8	18.7
38	28	20.3
40	29	21.2

From Table 4 and Figure 6, one can see a trend that correlation time increase with the solid volume fraction for the suspensions with and without fructose, indicating that with the increase solid volume fraction the water mobility goes down. However, correlation data (shown in Table 4) suggest that water molecules are more mobile when fructose is added, since the τ_c values of the suspensions with fructose are smaller than those of the suspensions without fructose correspondingly. Calculated τ_C values are practically same for the 25 vol.% suspensions with and without fructose, since the viscosity values for the 25 vol.% suspensions with and without fructose were also very similar. For this relatively dilute colloidal suspensions (25 vol.%), the influence of fructose on the relaxation of water is considered significant compared with that of alumina particles. Furthermore, correlation time for suspension with fructose remain more of less constant up to 32 vol.%, perhaps concentration of fructose high enough to decrease the viscosity and hence the correlation time to a level that the solids content does not change the mobility of the water for these cases.

3.2.4. Change of relaxation time of water during drying

In drying process, water molecules evaporate continuously and ratio of alumina to water (W_{Al2O3}/W_{H2O}) increases. If there were only one type of water molecules in the suspension,

the relaxation time of water molecules should remain constant with drying process independent of the W_{Al2O3}/W_{H2O} value.

The change of relaxation behavior of 25 vol.% alumina suspension during drying was monitored over 20 h at 50 °C. Both T_1 and T_2 times decreased with drying time (see Figure 7). The value of (R_2-R_1) which is proportional to $(P_b \cdot \tau_c)$ (cf. equation 4, and $\omega_1^2\tau_c^2 >> 1$) increases during drying. These results, as anticipated, indicate the presence of bound water molecules (strongly interacting with nanoparticle surfaces), and the water mobility decreases upon drying—due to increased fraction of bound water as the drying progresses. The value of (R_2-R_1) shown in Figure 7 changes slowly at the beginning of the drying process. At this period, P_b increased, but the correlation time (τ_c) is still short. Therefore, the product of $(P_b \cdot \tau_c)$ increases only slightly. However at later stages of drying, i.e. 8 to 16 hours, the value increased dramatically. In this period, both P_b and τ_c increased resulting sharp increase in (R_2-R_1) value. When the drying process approaches dry condition i.e., $P_b \rightarrow 1$, almost all water molecules were bound, resulting in an asymptotic value for the (R_2-R_1). The same trend of relaxation rate response was observed for the corn starch-water system when concentration of starch changes from 0-35 g starch/mole H_2O [29].

4. Conclusions

Addition of fructose dramatically reduces the viscosity of aqueous alumina nanoparticle suspensions. Rheology and NMR relaxation measurements indicated that the viscosity decrease is not a consequence of reduced interparticle solution viscosity.

Water mobility influences rheological properties of aqueous alumina suspensions, and ^{17}O NMR relaxation measurement is a suitable method in determining the mobility of water molecules in the aqueous suspensions. The overall relaxation time, T_1 and T_2, decrease with solid volume fraction. The present study showed that bound water layers are associated with lower molecule mobility. The overall mobility of the bound water decreases with the solid volume fraction. Calculated correlation time τ_c increases from 15.8 ns to 29.0 ns for 25, and 40 vol.% alumina suspension respectively. Upon adding 18 wt.% fructose in 40 vol.% alumina suspension, the correlation time τ_c was determined to be 21.2 ns. The results of correlation time suggest that the reduction of the suspension viscosity upon the addition of

fructose is a result of enhancing water mobility of bound water by fructose, since the correlation time is shorter for the suspension with fructose.

Acknowledgement

Ames Laboratory is operated for the U.S. Department of Energy by Iowa State University under contract number W-7405-ENG-82. This research was supported by the Office of Basic Energy Science, Materials Science Division. The authors also wish to thank M. Sikora, P. Tomasik, K. Schmidt-Rohr, B. Mavis, Andrew Thom, and M. Kramer for valuable assistance and discussions.

References

1. C. H. Schilling, M. Sikora, P. Tomasik, C. Li, V. Garcia, "Rheology of alumina-nanoparticle suspensions: effects of lower saccharides and sugar alcohols" *Journal of the European Ceramic Society*, **22**(6), 917-921, 2002.

2. C. Li and M. Akinc, "Role of Bound Water on the Viscosity of Nanometric Alumina Suspensions," submitted to *Journal of the American Ceramic Society*, 2004.

3. J. A. Glasel, K. H. Lee, "Interpretation of water nuclear magnetic resonance relaxation times in heterogeneous systems," *Journal of the American Chemical Society*. **96**(4), 970-978, 1974.

4. B. M. Fung, T. W. McGaughy, "Magnetic relaxation in heterogeneous systems," *Journal of Magnetic Resonance*, **43**(2), 316-323. 1981.

5. Y. Hirama, T. Takahashi, M. Hino, T. Sato, "Studies of water adsorbed in porous Vycor glass" *Journal of Colloid and Interface Science*, **184**(2), 349-359. 1996.

6. D. E. Woessner, "A NMR investigation into the range of the surface effect on the rotation of water molecules," *Journal of Magnetic Resonance*, **39**(2), 297-308. 1980.

7. A. Delville, M. Letellier, "Structure and dynamics of simple liquids in heterogeneous condition: An NMR study of the clay-water interface," *Langmuir*, **11**(4), 1361-1367, 1995.

8. S. H. Koenig, R. G. Bryant, K. Hallenga, G. S. Jacob, "Magnetic cross-relaxation among protons in protein solutions," *Biochemistry*, **17**(20), 4348-4358, 1978.

9. R. M. Pearson, "Wide-line nuclear magnetic resonance studies on transition aluminas: Distribution of protons between surface and bulk phases," *Journal of Catalysis*, **23**(3), 388-394, 1971.

10. B. R. Baker, R. M. Pearson, "Water content of pseudoboehmite: New model for its structure," *Journal of Catalysis*, **33**(2), 265-278, 1974.

11. F. Hanus, P. Gillis, "Relaxation of water adsorbed on the surface of silica powder," *Journal of Magnetic Resonance*, **59**(3), 437-445, 1984.

12. J. R. Zimmerman, W. E. Brittin, "Nuclear-magnetic-resonance studies in multiple-phase systems: lifetime of a water molecule in an adsorbing phase on silica gel," *Journal of Physical Chemistry*, 61, 1328-1333, 1957.

13. J. Clifford, B. A. Pethica, *Hydrogen-Bonded Solvent Systems*; Taylor & Francis: London, 1968; P 169.

14. A. F. P. Somasundaran, and N. J. Turro, "proton nuclear magnetic resonance study of water in flocs," *Langmuir*, 15, 4922-4926, 1999.

15. B. Halle, T. Andersson, S. Forsen, and B. Lindman, "Protein Hydration from water Oxygen-17 magnetic relaxation," *Journal of American Chemical Society*, 103, 500-508, 1981.

16. L. T. Kakalis and I. C. Baianu, "Oxygen-17 and deuterium nuclear magnetic relaxation studies of lysozyme hydration in solution: Field dispersion, concentration, pH/pD, and protein activity dependences," *Archives of Biochemistry and Biophysics*, **267**(2), 829-841, 1988.

17. A. Abragam, *The Principles of Nuclear Magnetism*, Clarendon Press, Oxford, 1961.

18. M. V. Cheshire, *Nature and Origin of Carbohydrates in Soils*, Academic Press, New York, 122-124, 1979.

19. B.A. Jucker, H. Harms, S.J. Hug, A.J.B. Zehnder, "Adsorption of bacterial polysaccharides on mineral oxides is mediated by hydrogen bonds," *Colloids and Surfaces B, Biointerfaces,* 9, 331-343, 1997.

20. P. Jones, J.A. Hockey, "Infrared studies of rutile surfaces," *Trans. Faraday Soc.* **67**(9), 2669-2678, 1971.

21. B. M. Fung, "Proton and deuteron relaxation of muscle water over wide range of resonance frequencies," *Biophys. J.* 18, 235-239, 1977.

22. R. Ruan, P. L. Chen, *Water in Foods and Biological Materials - A Nuclear Magnetic Resonance Approach*, Western Hemisphere, Technomic Publishing Company, Inc., 200-210, 1998.

23. P. Chinachoti, "Water mobility and its relation to functionality of sucrose - Containing food systems," *Food Technology,* **47**, 134-140, 1993.

24. P. Chinachoti and T.R. Stengle, "Water mobility in starch/sucrose systems: an oxygen-17 NMR study," *Journal of Food Science*, **55**(6), 1732-1734, 1990.

25. R. Khan, D. Stehli, L. Wei, and M. P. Steinberg, "Activity and mobility of water in sweetened whole soy concentrates and their rheological properties," *Journal of Food Science*, **54**(4), 931-935, 1989.]

26. L. T. Kakalis, I. C. Baianu, and T. F. Kumosinski, "Oxygen-17 and proton nuclear magnetic relaxation measurements of soy protein hydration and protein-protein interactions in solution," *J. Agric. Food Chem.* , 38, 639-647, 1990

27. B. Halle, T. Andersson, S. Forsen, and B. Lindman, "Protein hydration from water oxygen-17 magnetic relaxation," *J. Am. Chem. Soc.* **103**(3), 500-508, 1981.

28. L. Piculell, "Water spin relaxation in colloidal systems: Part 1.—17O and 2H relaxation in dispersions of colloidal silica," *J. Chem. Soc., Faraday Trans. 1*, 82, 387-399, 1986.

29. S. J. Richardson, M. P. Steinberg, R. E. De Vor and J. W. Sutherland, "Characterization of the oxygen-17 nuclear magnetic resonance water mobility response surface," *Journal of Food Science*, **52**(1), 189-193, 1987.

FIGURE CAPTIONS

Figure 1 SEM micrograph of the nanometric alumina particles

Figure 2 Effect of fructose addition on viscosity of alumina suspensions as a functionj of volume fraction of solids.

Figure 3 Change in viscosity and relaxation time for water with fructose concentration.

Figure 4 Dramatic effect of fructose addition on the flowability of nanometric alumina suspension. (a) 38 vol.% alumina suspension; (b) 38 vol.% alumina suspension with 18 wt.% fructose.

Figure 5 Variation of relaxation time with solid volume fractions with and without fructose.

Figure 6 Variation of correlation time, τ_C, as a function of solid volume fraction with and without fructose.

Figure 7 Variation of relaxation times T_1, T_2 and $(R_2\text{-}R_1)$ as a function of drying time for 25 vol.% nanometric alumina suspension.

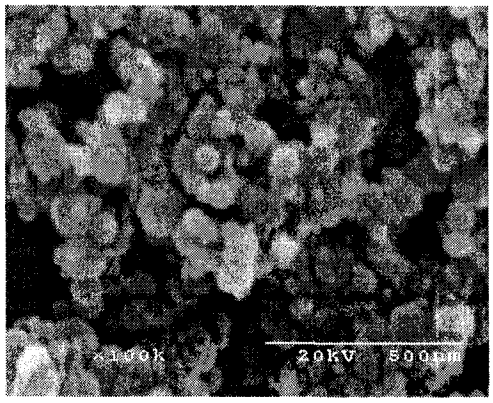

Figure 1

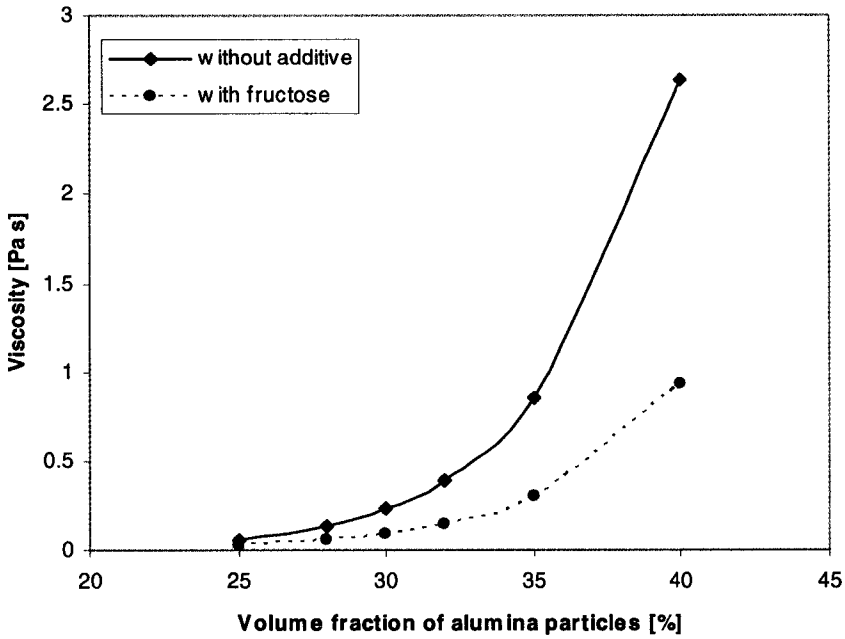

Figure 2

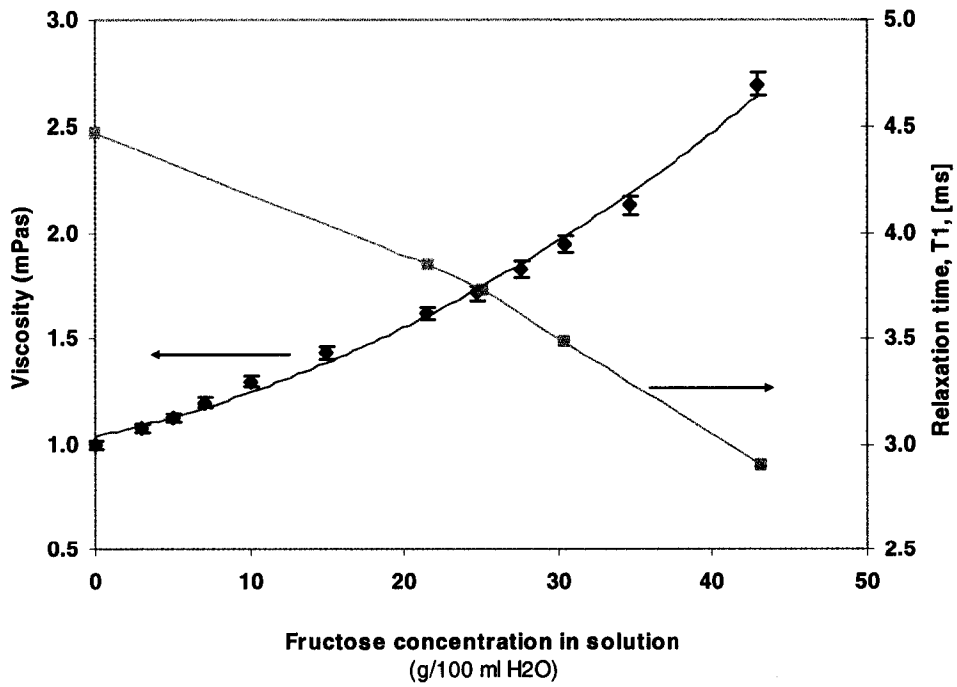

Figure 3

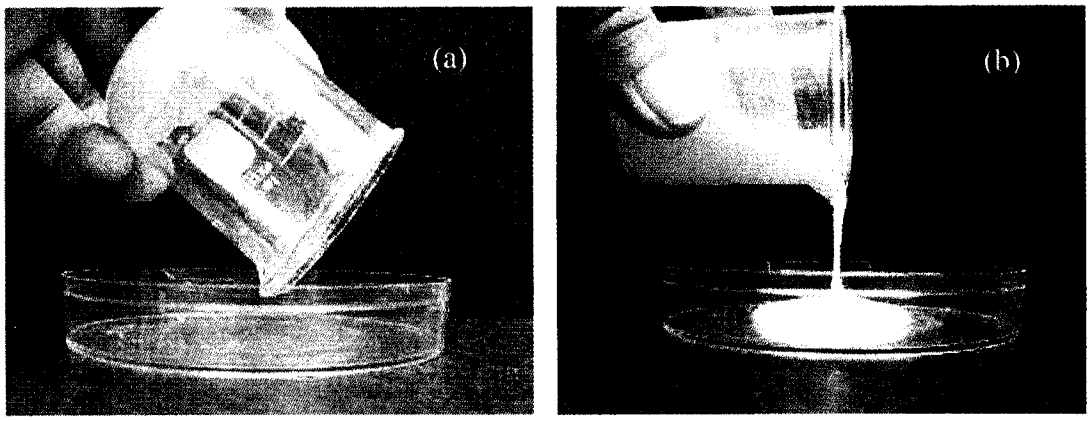

Figure 4

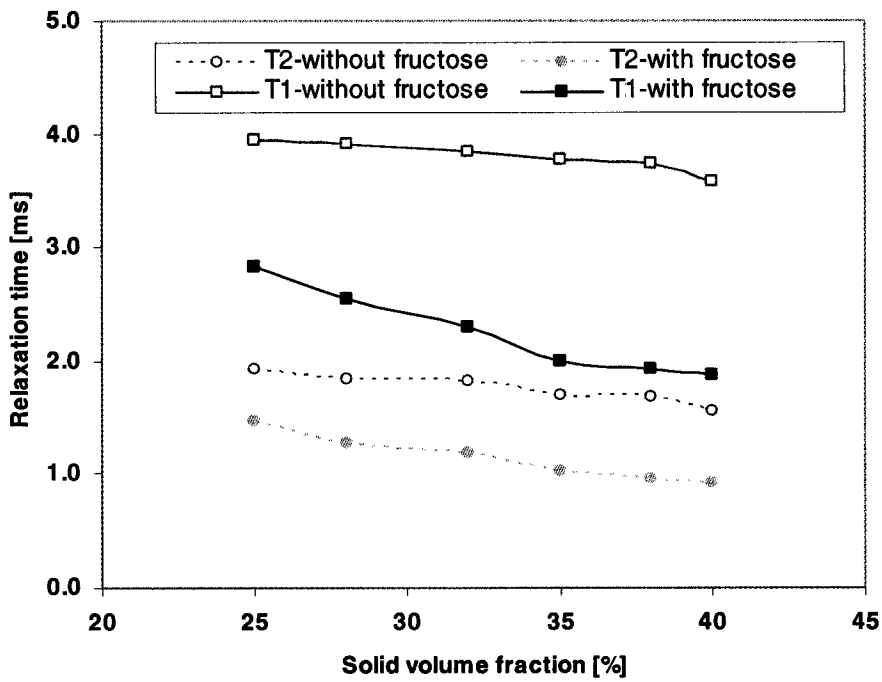

Figure 5

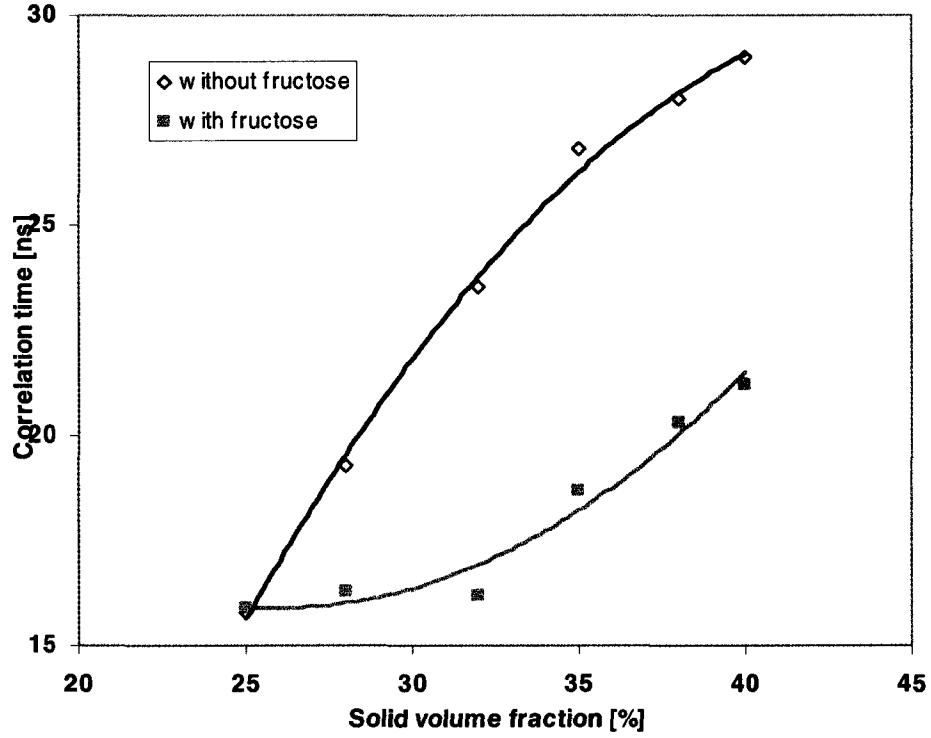

Figure 6

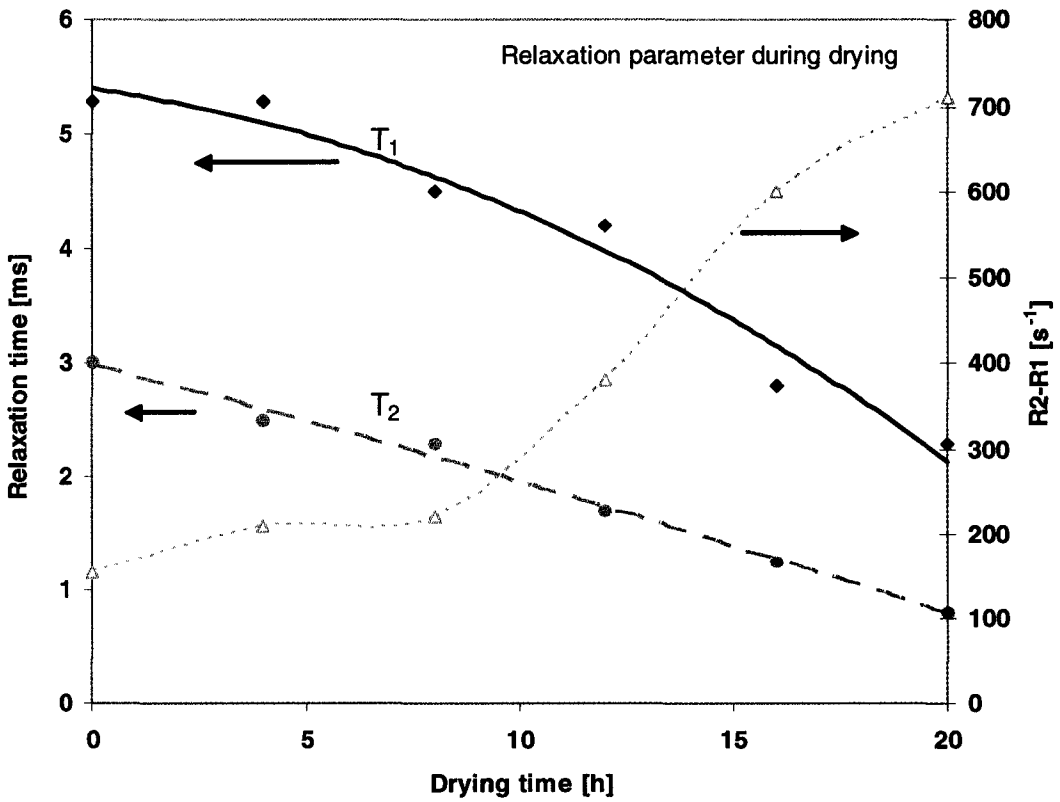

Figure 7

Chapter 4:

Interactions between Nanometric Alumina Particles in Fructose Aqueous Solutions

(A paper to be submitted)

Chuanping Li, James W. Anderegg, Mufit Akinc

Materials Science and Engineering, Ames Laboratory, Iowa State University

Ames, IA 50011

Abstract

Atomic force microscopy (AFM) was employed to measure the surface forces between a sharp alumina tip with a radius of 100 nm and a nanometric alumina particle (40 nm in diameter) in aqueous D-fructose solutions. In pure water, a repulsive force was observed at large separations (>9 nm) becoming attractive as tip approaches particle (< 3 nm). The results predicted by Derjaguin-Landau-Verwey-Overbeek (DLVO) theory agreed with the experimental data describing the interparticle forces in water. In aqueous fructose solutions, the interparticle forces were considerably smaller than they were in water. As fructose concentration increases from 0 to 10 wt.%, the critical distances for "jump-to-contact" decrease from 3.2 nm to 0.8 nm. The "pull-off" force was greatly reduced from 1.5 nN in water to 1.1, 0.7, and 0.4 nN for 3, 5, and 10% fructose solution respectively. The reduction in the interparticle force with fructose is inferred to be due to adsorption of fructose on the surface and hence alter the surface potential and/or Debye length. Adsorption of fructose on the particle surface may be responsible for weaker interaction between the particles.

1. Introduction

The surface properties of colloids are widely recognized as determining the flow and dispersive behavior of suspensions and particulate fluids. Recent work by Li and Akinc [1] showed that the viscosity of nanometric alumina aqueous suspensions is reduced dramatically by fructose addition. Chinachoti [2] also demonstrated a dramatic reduction in viscosity of starch-water mixture by sucrose addition.

In the dispersion or agglomeration of particles in liquids there is a need to understand the way in which the particles interact. This is because the macroscopic behavior of particulate systems is inextricably linked to the microscopic details of the interactions between the individual particles. Consequently, knowing the way in which the force varies between the particles and the associated modeling of these forces is of prime importance [3]. Moreover, a quantitative understanding of the changes in colloidal forces caused by chemical interactions between the particles and their chemical environment is critical for the prediction and control of colloidal processes

Recent advancements in technology have made direct force measurements possible in liquid by atomic force microscopy (AFM) [4,5]. Since then the use of the AFM for studies of this type has been reported by many workers on a wide range of tip-substrates and in various media. These studies have included a range of mineral oxides and solutions, for example, silicon nitride, Al_2O_3, glass, and diamond-mica and glass in electrolyte solutions [6], a glass sphere and a silica plate in aqueous solution [5], silica and α-alumina for different values of solution pH [7], silicon nitride tip-alumina in electrolyte solutions [8], zirconia [9], alumina [10], barium titanate [11], and cationic polyelectrolyte coated silica surfaces in water and in ethanol [12]. It was found [5] that the measured forces agree well with classical DLVO theory at large separation (>3 nm) and at conditions intermediate between constant charge and constant potential. An additional repulsive force at small separation prevents adhesion in a van der Waals minimum. Butt [6] found that in the presence of high concentrations (>3M) of divalent cations, where the electrostatic force can be completely ignored, another repulsive force was observed with silicon nitrde tips on mica. This force decayed roughly exponentially with a decay length of 3 nm and was ~0.07 nN strong. This repulsion is

attributed to the hydration force. Veeramasuneni *et al* [7] measured the interactions between silica and α-alumina at various pH values. They found that the experimental data were in good agreement with theoretical predictions based on electrostatic and van der Waals interactions. And when the force/radius values at a particular separation distance were plotted against pH, the transition from an attractive to a repulsive force occurred at pH 9.3 which is very close to the point of zero charge (pzc) of α-alumina as determined from electrophoresis experiments. Pedersen and Bergstrom [9] studied the forces between a sphere and a plane surface of yttria-partially-stabilized tetragonal-zirconia immersed in aqueous solutions of low-molecular-weight (M_w=10000) poly(acrylic acid) (PAA). They found the force results are comparable to rheological observations of zirconia suspensions stabilized by the same dispersant; the poor colloidal stability and high viscosity at low surface coverage of PAA are related to the attractive bridging interactions. Pedersen [10] also found the force value compared well to theoretically calculated DLVO curves and were found to be between the limits of constant surface potential and surface charge for α-alumina sphere-plate system in the solution at various NaCl concentrations and pH values. The steric layers of bis-hydrophilic diblock copolymers formed of poly(methacrylic acid) (PMAA) and poly(ethylene oxide) (PEO) on barium titanate surfaces was investigated by Sindel [11]. The attractive forces were never observed. It is believed that the electrolyte level through the hydration of the polymer affects the conformation of the stabilizing PEO chains. Increasing electrolyte levels disrupt the hydrogen bonding between the polymer and solvent needed to create an extended polymer conformation. The interactions of cationic polyelectrolyte coated silica surfaces in water and ethanol were investigated by McNamee *et al* [12]. It was found that no obvious Stern layer is formated in ethanol, and there is a depression of the force in ethanol compared to water due to the polarity difference between the solvent and surfactant. However, all of the researches that have been done on the measurement of interactions by AFM were limited to larger micron-sized particles. Due in part to experimental difficulties, interparticle forces beween nanoparticles have not been adequately addressed. They are focused on the effects of electrolytes, pH, and/or polymers on change of the interactions.

The questions were raised: will DLVO still hold for describing the interactions in water between nanometric particles? Why and how does fructose change the viscosity of the nanoparticle suspension, although it is neither an electrolyte nor a polymer?

The primary objective of this study is to determine the interparticle forces between nanosized alumina particles in an aqueous solution and understand the role fructose, a non-electrolyte, plays in altering the interaction between the particles in the aqueous suspension.

2. Experimental procedure

2.1. Materials.

The nanosize alumina powders (99.99% Al_2O_3) were purchased from Nanophase Technologies Corporation (Burr Ridge, IL). The surface area of the alumina particles was measured to be 37.9±0.2 m^2/g by nitrogen adsorption, corresponding to an equivalent spherical particle diameter of 40 nm. A TEM micrograph shows that the particle shape is spherical with a considerable size distribution and are agglomerated (Figure 1). The nanosized alumina used in this investigation was pure γ-alumina phase, as stated by the manufacturer and confirmed by XRD pattern. The specific gravity of the γ-alumina was measured to be 3.6 g/cm^3.

D-Fructose was purchased from SIGMA Corporation (St. Louis, MO). Chemical analysis, as provided by the manufacturer, indicated that it was 99.9% pure. All materials were used as received, without further purification.

2.2. Experimental.

2.2.1 ζ-potential Measurements.

Zeta potential measurements were provided by Matec (Matec Instrument Companies, Inc. Northborough, MA) employing ESA-9800 Zeta Potential Analyzer. Solids content was kept at 20 vol.% while pH was varied from pH = 3.8 to 12 (See Figures 2 and 3).

2.2.2 Classification of Particles.

For accurate description of interparticle forces and appropriate modeling a narrow particle size distribution was needed. As received nanosize particles were classified by

centrifugation of a 10 wt.% alumina aqueous suspension at 4000 rpm for given time according to the Svedberg Equation [13],

$$d = \frac{6}{\omega}\sqrt{\frac{\eta \ln \frac{x_2}{x_1}}{2(\rho_1 - \rho_2)t}} \qquad (1)$$

where x_1 is the distance from the axis of rotation to the bottom of the centrifuge tube, x_2 is the distance from the axis of rotation to the meniscus of the suspension, ω is the angular velocity, t is the time needed for a given particle to travel the distance from x_1 to x_2, η is the viscosity of the medium, and ρ_1 and ρ_2 are the density of the particle and the medium respectively. In our case, x_1=10.16 cm, and x_2=15.24 cm; ω=4000 rpm; ρ_1 = 3.6 g/cm^3 and ρ_2 = 1.0 g/cm^3. Sedimentation time for several particle sizes were calculated using the equation (1) and it was determined that for a narrow particle size range a centrifugation time of 17 to 22 minutes would be sufficient.

The 10 wt.% suspension was sonicated for 30 min before centrifuging. Eight centrifuge cycles, in the time range of 22.2 to 17.0 min, were used to collect 35 to 40 nm particles. The suspension was first centrifuged for 17 min and the supernatant was collected. A new suspension was prepared and centrifuged for 22.2 min, and the sediment was collected. The sediment was redispersed and the centrifugation cycle was repeated for a total of eight times to get a relatively narrow particle size distribution. The classified particles were dried at 80°C (to avoid hard agglomerate formation at higher temperature, e.g. 100°C) in an oven for 24 h.

2.3 Sample preparation.

In this study sharp tips with low spring constants (k≈0.06N/m) were used to capture weak interactions between the nanosize particle and the measuring tip. Ultra sharp contact silicon cantilevers, with the tip radius of approximately 30 nm, were used (MikroMasch USA, Portland, OR). Typically, colloid probes are usually prepared by gluing spherical particles on AFM cantilever springs [5]. Due to experimental limitations, only large (D>1μm) particles were studied by this technique. In addition, deformation of the glue under the applied force adds an unknown but significant error to the measurements. In the present work, a thin alumina layer was applied to obtain desired surface chemistry. The tips were coated with a 10

nm aluminum layer by electron beam-physical vapor deposition (EB-PVD) for 50 seconds (Temescal BJD-1800 E, Semicore Equipment, Inc., Livermore, CA). The aluminum layer was converted to an alumina layer by oxidizing in air at 500 °C for five minutes.

Pieces of silicon wafer measuring 1.5×2.0 cm used as substrate for particles were also coated with a thin layer (10 nm) of aluminum in the EB-PVD chamber. A tapping mode of an AFM scan shows that the thickness of the layer was 10.4 nm.

A dilute suspension (0.1 wt.% particles in DI-water) of narrow-size particles (35-40 nm in diameter) was dispersed in an ultrasonic bath for 30 minutes. A drop of the dispersed suspension was spin-coated on the aluminum coated silicon wafer at a speed of 200 rpm. and dried in oven at 80 °C for 10 hours. Figure 2 shows a schematic drawing of nanoparticles mounted on aluminized wafer substrate.

2.4 Measurements.

SEM/AES and AFM in tapping mode were employed to observe the colloid probe and the particle sample. Figure 3 shows the AFM image of the well-dispersed nanosize (35-40 nm) alumina particles. It is clear that the classification procedure described above was able to produce a narrow size distribution in contrast to as received particles shown in Figure 1.

SEM/AES was down on a Jeol 7830 F Field Emission Auger Microprobe (JEOL USA, Inc., Peabody, MA 01960) at Ep=10.0 keV and Ip=1.00×10^{-9} A. The SEM micrographs of the AFM tip before and after alumina coating indicates that the tip curvature increased from 30±5 nm for as received tip to approximately 100 nm after alumina coating (Figure 4). Chemical analysis of the tip by Auger spectroscopy indicates that the treated tip was coated with an alumina layer as expected as shown in Figure 5.

Force between particle and the tip were measured by a Veeco Dimension 3100 AFM system (Veeco Instruments Inc., Woodbury, New York) in deionized water, and in aqueous fructose solutions.

Approximately 1 mL solution was added onto the surface of the substrate which contained nanosize alumina particles. The colloid probe was then completely immersed into solution. The experiments were carried out in an environment where the temperature was

25±2 °C throughout the procedure. The Z scan rate was set at 1.00 Hz and image scan rate was at 20.3 Hz. The scan area of 1.00 μm×1.00 μm was selected. The force-distance values of 256 spots on the whole area of 1 μm×1 μm were collected. The zero distance was determined when the tip and the sample were just "in contact", that is, when the deflection of the tip was the same as the displacement of the tip. At large separations the interparticle force was set to zero at which the deflection was constant. The forces were calculated by multiplying the tip deflection by its spring constant.

2.5 Spring constant determination.

The cantilevers that were used for detecting force values in water and in the fructose solutions have a nominal spring constant of 0.06 N/m (supplied by the manufacturer). The spring constant can vary from batch to batch and tip to tip due to small differences in the thickness. The treatment (alumina coating and baking) for the tips may also change the spring constant. Spring constants of the cantilevers were determined by "Cantilever-against-Cantilever" technique [14] immediately after each measurement. The technique depends upon comparing a simple physical measurement of the cantilever against known, pre-calibrated cantilevers. Figure 6 shows the schematic drawing of the technique. The force balance at point O is given by,

$$F' = F \qquad or \qquad k \times h = k_{known} \times h' \tag{2}$$

Where k_{known} = 0.22 N/m; h' is the deflection of the known cantilever, $h' = H - h$; H is the Z position of the tested cantilever; h is the deflection of the tested cantilever. For a given batch the manufacturer states the force constant to be k=0.06 N/m which is in good agreement with the measured value of k = 0.0627 N/m.

3. Results and Discussion

3.1 ζ-potential.

The ζ-potential of 20 vol.% nanometric alumina aqueous suspension as a function of pH is shown in Figure 7 with the isoelectric point at approximately pH=9.3. The ζ-potential remained more or less constant from pH = 3.8 to about 6.5 at about 40 mV. At higher pH values it decreases at a steady rate before crossing zero at pH = 9.3. In order to isolate the

role fructose play independent of the pH, ζ-potential of the suspension was also measured as a function of fructose concentration. Figure 8 shows that ζ-potential and pH changes slightly with increasing fructose concentration. Realizing that the solution is quite acidic to begin with and changes by about 0.5 pH unit (corresponding to a reduction in [H+] of approximately $2x10^{-4}$ M), is a significant change. Exact cause of this reduction in hydronium ion concentration is not clear. Since the variation in ζ-potential for the same range is only couple of millivolts, stripping hydroxyl groups from surface is not likely. Our previous work [1] showed that fructose may cover up to 22 % of the particle surfaces. The pH change caused by the addition of fructose indicates that the adsorption of fructose on the particle surfaces may weaken the hydration force between the particle surface and water molecules. Even though fructose is not an electrolyte and dielectric constant of 2.5 wt.% solution is similar to that pure water [15], it still can alter the electrostatic properties of the particle surface by steric shielding and cause the ζ-potential to decrease.

3.2 Interparticle forces in water.

Interaction between the nanosized hemispherical apex of alumina tip and the nanosize alumina particle in deionized water was measured to mimic the interaction between the two nanosize alumina particles. Although neither particle behaves as a free, spherical particle in the solution, the experimental set up described above was considered to represent the behavior of two nanosize particles in suspension. Figure 9 shows a typical interaction force (both on approach and separation) as a function of distance. On the approach curve shown in Figure 9, a slight repulsive force was observed below 100 nm separation. Repulsion force showed a maximum around 9 nm, below which repulsive force decreased sharply and at a separation of 3.2 nm, the tip "jumped-to-contact" with the particle. The particle-tip interaction may be explained by the classical DLVO theory, i.e. at large separations ($9<z<100$ nm), interaction is dominated by the repulsive electrostatic forces and at short separations ($0<z<9$ nm), attractive van der Waals forces are dominant. At a separation less than 3.2 nm, the net interaction force becomes attractive leading to spontaneous jump to the surface. The DLVO theory was used to fit the experimental data to the approach curve. The

net interaction force between two spherical particles with radii of R_1 and R_2 at a surface separation z is expressed by following equation [16]:

$$F = 4\pi\varepsilon_r\varepsilon_0 \frac{R_1R_2}{R_1+R_2}\frac{\psi_0^2}{\kappa^{-1}}\exp(\frac{-z}{\kappa^{-1}}) - \frac{A_H}{6z^2}\frac{R_1R_2}{R_1+R_2} \qquad (3)$$

where, ε_r is relative dielectric constant of the medium (for water is 78.36); ε_0 is the permeability of vacuum and equal to 8.8542×10^{-12} F m^{-1}; ψ_0 is the surface potential; κ^{-1} is so called the Debye length and given by $(2n_0Z^2e^2/\varepsilon_0\varepsilon k_BT)^{-1/2}$ [16], where n_0 is the number concentration of ions, z is the valence of ions, e is the elementary charge of electron, k_B is the Boltzmann constant and A_H is the Hamaker constant. For Al_2O_3-H_2O system, the value of $A_H=36.7\times10^{-21}$ J was used[17].

Using the surface potential, ψ_0, and Debye length, κ^{-1}, as adjustable parameters, DLVO expression was fitted to the experimental data. Figure 10 shows that equation (3) describes the net interaction force between particles accurately for the whole range. The agreement between experimental results and the DLVO theory was excellent (except for the very short range at which discontinuous jump was observed), Best fit was obtained for the surface potential, ψ_0 = 151 mV and Debye length, κ^{-1} = 70 nm. The value of the surface potential is reasonable estimate for a ζ-potential of 38 mV which was given above for 20 vol.% nanometric alumina aqueous suspension. The surface potential obtained by fitting the data to DLVO expression is comparable with the values reported in the literature [7, 10, 18], where the ζ-potential of α-alumina is 37 mV at pH 4.0 [7] and the surface potential of α-alumina is 26 mV at pH 6.2 and 0.0001 M NaCl solution [10]. For the γ-alumina, ζ-potential of 40 mV was reported at pH 6.5 with low concentration of NaCl solution (1×10^{-3} mol dm^{-3}) [18]. Figure 10 is an experimental verification that DLVO theory can predict the net interparticle forces for nanosize particle suspensions as it does for micron size particle system.

Comparison of approach and separation plots shows a significant hysteresis. This irreversible behavior is not surprising and implies that there is an activation barrier in detaching the particles which manifests itself with 1.5 nN "pull-off" force. It is anticipated that once the particles come in physical contact they form relatively strong hydrogen bonds between hydrated surface functional groups.

3.3 Particle Interactions in fructose solutions.

The net interaction force between the alumina tip and the nanosize alumina particle as a function of distance in 3, 5, and 10 wt.% fructose solution is shown in Figure 11. For each concentration, the net repulsive force upon approach is lower than that was for water (see inset in Figure 11). Also, the distance at which the tip starts to jump to contact with the particle was reduced by adding fructose implying that the attractive force was also reduced. Although the reduction in interaction force for all concentrations is indisputable, there is no obvious trend in reduction in the interaction force with fructose concentration.

DLVO theory was also applied to this set of experimental curves using Equation (3). The dielectric constant for each solution was only slightly less than pure water (78.4 v.s. 78.3 for all fructose concentrations) [15]. According to Lifshitz theory [17], the van der Waals attractive force (Hamaker constant) should not change significantly due to the small change in the dielectric constant. Based on this, the Hamaker constant, A_H, was assigned a fixed value of 3.67×10^{-20} J for the Al_2O_3-fructose solution. The results of best fit are shown in Figure 11 (inset) and summarized in Table 1. The surface potential and Debye length values obtained from best fit are reasonable except for the 3 wt.% fructose solution. The unusual behavior is also reflected in the experimental data for the same solution and this particular set of data should be considered anomalous. The source of this anomaly is not known but may be due to instrument calibration for that particular sample. In general, it is clear that the surface potential was lowered by fructose addition, implying partial neutralization of surface charges possibly by fructose adsorption. However, the reduction in surface potential is not reflected in similar reduction in ζ-potential. ζ-potential is reduced by only few mV by the fructose addition. Alternatively, one might consider screening of electrostatic forces by the addition of fructose which has amphibilic character. With what mechanism fructose alters the interactions between nanosized alumina particles is still unclear.

Table 1: Interaction parameters from AFM measurements

C_f wt.%	Ψ_o mV	κ^{-1} nm	x* nm	F_{Pull}* nN	W_{adh}* mJ/m^2	γ_{AlOH}* mN/m
0	150	64	3.2	1.5	14.3	7.2
3	20	1.8	1.8	1.1	10.5	5.3
5	68	60	1.6	0.7	6.7	3.3
10	102	60	0.8	0.4	3.8	1.9

*x ="jump-to-contact", F_{Pull} = Pull-out force, W_{adh} = work of adhesion, γ_{AlOH} = surface tension

More important than the magnitude of repulsive forces at large separation is the "jump-to-contact" values in fructose solutions. Whenever the attractive force between two surfaces exceeds the spring constant of the cantilever, the tip jumped to contact the particle surface. The spring constant of the cantilever used in this work was 0.0627 N/m. Figure 11 shows that the distance for jump-to-contact decreased with increasing fructose concentration. Table 1 gives the jump-to-contact distances as well as the depth of the force corresponding to this jump for several fructose concentrations. Since the spring constant of the cantilever is constant, the correlation between the jump-to-contact distance and adhesion force is also obvious. It is believed that this change of short range interactions is strongly related to the change of the structure and orientation of vicinal water molecules on the surfaces. The contribution of the hydration layer should also be taken into account in the very short range.

Pull-out forces between the tip and the particle in water and fructose solutions were measured during retracting the tip from the particle surface. The retraction curves show clearly that pull-off forces in the fructose solution were much weaker than those in water yet for each solution the pull-out force was much greater than that of adhesion force (see Figs. 11 & 12). Figure 12 shows that the higher the concentration of fructose in the solution, the weaker the pull-off force As shown in Table 1, pull-off force was reduced almost four-fold going from water (F_{Pull} = 14.3 nN) to 10wt% fructose (F_{Pull} = 3.8 nN) solution.

Bradley [19] showed that the adhesion force between two rigid spheres is:

$$F_{Pull} = 2\,\pi R_1 R_2/(R_1+R_2)\, W \qquad (4),$$

where R1 and R2 are the radii of the two spheres and W is the adhesion work, which is defined as the work necessary to create an interface area of 1 cm^2 between two different materials or to separate them. Work of adhesion is given by the sum of surface tension

tensions γ_1, γ_2, and γ_{12}, where γ_1 and γ_2 are the surface tensions for sphere-1 and sphere-2, respectively, and γ_{12} is the interfacial surface tension between the two spheres which vanishes if the spheres are of same material and the adhesion work becomes equal to 2γ. In the present case, the surface tension is taken as that of hydroxylated alumina surface in fructose solution:

$$W = \gamma_{AlOH\text{-}Sol'n)} + \gamma_{AlOH\text{-}Sol'n)} - \gamma_{AlOH\text{-}AlOH}$$
$$\approx 2\gamma_{AlOH\text{-}Sol'n)} \qquad (5)$$

Using the above expressions and the measured force of adhesion, the work of adhesion and particle-solution interfacial tension was calculated. The results are given in Table 1. The surface tension value in water is significantly lower than that in the literature [20], where 43.7 mN/m was reported for α-alumina. It is not clear if the behavior of α-alumina resembles closely to that of γ-alumina in solution and of the particle size has an effect as it approaches to nano scale. The results clearly show that addition of fructose decreases particle-solution interface significantly, another evidence for the observed reduction in viscosity of the suspension with fructose addition.

3.4 Water structure effects and hydration force.

Although the DLVO theory predicts the net interaction forces between particles for nanosize alumina suspensions quite accurately at large separations, the theory and experimental data diverge as particles approach to contact.. Forces in addition to electrostatic and van der Waals must exist at least for the system under consideration.

A number of previous studies [21, 22, 23, 24] have shown that the DLVO theory leaves many observations unexplained. Langmuir [25] and Derjaguin [26] postulated the existence of an additional structural force that seemed to be unique to water. This hydration, or structural, force is believed to arise from the strongly bound and oriented first layer of water molecules on surfaces, which may prevent two surfaces of particles from approaching any closer than 0.5-0.6 nm, the thickness of two water molecules. In order for these forces to influence the interparticle forces beyond a couple of layers, they must propagate further than one or two molecular layers. It seems reasonable that the first strongly oriented water layer could impose structural orientation on to the second and subsequent layers as suggested by

Israelachvili and Wennerstrom [27]. The range of this interaction was suggested to extend from nanometers [28, 29, 30, 31], to micrometers [32]. Our observations indicate that long range forces extend to about 6 nm. The previous work done in our lab [1] also showed that up to 20 water layers may be 'bound' on the particle surfaces for suspensions containing 32 vol.% nanometric alumina. At even higher solids contents, the bound water layers overlap resulting in dramatic increase in viscosity. However, the number of the bound water layers can be reduced by adding fructose to the suspension [1]. Although the exact mechanism by which the reduction of suspension viscosity with fructose addition has not been established yet, there is a compelling evidence that fructose molecules disturb the structural order the water molecules assume in the vicinity of the particle surface. The reduction in short range interaction (both repulsive and attractive) and particle-solution interfacial tension with the addition of fructose lead to a reduction in the thickness of the bound layers and hence reduction in the viscosity of the suspension. Of course, as the particle size approaches nano scale, these effects become significant and perhaps dominate the flow behavior of suspensions.

The change in the extent and structure of the hydration layer around a particle by fructose leads to certain implications. The hydration layer must be overcome before two colloidal particles can come into contact. Thus, the overall energetics of any association or dissociation process in water also involves what is commonly referred to as dehydration or hydration of the interacting surface groups. This in turn, determines the agglomeration behavior of the particles in dense suspensions. The overall energy balance that favors the association of two particles in water with fructose depends on a competition between particle-solute (fructose), solute-solute, solute-solvent (water), and solvent-solvent interactions (including hydrogen bonds) which have yet to be elucidated.

4. Conclusion

For the most part, DLVO theory describes the interactions between nano sized alumina particles in aqueous solutions. The fit between the theoretical curve and the experimental data was found to diverge somewhat for fructose solutions especially at short separation distances. The experimental data showed that the interactions between the particles are

reduced by fructose addition. The spontaneous attraction (jump-to-contact) distance was found to decrease from 3.2 nm for water to 1.8, 1.6, and 0.8 nm for 3, 5, 10 wt.%, fructose solution respectively. Similarly, the pull-off force was greatly reduced from 1.5 nN in water to 1.1, 0.7, and 0.4 nN for 3, 5, and 10% fructose solution respectively. The reduction in the viscosity of nanometric alumina aqueous suspension by fructose was attributed to the reduction in particle-particle interaction in aqueous solution.

Acknowledgment

Ames Laboratory is operated for the U.S. Department of Energy by Iowa State University under Contract No. W-7405-ENG-82. This research was supported by the Office of Basic Energy Science, Materials Science Division. Professor Tuttle's assistance in PVD, Mr. Oja's in ζ-potential and Mr. Shulha's assistance in AFM measurements are greatly appreciated. The authors also wish to thank Professors Tsukruk, Schilling, Kramer and Tomasik and Drs. Thom, .Mavis, and Sikora, for valuable assistance and discussions.

References

1. C. Li and M. Akinc, "Role of Bound Water on the Viscosity of Nanometric Alumina Suspensions," submitted to *Journal of the American Ceramic Society*, 2004.
2. P. Chinachoti, "Water mobility and its relation to functionality of sucrose-containing food systems," *Food Technology*, Vol. **47**, 134-140, January 1993.
3. C. S. Hodges, J. S. Cleaver, M. Ghadiri, R. Jones, and H. Pollock, "Forces between polystyrene particles in water using the AFM: pull-off force vs particle size," *Langmuir* **18**, 5741-5748, 2002.
4. W. A. Ducker, T. J. Senden and R. M. Pashley, "Direct measurement of colloidal force using an atomic force microscope," *Nature*, **353**(6341), 239-241, 1991.
5. W. A. Ducker, T. J. Sender, and R. M. Richard, "Measurement of forces in liquids using a force microscope," *Langmuir*, **8**(7), 1831-1836, 1992.
6. H. J. Butt, "Measuring electrostatic, van der Waals, and hydration forces in electrolyte solutions with an atomic force microscope," *Biophysical Journal*, **60**, 1438-1444, 1991.
7. S. Veeramasuneni, M. R. Yalamanchili and J. D. Miller, "Measurement of interaction forces between silica and α-alumina by atomic force microscopy," *Journal of Colloid Interface Science*, **184**(2), 594-600, 1996.
8. H. J. Butt, "Measuring local surface charge densities in electrolyte solutions with a scanning force microscope," *Biophysical Journal,* **63**(2), 578-582, 1992.
9. H. G. Pedersen and L. Bergstrom, "Forces measured between zirconia surfaces in Poly(acrylic acid) solutions," *J. Am. Ceram. Soc.* **82** (5) 1137-1145 1999.
10. H. G. Pedersen, "Aluminum oxide probes for AFM force measurements: Preparation, characterization, and measurements," *Langmuir*, **15**, 3015-3017, 1999.
11. J. Sindel, N. S. Bell, and W. M. Sigmund, "Electrolyte effects on nonionic steric layers: bis-hydrophilic PMAA-PEO diblock copolymers adsorbed on barium titanate," *J. Am. Ceram. Soc.* **82** (11), 2953-2957, 1999.
12. C. E. McNamee, M. Matsumoto, P. G. Hartley, P. Mulvaney, Y. Tsujii and M. Nakahara, "Interaction forces and zeta potentials of cationin polyelectrolyte coated

silica surfaces in water and in ethanol: Effects of chain length and concentration of perfluorinated anoionic surfactants on their binding to the surface," *Langmuir*, **17**, 6220-6227, 2001.

13. T. Svedberg, and K. O. Pedersen, "*The Ultracentrifuge*" Oxford University Press, London, 1940.
14. A. Torii, M. Sasak, K. Hane and S. Okuma, "A method for determining the spring constant of cantilevers for atomic force microscopy," *Meas. Sci. Technol.*, **7**, 179-184, 1996.
15. K. Fuchs and U. Kaatze, "Molecular dynamics of carbohydrate aqueous solutions. Dielectric relaxation as a function of glucose and fructose concentration," *J. Phys. Chem. B*, **105**, 2036-2042, 2001.
16. J. N. Israelachvili, in *Intermolecular and Surface Force with Applications to Colloidal and Biological Systems*, London, Academic Press, 139, 184, 1985.
17. L. Bergstrom, "Hamaker constants of inorganic materials," *Advances in Colloid and Interface Science*, **70**, 125-169, 1997.
18. I. Sondi, O Milat, and V. Pravdic, "Electrokinetic potentials of clay surfaces modified by polymers," *Journal of Colloid and Interface Science* **189**, 66-73, 1997.
19. R. S. Bradley, "The cohesive force between solid surfaces and the surface energy of solids," *Philosophical Magazine*, **13**, 853-862, 1932.
20. L. Holysz, and E. Chibowski, "Surface free energy components of α-alumina from thin-layer wicking," *Langmuir*, **8**(2), 717-721, 1992.
21. J. N. Israelachvili, *Intermolecular and Surface Forces* 2nd ed, Academic, New York, 1991.
22. R. G. Horn, "Surface forces and their action in ceramic materials," *J. Am. Ceram. Soc.*, **73**(5) 1117-1135, 1990.
23. H. Yotsumoto and R-H Yoon, "Application of extended DLVO theory: I. Stability of rutile suspensions," *Journal of Colloid and Interface Science* **157**, 426-433, 1993.
24. D. Grasso, K Subramaniam, M. Butkus, K. Strevett and J Bergendahl, "A review of non-DLVO interactions in environmental colloidal systems," *Re/Views in Environmental Science & Bio/Technology* **1**, 17-38, 2002.

25. I. Langmuir, "The role of attractive and repulsive forces in the formation of tactoids, tixotropic gels, protein crystals and coacervates," *Journal of Chemical Physics.* **6**, 873-896 1938.

26. B. V. Derjaguin, "Properties of water layers adjacent to interfaces," in *Fluid Interfacial Phenomena* (ed. Croxton, C. A.) 663-738, Wiley, Chichester, 1986.

27. J. N. Israelachvili and H. Wennerstrom, "Role of hydration and water structure in biological and colloidal interactions," *Nature*, **379,** 18 January 1996.

28. R. P. Rand and V. A. Parsegian, "Hydration forces between phospholipic bilayers," *Biochimica et Biophysica Acta* **988**(3), 351-376, 1989.

29. R. M. Pashley, "Hydration force between mica surfaces in electrolyte solutions," *Advances in Colloid and Interface Science*. **16**, 57-62, 1982.

30. J. N. Israelachvili and R. M. Pashley, "Double-layer, van der Waals and hydration forces between surfaces in electrolyte solutions," in *Biophysics of Water* (eds Franks, F. and Mathias, S.) 183-194, Wiley, Chichester, 1982.

31. J.N. Israelachvili, "Measurement of hydration forces between macroscopic surfaces," *Chemica Scripta* **25**(1), 7-14, 1985.

32. W. D. Hansen, "The occurrence and extent of vicinal watr," in *Biophysics of Water* 163-169, (eds Franks, F. and Mathias. S.), Wiley, Chichester, 1982.

FIGURE CAPTIONS

Figure 1. TEM image of nano size alumina particles.

Figure 2. Schematic drawing of mounting particles on a wafer substrate.

Figure 3. AFM image of nano size alumina particles on a wafer substrate.

Figure 4. SEM images of AFM cantilever tip. (a) and (b) as received tip; (c) Alumina coated tip; (d) selected spots for the Auger analysis of the coated tip.

Figure 5. Auger Electron Spectra of spots shown. Spots 1 and 4 are on the sharp end of the tip; spots 2 and 3 are on the arm of the tip. (see Figure 4)

Figure 6. Schematic diagram of the "cantilever-against-cantilever" technique for determining spring constant of a cantilever tip.

Figure 7. ζ-potential vs. pH plot of 20 vol.% nanosize alumina aqueous suspension.

Figure 8. Effect of fructose on the pH and ζ-potential of 20 vol.% nanosize alumina suspension.

Figure 9. Interaction force as a function of distance between the alumina tip and the particle in water during approach and detach.

Figure 10. Force-distance plot for nanosize alumina suspensions in water. Solid curve shows the net interaction force as defined by DLVO theory. Note surface potential and Debye Length are used as adjustable parameters in Equation (3).

Figure 11. Interaction force as a function of distance between the alumina tip and the particle in fructose solutions during approach. Inset shows the DLVO best fit curves to the AFM data.

Figure 12. Force-distance plots for nanosize alumina suspensions for various fructose concentrations.

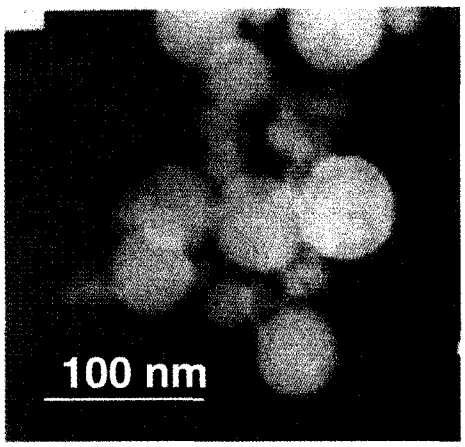

Fig. 1

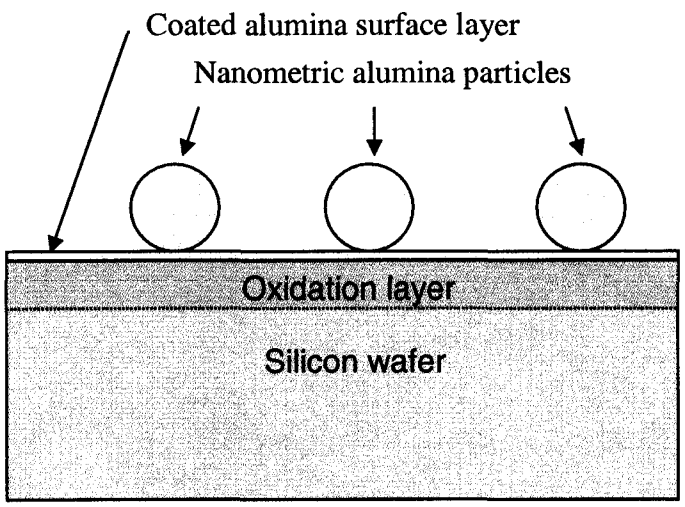

Fig. 2

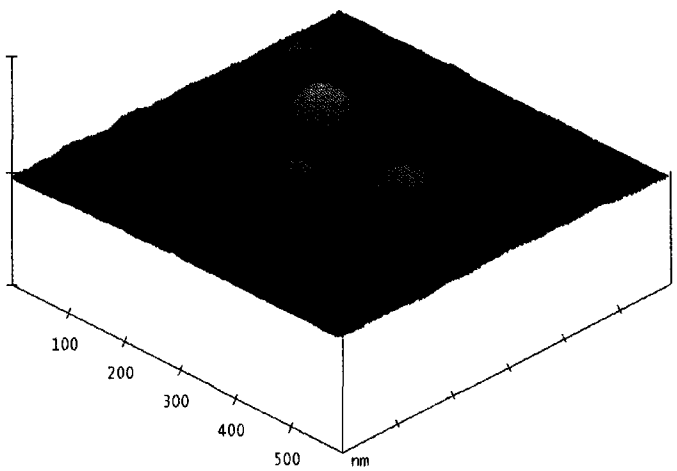

Fig. 3

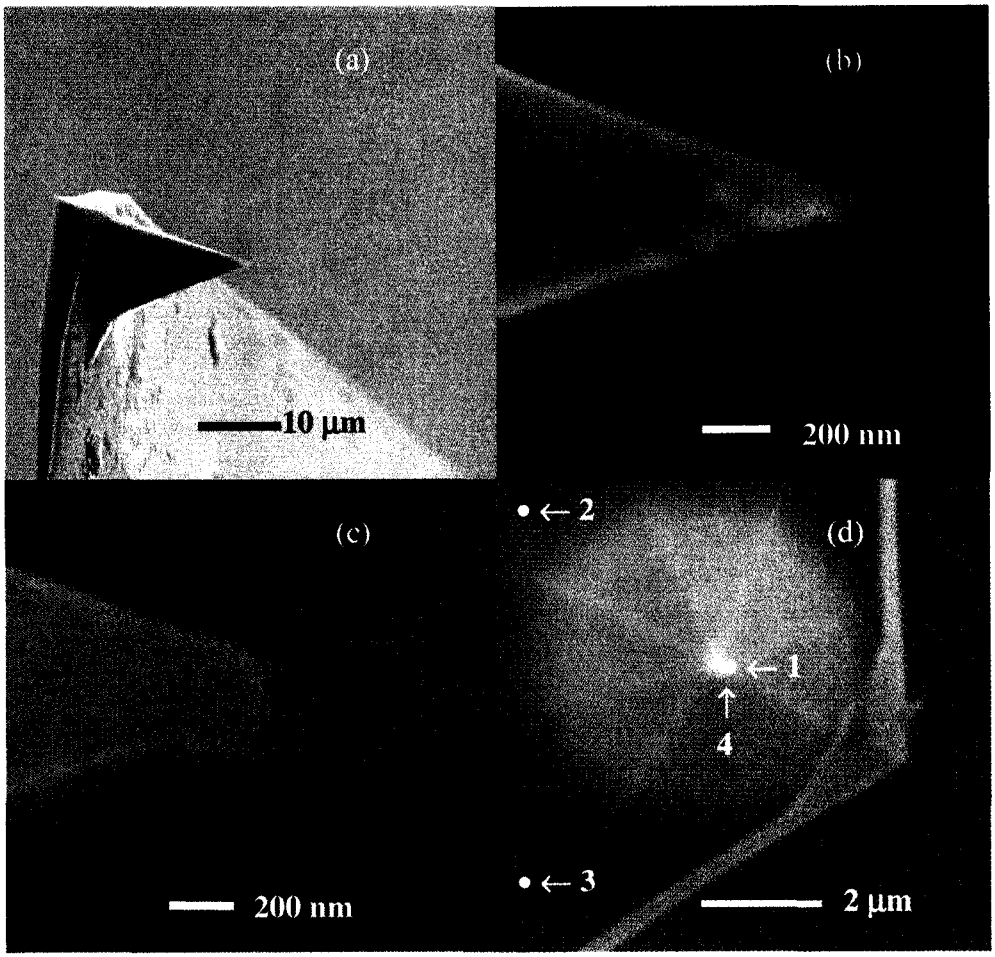
(a)
10 μm
(b)
200 nm
• ← 2
(c)
(d)
← 1
4
• ← 3
200 nm
2 μm

Fig. 4

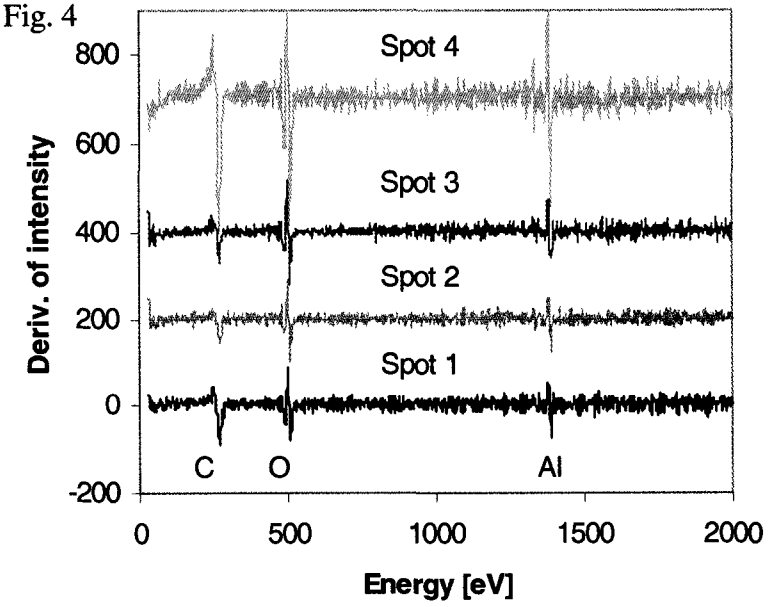
Spot 4
Spot 3
Spot 2
Spot 1
Deriv. of intensity
800
600
400
200
0
-200
C
O
Al
0
500
1000
1500
2000
Energy [eV]

Fig. 5

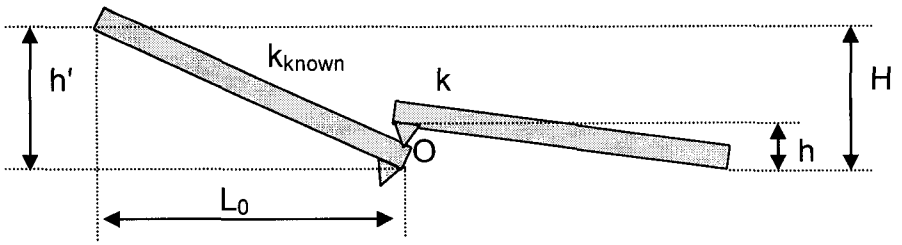

Fig. 6

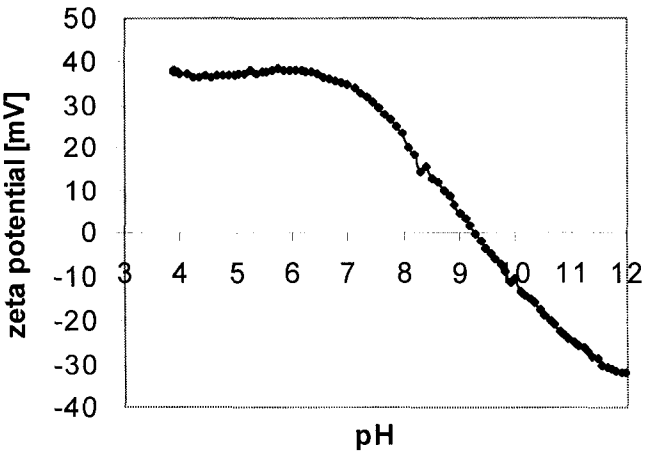

Fig. 7

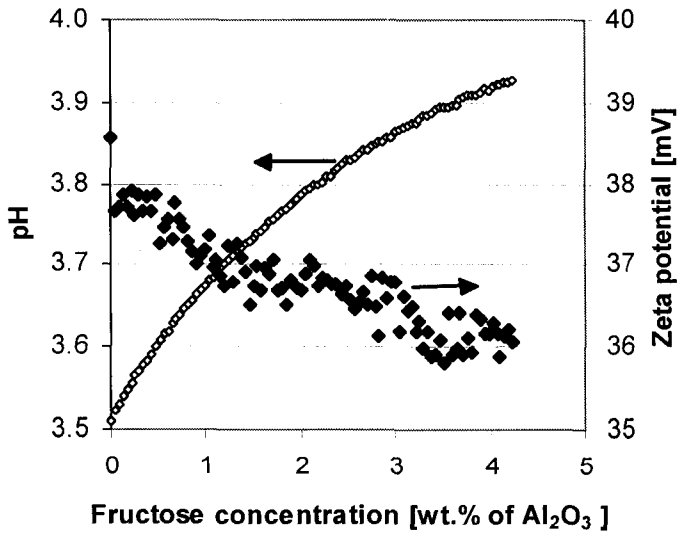

Fig. 8

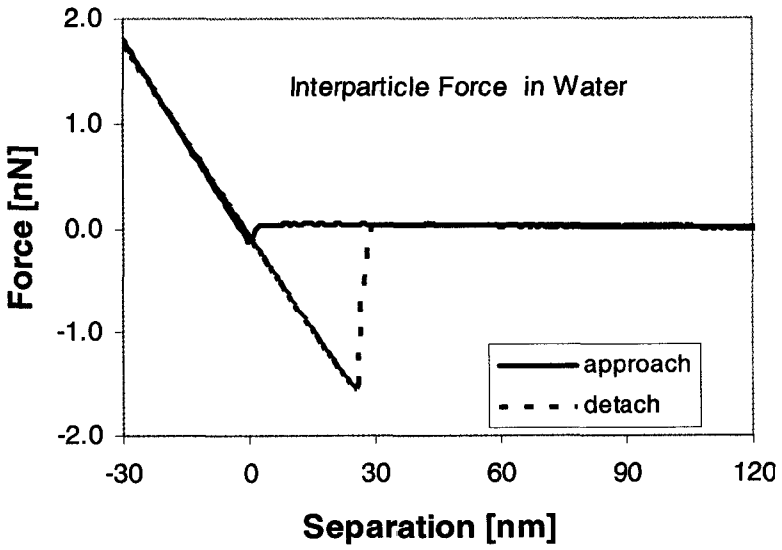
Interparticle Force in Water
Force [nN]
Separation [nm]
approach
detach
2.0
1.0
0.0
-1.0
-2.0
-30
0
30
60
90
120

Fig. 9

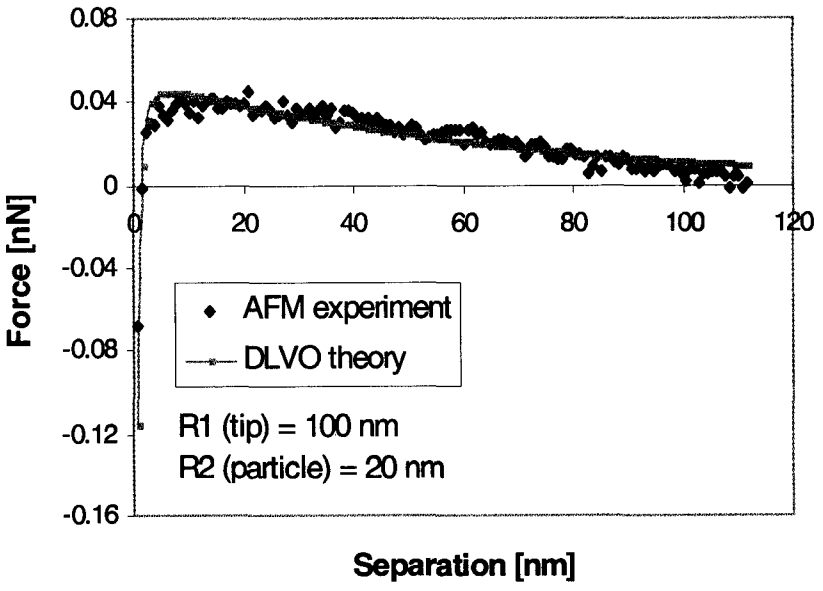
Force [nN]
Separation [nm]
AFM experiment
DLVO theory
R1 (tip) = 100 nm
R2 (particle) = 20 nm
0.08
0.04
0
-0.04
-0.08
-0.12
-0.16
0
20
40
60
80
100
120

Fig. 10

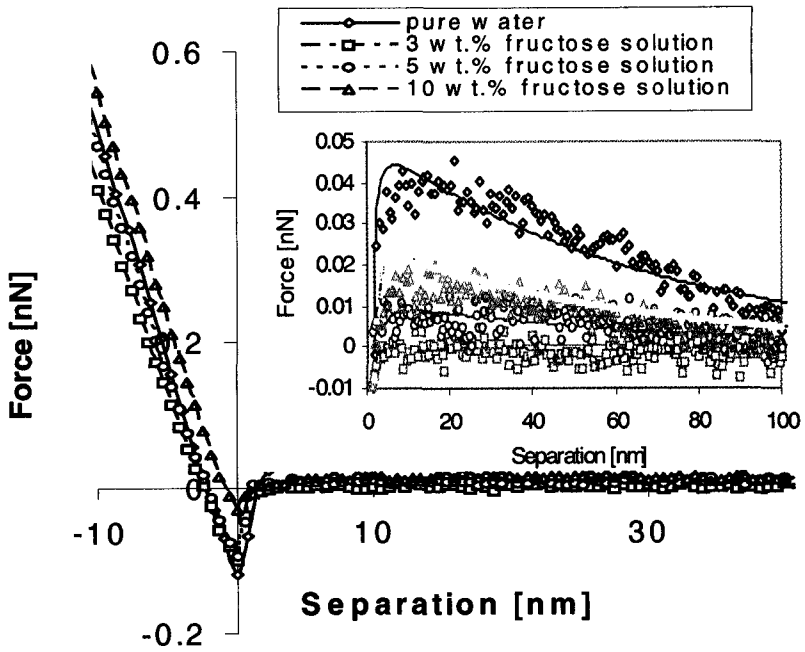
pure w ater
3 w t.% fructose solution
5 w t.% fructose solution
10 w t.% fructose solution
Force [nN]
Separation [nm]
0.6
0.4
0.2
0
-0.2
-10
10
30
0.05
0.04
0.03
0.02
0.01
0
-0.01
0
20
40
60
80
100

Fig. 11

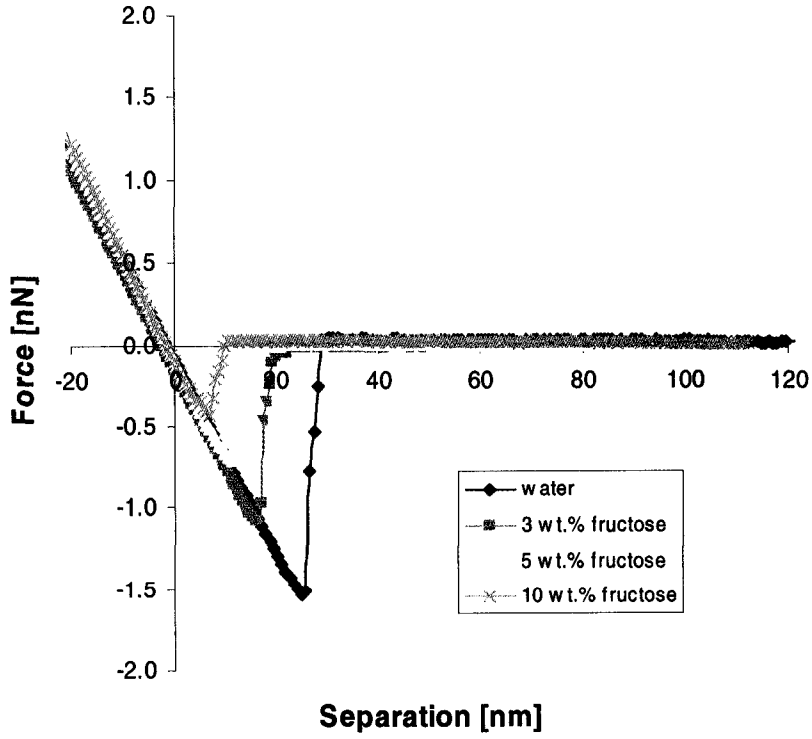
Force [nN]
Separation [nm]
2.0
1.5
1.0
0.5
0.0
-0.5
-1.0
-1.5
-2.0
-20
0
20
40
60
80
100
120
w ater
3 w t.% fructose
5 w t.% fructose
10 w t.% fructose

Fig. 12

Chapter 5: General Conclusions

The rheological properties are crucial to the formation of ceramic components, the physical properties of dried and sintered materials, and the reliability of the final products, especially for nanometric particles. This thesis addresses the problem of rheological properties in colloidal particle aqueous suspensions that arise during ceramic shaping. It is focused on four main aspects: (i) the changes in viscosity with particle volume fraction and by D-fructose addition, a non-electrolyte, mono saccharide; (ii) the nature of water layers on nanometric alumina particle surfaces and their influence on the rheology; (iii) the role of water mobility in the suspension and its relation with the rheology; (iv) the interactions between the nanometric alumina particles in aqueous fructose solutions.

Low viscosity suspensions with high solid loading are usually needed in ceramics forming process in order to achieve defect-free and reliable ceramic components. The research shows that fructose and several other mono-, di- saccharides, are effective in reducing the viscosity of dense nanometric alumina aqueous suspensions. Dense and fluidic nanometric alumina aqueous suspensions (40 vol.% solid loading) can be made by adding fructose. Why and how these kinds of molecules, e.g. fructose, influence the rheology?

Although extensive work has been reported regarding the rheological properties of colloidal particle suspensions, majority of the work was on the role of pH, the additive like electrolytes/polyelectrolytes, and polymers on the rheology. These additives certainly change the rheology of suspensions since they can vary the electrostatic forces and/or bring the steric forces onto particle surface. To the best knowledge of this author, no research has been carried out to study the effect of small, non-electrolyte molecules, on rheology of nanoparticle suspensions.

It is known that the rheology of colloidal suspensions strongly depend on the interactions between particle-particle and particle-medium. The research showed the high surface area nanometric alumina particles strongly interact with water in aqueous suspension, causing the pH down to 4. The interactions between the particle surface and water influence the viscosity of the suspension. TGA and SZT-DSC experiments identified three types of water in nanometric alumina aqueous suspensions: bulk (free) water, physically bound water, and

chemically bound water. Chemically bound water represents the monolayer of water molecules on the particle surface. In addition, multiple layers of water were physically bound on the particle surface. The physically bound water melts at the temperature below 0°C with low heat of fusion. These bound water layers strongly affect the viscosity of the suspension, especially when the solid volume fraction is higher than 30 %. SZT-DSC analysis indicated the number of bound water layers on the particle surface approaches 20 at high solids contents (ϕ>30 vol.%). At this level, bound water layers overlap, resulting in a dramatic increase in the viscosity of the nanometric alumina suspensions.

The variation of viscosity by fructose must result from the change of interactions between the nanometric alumina particles and water in the aqueous suspension. The research shows that the interactions do vary with the presence of fructose.

The results of fructose adsorption measurements showed that only fraction of alumina surface was covered by fructose. However, it is likely that this small amount of adsorbed fructose is responsible for the pH increase and decrease of the zeta potential of the alumina particles. It is believed that the addition of fructose weakens the interactions between particle surface and water molecules, as a consequence, water molecules rendered more mobile. Therefore, the reduction of viscosity upon addition of fructose is due to availability of higher fraction of water contributing to the flow. The overall level of water mobility was enhanced as determined by ^{17}O NMR spectroscopy. SZT-DSC results indicated that the bound water fraction was reduced after adding fructose. According to equation (4) in chapter 3, fractions of the bound water in the suspensions could also be determined by NMR technique, if the order parameter of water molecules, S, was known. Unfortunately, the bound water structure is unclear, which hinders determining the fraction of bound water through NMR technique. The presence of fructose in the suspension makes the structure even more complicated to assess.

The variation of interaction between the nanoparticles in water and fructose solutions was directly measured using AFM. The AFM experimental data showed that the interaction between the particles is reduced by fructose addition. The spontaneous jump-to-contact distance was found to decrease from 3.2 nm for water to 1.8, 1.6, and 0.8 nm for 3, 5, and 10 wt.%, fructose solution respectively. Similarly, the pull-off force was greatly reduced from

1.5 nN in water to 1.1, 0.7, and 0.4 nN for 3, 5, and 10 wt.% fructose solution respectively. The reduction in the viscosity of nanometric alumina aqueous suspension by fructose was also attributed to the reduction in particle-particle interaction in aqueous solution. For the most part, DLVO theory describes the interactions between nano sized alumina particles in aqueous solutions quite well. The fit between the theoretical curve and the experimental data was found to diverge somewhat for fructose solutions especially at short separation distances.

The research demonstrated that even nonionic, small molecules may dramatically influence the interactions between nanopartic-nanoparticle and nanoparticle-water in aqueous suspension. Therefore, these kinds of molecules may become new dispersants for suspensions with nanometric ceramic powders

This research has, in the opinion of the author, shed some light into the rheological behavior of nanosized alumina suspensions and the role fructose play in altering this behavior. Though some strong signs were observed as to how fructose influence the viscosity of nanometric alumina suspensions, proof and details of fundamental particle/solute/solvent interactions as they related to rheological behavior have yet to be elucidated.